Ministry of Higher Education
and Scientific Research
University of Babylon / College of Science
Department of physics

Effect of Beta particles Irradiation on Structural and Optical Properties of Metal –Phthalocyanine Thin Films

A Thesis

Submitted to the College of Science /University of Babylon

in Partial Fulfillment of the Requirement for the Degree of Master of Science in Physics

By

Reham Khalid Kareem Kadum

B.Sc. in Physics / (2016)

Supervised by

Dr. Addnan Hammood Muhammad Abdul Husain

2022 A.D **1444 A.H**

Supervisors Certification

I certify that this thesis entitled ***"Effect of Beta Particles Irradiation on Structural and Optical Properties of Metal –Phthalocyanine Thin Films"*** was prepared by (**Reham Khalid Kareem Kadum**) under my supervisions at Department of Physics , College of Science, University of Babylon, as a partial fulfillment of the requirements of Master in physics science

Signature:

Supervisor: Dr. Addnan Hammood Mohammad Abdul Husain

Title: Lecturer

Address: Department of Physics –university of Babylon

Date: / / 2022

Certification of the Head of the Department

In view of the available recommendation, I forward this thesis for debate by the examination committee.

Signature:

Name: Dr. Samira Adnan Mahdi

Title: Assistant Professor

Address: Head of the Department of Physic - College of Science – University of Babylon

Date: / / 2022

Dedication

To….

My Father

My Mother

My sisters & brother

My grand father

My friends

with my love and respect

Reham

Acknowledgments

First of all, I would like to thank God Almighty for helping me complete my thesis.

*I would like to express my thanks and gratitude to my supervisor, **Dr. Adnan Hammoud Al-Aarajiy**, for his suggestion of the topic to me and for his efforts, advice and guidance that helped avoid all the difficulties that faced me during my work*

I thank all of my friends so much.

*I thank the head of the Physics Department at the College of Science at University of Karbala **Asst .Prof. Dr. Rajaa Abd-ALAmeer** . Many thanks and gratitude to all my family members who always support me and alleviate the difficulties I faced during my work*

Reham

Summary

Copper phthallocyanine (CuPc) solution was prepared from copper phthallocyanine powder dissolved in chloroform at a concentration of (0.15 g/l) and irradiated with two different sources :beta nuclear rays plus(Na-22) with a source of energy (0.544 Mev) and minus beta ray (Sr-90) with energy source (0.546 Mev) .

The optical properties were measured before and after irradiation and it was found that the absorbance and reflectance decrease with the increase of the irradiation time and the transmittance and the optical energy gap with indirect transmission increase. The optical constants such as the absorption coefficient, refractive index, extinction coefficient , real and imaginary dielectric constant and optical conductivity were also calculated before and after irradiation.

CuPc solutions with concentrations (0.1, 0.15, 0.2 g/l) were also prepared and irradiated with plus beta nuclear rays (Na-22) and minus beta sources (Sr-90). The optical properties were measured before and after irradiation and it was found that the absorbance and reflectance increased with increasing Irradiating time, transmittance decrease, and optical energy gap with indirect transmission. Optical constants such as absorption coefficient, refractive index, extinction coefficient, real and imaginary dielectric constant and optical conductivity were calculated before and after irradiation.

CuPc thin films of constant thickness and room temperature were prepared using (Spin Coating) technique on a glass substrate with thickness (197, 214) nm using the Ellipsometry technique , then these films were irradiated with two different sources of plus and minus beta rays .

CuPc powder was diagnosed by Fourier Transform Infrared (FTIR) then chemical bonds were determined, The absorbance , transmittance and reflectance were test by UV- Visible.

UV-Vis assays showed that CuPc thin films have decreased in absorbance and reflectance , increase in transmittance, and optical direct energy band gap, optical constants such as absorption coefficient, reflection coefficient, extinction coefficient, and fluorescence spectra were calculated.

The structural properties of CuPc powder and thin films were tested by X-ray diffraction and average crystal size was determined before and after irradiation, The X-ray diffraction results showed that the CuPc powder is polycrystalline, triclinic system and average crystal size increased with the increase in irradiating time

Atomic force microscopy (AFM) was used to investigate the surface morphology of copper phthalocyanine thin films, and it was showed that grain size and roughness decreased with increasing irradiating time for both beta-ray sources.

List of Contents

No.	Subject	Page No.
	Contents	I
	List of Figures	V
	List of Tables	XII
	List of Symbols and Abbreviations	XV
	Chapter One: Theoretical Part	
1.1	Introduction	1
1.2	Organic Semiconductors	2
1.3	Phthalocyaninces ,MPc , Pcs	3
1.4	Copper phthalocyanine	6
1.5	Literature Survey	9
1.6	Aim of Research	13
	Chapter Two: Theoretical Part	
2.1	Introduction	14
2.2	Beta Ray	14
2.2.1	Beta Minus Decay(β-)	15
2.2.1.1	Sr-90	15
2.2.2	Positron/Beta Plus Decay(β+)	16
2.2.2.1	Na-22	17
2.3	Optical Properties	18
2.3.1	FT-IR Emission	19
2.3.2	Optical Properties of Semiconductors	21

No.	Subject	Page No.
2.3.2.1	Direct Transition	23
2.3.2.1.1	Allowed Direct Transition	23
2.3.2.1.2	Forbidden Direct Transition	24
2.3.2.2	Indirect Transition	24
2.4	Optical Constants	25
2.5	Photoluminescence Spectrum	27
2.6	Structural Properties	29
2.6.1	X-ray Diffraction	29
2.7	Surface Morphology	32
2.7.1	AFM – Atomic Force Microscopy	32
Chapter Three: Experiment Procedure and Measurements		
3.1	Introduction	34
3.2	Solution Preparation	35
3.3	Preparation of Blue CuPc Thin Films	35
3.4	Beta Ray Sources	36
3.5	Thickness Measurements	37
3.6	Optical Measurements	38
3.6.1	UV-Vis. Measurements	38
3.6.2	Photoluminescence Measurements	39
3.7	Structural Measurements	40
3.7.1	FT-IR Measurements	40

No.	Subject	Page No.
3.7.2	X–Ray Diffraction	41
3.8	Surface Morphology Measurements	42
3.8.1	Atomic Force Microscope Measurements	42
	Chapter Four: Results and Discussions	
4.1	Introduction	44
4.2.1	FT-IR Transmittance spectra	44
4.3	Optical properties for CuPc	45
4.3.1	Effect of irradiation time on Optical properties for CuPc Solution Irradiated by Beta ray	45
4.3.2	Concentrations Effect Solution Irradiated by Beta ray for Cupc on the Optical Properties	57
4.3.3	The Optical Properties of CuPc Thin Films	68
4.4	Photoluminescence Spectra	88
4.5	Result of Structural properties and Surface Morphology	91
4.5.1	XRD Results of CuPc	91
4.5.1.1	XRD Results of CuPc Powder	91

No.	Subject	Page No.
4.5.1.2	XRD for CuPc thin films for plus Beta ray (β+)	92
4.5.1.3	XRD for CuPc thin films for Minis Beta ray (β-)	94
4.5.2	Surface Morphology	96
4.5.2.1	Atomic Force Microscope	96
	Chapter Five: Conclusions and Suggestions	
5.1	Conclusions	105
5.2	Suggestions for Future Work	106
	References	107

List of Figures

Figure No.	Subject	Page No.
1.1	Molecular shape of mineral and non-mineral phthalocyanine	**4**
1.2	Typical function of phthalocyanine derivatives	**5**
1.3	The structure of copper phthalocyanine(CuPc)	**6**
2.1	Schematic of Sr-90 decay	**16**
2.2	Schematic of Na22 decay	**17**
2.3	Oscillations observed in diatomic molecules.	**19**
2.4	Schematic Representation of FT-IR spectrometer	**20**
2.5	The Optical Transition (a) Allowed Direct Transition (b) The Forbidden Direct Transition ; (c) Allowed Indirect transition (d) The Forbidden Indirect Transition	**24**
2.6	Representation of the energy transfer involved in the process of fluorescence (Jablonski diagram)	**26**
2.7	Typical (a) absorption and (b) fluorescence emission spectra of a symmetrical D_{4h} type MPc	**27**
2.8	Reflection of X-ray beam of wavelength λ from a particular set of atomic planes separated by equal distances d. θ is the complement of the angle of incidence	**29**
2.9	Scheme of AFM device	**31**
3.1	Schematic diagram for the experimental work.	**34**
3.2	Spin Coating method	**36**

Figure No.	Subject	Page No.
3.3	Beta Sources	**36**
3.4	Typical Configuration in Ellipsometer	**38**
3.5	UV-Vis spectrophotometer	**39**
3.6	Photoluminescence Spectrometer	**40**
3.7	FTIR spectrophotometer	**41**
3.8	Schematic illustration of X-ray diffraction instrument	**42**
3.9	AFM Device	**43**
4.1	FT-IR spectra for CuPc Powder	**45**
4.2	a. Absorbance spectra with CuPc solutions concentration (0.15)g/l for β+ Irradiated samples in period time . b. The Maximum Absorption vs. the Irradiating time for β+ CuPc solutions at 600nm	**46**
4.3	a. Absorbance spectra with CuPc solutions concentration (0.15)g/l for β-Irradiated samples in period time . b. The Maximum Absorption vs. the Irradiating time for β- CuPc solutions at 600nm	**47**
4.4	a. Reflectance spectra with CuPc solutions concentration (0.15)g/l for β+Irradiated samples in period time . b. The	**48**

Figure No.	Subject	Page No.
	Maximum Reflection vs. the Irradiating time for β+ CuPc solutions at 600nm	
4.5	a. Reflectance spectra with CuPc solutions concentration (0.15)g/l for β-Irradiated samples in period time . b. The Maximum Reflection vs. the Irradiating time for β- CuPc solutions at 600nm	**48**
4.6	a. Transmittance spectra with CuPc solutions concentration (0.15)g/l for β+Irradiated samples in period time . b. The Maximum Transmittance vs. the Irradiating time for β+ CuPc solutions at 600nm	**49**
4.7	a. Transmittance spectra with CuPc solutions concentration (0.15)g/l for β-Irradiated samples in period time . b. The Maximum Transmittance vs. the Irradiating time for β- CuPc solutions at 600nm	**50**
4.8	a. Determined indirect energy band gap CuPc solutions concentration (0.15)g/l for β+ Irradiated samples in period times. b. The Maximum indirect energy band gap vs. irradiating time for β+CuPc solutions at 600 nm	**51**
4.9	a. Determined indirect energy band gap CuPc solutions concentration (0.15)g/l for β+ Irradiated samples in period times. b. The Maximum indirect energy band gap vs. irradiating time for β+CuPc solutions at 600 nm	**51**

Figure No.	Subject	Page No.
4.10	a. Absorbance spectra with CuPc solutions concentrations (0.1 ,0.15,0.2)g/l for β+Irradiated samples in (5 day) . b. The Maximum Absorbance vs. the concentrations for β+ CuPc solutions at 600nm	**54**
4.11	a. Absorbance spectra with CuPc solutions concentrations (0.1 ,0.15,0.2)g/l for β-Irradiated samples in (5 day) . b. The Maximum Absorbance vs. the concentrations for β- CuPc solutions at 600nm	**54**
4.12	a. Reflectance spectra with CuPc solutions concentrations (0.1 ,0.15,0.2)g/l for β+Irradiated samples in (5 day) . b. The Maximum Reflectance vs. the concentrations for β+ CuPc solutions at 600nm	**55**
4.13	a. Reflectance spectra with CuPc solutions concentrations (0.1 ,0.15,0.2)g/l for β-Irradiated samples in (5 day) . b. The Maximum Absorbance vs. the concentrations for β- CuPc solutions at 600nm	**56**
4.14	a. Transmittance spectra with CuPc solutions concentrations (0.1 ,0.15,0.2)g/l for β+Irradiated samples in (5 day) . b. The Maximum Transmittance vs. the concentrations for β+ CuPc solutions at 600nm	**57**
4.15	a. Transmittance spectra with CuPc solutions concentrations (0.1 ,0.15,0.2)g/l for β-Irradiated samples in (5 day) . b. The Maximum Transmittance vs. the concentrations for β- CuPc solutions at 600nm	**57**

Figure No.	Subject	Page No.
4.16	a. Determined indirect energy band gap for β+ ray CuPc solution with Concentrations(0.1, 0.15,0.2) g/l. b. The Maximum indirect energy band gap vs. Concentrations at 600nm	**58**
4.17	a. Determined indirect energy band gap for β- ray CuPc solution with Concentrations(0.1,0.15,0.2)g/l . b. The Maximum indirect energy band gap vs.Concentrations at 600nm	**59**
4.18	a.Absorbance spectra for β+ Cupc thin film with thickness (197) nm in period times . b. The Maximum Absorbance vs. irradating time for β+ Cupc thin film at 600 nm	**61**
4.19	a.Absorbance spectra for β- Cupc thin film with thickness (197) nm in period times . b. The Maximum Absorbance vs. irradating time for β- Cupc thin film at 600 nm	**62**
4.20	a.Absorbance spectra for β+ Cupc thin film with thickness (214) nm in period times . b. The Maximum Absorbance vs. irradating time for β+ Cupc thin film at 600 nm	**62**
4.21	a.Absorbance spectra for β- Cupc thin film with thickness (214) nm in period times . b. The Maximum Absorbance vs. irradating time for β- Cupc thin film at 600 nm	**63**
4.22	a.Reflectance spectra for β+ Cupc thin film with thickness (197) nm in period times . b. The Maximum Reflectance vs. irradating time for β+ Cupc thin film at 600 nm	**64**

Figure No.	Subject	Page No.
4.23	a.Reflectance spectra for β- Cupc thin film with thickness (197) nm in period times . b. The Maximum Reflectance vs. irradating time for β- Cupc thin film at 600 nm	**64**
4.24	a.Reflectance spectra for β+ Cupc thin film with thickness (214) nm in period times . b. The Maximum Reflectance vs. irradating time for β+ Cupc thin film at 600 nm	**65**
4.25	a.The relation between Reflectance(R) and wavelength (λ) for β- CuPc thin film with thickness (214) nm in period times . b. The relation betweenMaximum Reflectance and irradating time for β-CuPc thin film at 600 nm	**65**
4.26	a.Transmittance spectra for β+ Cupc thin film with thickness (197) nm in period times . b. The Maximum Transmittance vs. irradating time for β+ Cupc thin film at 600 nm	**66**
4.27	a.Transmittance spectra for β+ Cupc thin film with thickness (197) nm in period times . b. The Maximum Transmittance vs. irradating time for β+ Cupc thin film at 600 nm	**67**
4.28	a.Transmittance spectra for β+ Cupc thin film with thickness (214) nm in period times . b. The Maximum Transmittance vs. irradating time for β+ Cupc thin film at 600 nm	**67**
4.29	a.Transmittance spectra for β- Cupc thin film with thickness (214) nm in period times . b. The Maximum	**68**

Figure No.	Subject	Page No.
	Transmittance vs. irradating time for β- Cupc thin film at 600 nm	
4.30	a. Determined Direct energy band gap for β+ ray CuPc Thin film with thickness(197)nm in period time b. The Maximum Direct energy band gap vs.Irradiating time at 600nm	**69**
4.31	a. Determined Direct energy band gap for β- ray CuPc Thin film with thickness(197)nm b. The relation between Maximum Direct energy band gap and irradiating time at 600nm	**69**
4.32	a. Determined Direct energy band gap for β+ ray CuPc Thin film with thickness(214)nm b. The relation between Maximum Direct energy band gap and irradiating time at 600nm	**70**
4.33	a. Determined Direct energy band gap for β- ray CuPc Thin film with thickness(214)nm b. The relation between Maximum Direct energy band gap and irradiating time at 600nm	**70**
4.34	Photoluminescence spectra for CuPc un radiation thin films	**74**
4.35	Photoluminescence spectra for CuPc thin films at different irradiation time of (β+)	**74**
4.36	Photoluminescence spectra for CuPc thin films at different irradiation time of (β-)	**75**

Figure No.	Subject	Page No.
4.37	XRD spectrum for CuPc Powder	**77**
4.38	XRD pattern for CuPc thin films irradiated by Plus Beta ray source (Na-22) at different irradiation time	**79**
4.39	XRD pattern for CuPc thin films irradiated by Minis Beta ray source (Sr-90) at different irradiation time	**80**
4.40	3D AFM images with different irradiating time for CuPc thin film irradiated Beta ray source (β+)	**83**
4.41	granular distribution diagrams of a surface CuPc thin films with a thickness of 214 nm and irradiated with β+ at different irradiating times	**84**
4.42	3D AFM images with different irradiating time for CuPc thin film irradiated plus Beta ray source (β-)	**86**
4.43	granular distribution diagrams of a surface CuPc thin films with a thickness of 214 nm and irradiated with β- at different irradiating times	**87**

List of Tables

Table No.	Subject	Page No.
1.1	Comparison of the Electrical Properties of the Inorganic Semiconductor Germanium and Organic Semiconductor	**2**
1.2	Properties of CuPc blue pigment	**7**
3.1	Beta Source isotopes	**37**
4.1	Optical Constants For β+ Cupc Solution	**52**
4.2	Optical Constants For β - CuPc Solution	**53**
4.3	Optical Constants for different Concentrations β+ CuPc sol	**60**
4.4	Optical Constants for different Concentrations β- CuPc sol	**60**
4.5	Optical Constants for β+CuPc thin film at thickness 197 nm	**71**
4.6	Optical Constants for β-CuPc thin film at thickness 197 nm	**72**
4.7	Optical Constants for β+CuPc thin film at thickness 214 nm	**72**
4.8	Optical Constants for β-CuPc thin film at thickness 214 nm	**73**
4.9	Energy gap obtained by Photoluminescence and Tauce method at different irradiating time of plus beta ray(β+)	**75**
4.10	Energy gap obtained by Photoluminescence and Tauce method at irradiating time Minis beta ray(β-)	**76**
4.11	The lattices constants and angels of CuPc powder Parameter	**77**
4.12	The structural parameters of CuPc polycrystalline structural powder	**78**
4.13	structure parameters of CuPc thin films irradiated β+ ray	**79**

Table No.	Subject	Page No.
4.14	structure parameters of CuPc thin films irradiated β- ray	**81**
4.15	AFM measurements for CuPc irradiated with plus beta ray(β+)	**85**
4.16	AFM measurements for CuPc irradiated with minis beta ray(β-)	**88**

List of Symbols and Abbreviations

Symbol	Description
A	Absorbance
A1	Activity of Beta ray
a	Lattice Constant
α	Absorption Coefficient
E_g	Energy Gap
C.B	Conduction Band
V.B	Valence Band
$d_{(hkl)}$	The Inter Planar Distance
λ	Wavelength
n	Refractive Index
N	Complex Refractive Index
P	Proton
n1	Neutron

Symbol	Description
ν	Neutrino
$\bar{\nu}$	Antineutrino
Na	Sodium
Sr	Strontium
r	Constant in Tauc Formula
T	Transmittance
R	Reflectance
ε_i	Imaginary Part of Dielectric Constant
ε_r	Real Part of Dielectric Constant
T	Transmittance
t	Film Thickness
UV	Ultra Violet Spectrum
XRD	X-Ray Diffraction
CuPc	Copper Phthalocyanine
PL	Photoluminescence
PDT	Photodynamic Therapy
FTIR	Furrier Transform Infrared
AFM	Atomic Force Microscope
c	Velocity of Light
FWHM	Full Width at Half Maximum
h	Blank Constant

Symbol	Description
hν	Photon Energy
IR	Infrared
k	Extinction Coefficient
LED	Light Emitting Diode
θ	Diffraction Angle
G.S	Grain Size
D	Average Crystal Size
RMS	Square Root Mean of Roughness
σ	Optical conductivity
Eg	Energy Band Gap
H_2pc	free phthlocyanine
Mpc	Metal phthlocyanine

Chapter One

General introduction

1.1 Introduction

Phthalocyanine and its metal complexes have been known in1907. The metal-free phthalocyanine was first discovered by Braun and Tchernia [1]. Copper Phthalocyanine is an organic semiconductor widely used as an optoelectronics devices as thin films[1][2]. Thin-film technologies are being developed as a means to substantially reduce the cost of electronic systems. Thin film modules are expected to be cheaper to manufacture owing to their reduced material costs [3], [4] Recently, metal phthalocyanine (MPc) complexes have been used in light emitting diodes (LEDs) [5–7], device for limiting light optically, gas sensors[8–10], biosensors, photovoltaic cells, photodynamic treatment, and semiconductor materials. In bio sensing, a copper phthalocyanine chemoresistor was utilised as a transducer [11]–[13] ,digital cameras[14][15], mobile phones, and personal computers, because of their versatility, architectural flexibility, nontoxicity, and simplicity of processing [16]. There are several potential areas in photodynamic therapy (PDT) which involves the use of phthalocyanine derivatives as photosensitizers to treat various diseases, such as psoriasis and cancer [17][18][19][20] Colorful phthalocyanines can withstand a wide range of chemical and thermal conditions without losing their quality [21].

1.2 Organic Semiconductors

Semiconductors are significantly used in modern electrical devices. For the most part, they may be separated into inorganic and organic semiconductors. Despite the widespread usage of inorganic semiconductors like germanium and silicon in electronics, organic semiconductors are likely to take their place in the near future. The following Table(1.1) offers a comparison between the properties of an a conventional semiconductor (Germanium) and an organic semiconductor.

Table 1.1: A Contrast of comparing the Electrical Properties of the Inorganic Semiconductor Germanium with those of the Organic Semiconductor Gallium Arsenide [5]

Properties	**Inorganic**	**Organic**
Mobility(cm^2/sec)	3900	0.02
Carrier concentration(cm^{-3})	2.5×10^{13}	8×10^{7}
density (gm/cm^3)	-	10^{12}-10^{14}
Resistivity (ohm.cm)	43	10^{14}
Band gap (eV)	0.67	3.02

More research is being done on organic semiconductors as a potential replacement for some inorganic semiconductors. Organic semiconductors are organic compounds that show the characteristics of semiconductors. Most organic semiconductors are composed mostly of carbon and hydrogen atoms [22]. The molecules in an organic crystal are held together by weak Van der Waals interactions, which result in low melting points and electronic conductivities. The sensitivity of organic molecules to physical and chemical changes encouraged the usage of the organic semiconductors for bio-sensing applications [23]. The use of

organic thin film interfaces in organic based solar cell architectures can significantly increase the occurrence of fast charge transfer rate at the interfaces and hence achieve higher quantum efficiency. Organic semiconductors owe their semiconducting properties due to presence of conjugated double bonds in their molecular structure[24]. Carbon atoms, forming conjugated double bonds, are sp^2 hybridized and give rise to both σ- and π-bonds, whose energy levels are split into occupied bonding orbitals with a lower energy and unoccupied anti-bonding orbitals of higher energy [25]

Conjugated double bonds, which are present in the molecular structure of organic semiconductors, are responsible for the molecules' ability to behave as semiconductors [26].

1.3 Phthalocyaninces ,*MPc* , *Pcs*

Phthalocyanines are a type of very stable organic semiconductors that have garnered a lot of interest due to the fact that they are quite inexpensive and have a minimal risk of poisoning [27][28]. It has a vivid blue-green hue. Phthalocyanines are attracting a lot of interest because of their potential usage in organic electronic devices as an active layer[29]. The first phthalocyanine was produced accidentally in 1907[30]. The word phthalocyanine comes from a combination of two Greek terms that specify exactly the properties of The color of this material. This is cyanide and naphtha, often known as rock oil (dark blue)[31]. The blue dye has been known for many years. Pcs are porphyrin derivatives with high symmetry, planarity and electron de-localization, with four nitrogen atoms at the meso positions of the aromatic rings attached to the pyrrolerings in coplanar position[32]. The term 'Phthalocyanine' was first used by L instead to describe this particular class of compounds. Phthalocyanines are aromatic hydrocarbons exhibiting semiconducting properties, which come under the class of organic

semiconductors[33]. They are known as phthalocyanins, or phthalocyanins. It was first synthesised by Braun and Tcherniac, and subsequent research has focused on the unique properties of phthalocyanine [34]. It is anticipated that their commercial usage in the production of semiconductor devices would have substantial repercussions throughout this decade due to the fact that they are projected to have these implications[35]

The phthalocyanine (H_2Pc) that does not include any metals ($C_8H_4N_2$) $4H_2$ has the chemical formula $C_{32}H_{18}N_8$ Aza nitrogen atoms join together four identical isoindole units, and in the centre there are two hydrogen atoms linked together[36]. The phthalocyanine polymers are becoming one of the most researched of all organic functional materials and have lately gained a great amount of attention owing to the fact that they are both thermally and chemically stable[37]

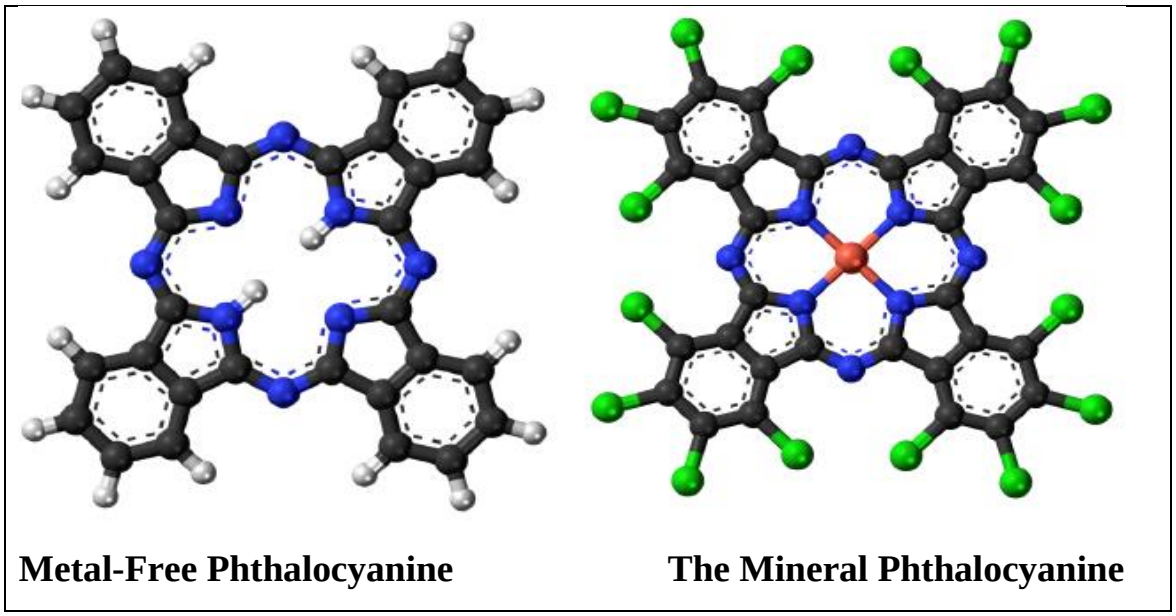

Figure (1.1): Structure of mineral and non-mineral phthalocyanine at the molecular level [38]

One of the most promising organic semiconductors for use in solar cells, nonlinear optics, electro-catalysis, and other photo-electronic devices is metal phthalocyanine (MPc) [39]. cancer photodynamic therapy (PDT)

photosensitizers are also known to have potential such that they can absorb far-red light, which has stronger tissue penetration qualities, as well as photosensitize singlet oxygen to a suitable degree. For the most part, metal phthalocyanine (MPc) films that are vacuum-sublimed are p-type semiconductors[40]

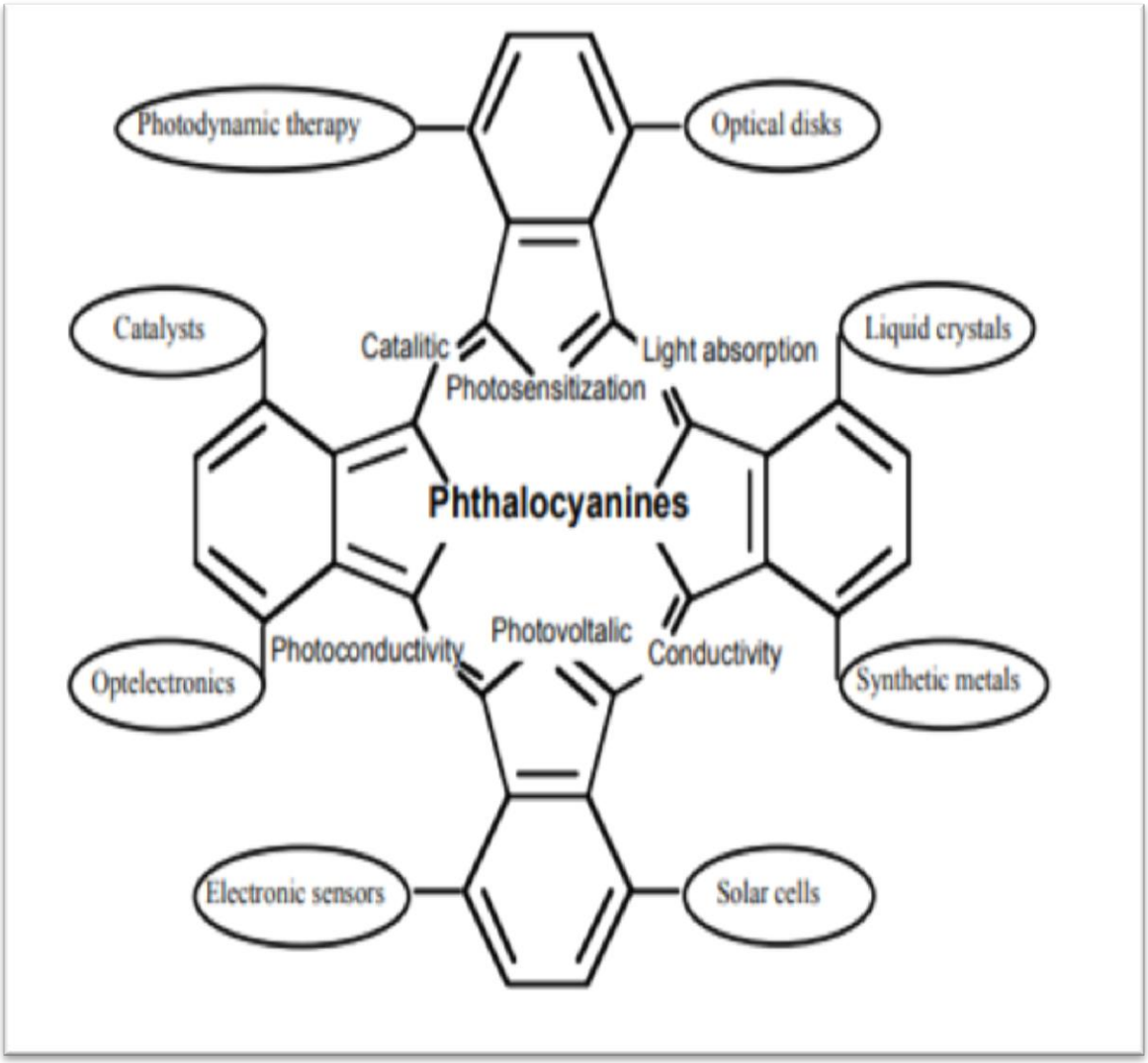

Figure (1.2): Typical function of phthalocyanine derivatives [41]

1.4 Copper *Phthalocyanine*

Copper phthalocyanine ($C_{32}H_{16}N_8Cu$) belongs to a group of compounds that are the simplest its molecules are the hydrogen molecule (H_2), which occupies the central position. Other types of Phthalocyanins in the presence of transition metals other than copper, such as Fe, Co, Ni, Zn, and Mg[42]. Figure (1-3) depicts the copper-substituted phthalocyanine structure.

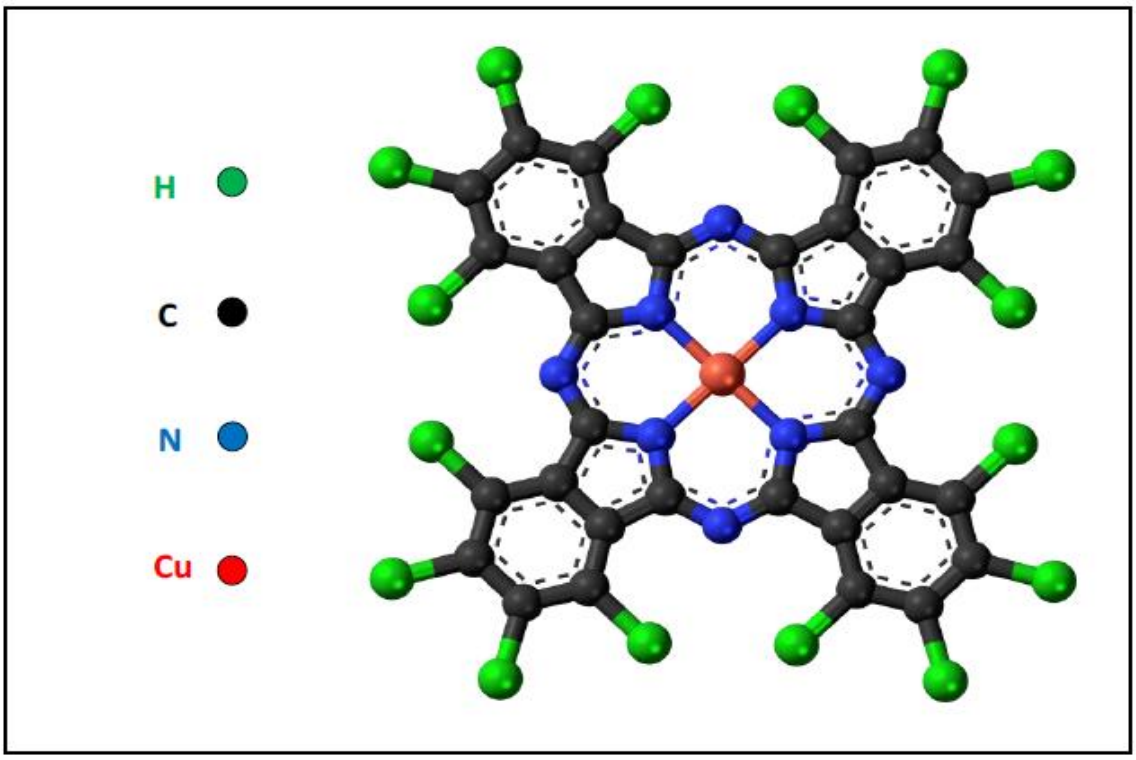

Figure(1.3):Diagramming the copper phthalocyanine's molecular framework (CuPc)[43]

Copper phthalocyanine is capable of forming crystalline structures; meaning that it is possible to define a unit cell. Several unit cells have been discovered for phthalocyanines with the most common phases labeled as α- and β-phase. The unit cell can have multiple copper phthalocyanine molecules that form the basis of the crystal structure so that it includes hundreds of atoms[44]. The basis of an inorganic crystal is the smallest physical unit of the system and is defined as the smallest set of atoms which can be transposed linearly determined by a set of

vectors such that the crystalline pattern can be produced [45] Typically, the basis of inorganic crystals is composed of a relatively small set of atoms.

Copper-phthalocyanine (CuPc) is one of four macrocyclic compounds in the CuPc family, each containing four isoindole units linked by four nitrogen atoms and containing an ion of copper II. There are several electrical properties emitted by the metal at the molecule's centre. The conductivities of these molecules range from (10^{12}- 10^{-14} s/m) for all of them. CuPc has an optical gap of and a molecular weight of 576.08 g/mol (1.7 ev) Around (3500 C)[43] , it's a reasonably stable molecule that begins to evaporate. Some polymorphic phases have been found, two of which are known as and respectively

Organic crystalline solids, such as copper phthalocyanine, have a basis composed of multiple molecules which includes hundreds of atoms. Copper phthalocyanine, a non-polymeric organic system, has a basis with which the molecules are bonded together by Van der Waals forces[46]

Table(1.2) :Properties of CuPc blue pigment

Name	Copper Phthalocyanine
Molecular Structure	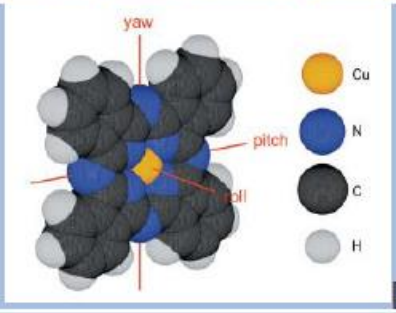 [25]
Molecular Formula	$C_{32}H_{16}CuN_8$
Molecular Weight	576.08
Melting Point	600 °C (dec.)
Water Solubility	<0.1 g/100 mL at 20 °C
Crystal system	Triclinic (anorthic)
Cell Parameters	a= 12.88600 Å, b= 3.76900 Å, and c= 12.06100 Å, α= 96.220°, β= 90.620 °, and γ= 90.320 °
Density	1.64300 g/cm³

In most pigment-consuming industries, it is used to create blue hues because of its strong general resistance to organic solvents [47]. (Cu-Pc) is an organic semiconductor with a positive charge. Furthermore, this material is very stable both thermally and chemically. One of the most significant colourants, it has exceptional features such as light fastness, resistance to alkalis and acids with tinting power [48].

There are many remarkable properties of copper phthalocyanine (CuPc), which was produced as the first derivative[49]. Insoluble in conventional solvents and polymer melts because CuPc is nonpolar, polycyclic, and planar. In contrast, the solubility of concentrated acids is affected. CuPc may be employed in high-temperature procedures because of its strong thermal stability (it sublimes at -550 C)[50].

Compound sensors [51], catalysis [52][53], optical plates, xerography [54], non-directional optics [55], photovoltaic cells, and photo sensitizer for photodynamic therapy are just a few of the many uses for copper phthalocyanine blue[56]. Because of its utility in mechanical supplies, such as the capacity to structure, the very stable metal intricacy with metal cation, and the force brightness and perfection of colours, copper phthalocyanine amalgam is being examined by a large scientists.

1.5 *Literature Survey*

In (2010) , Priyanka. S et al . [57] measured Various MPcs thin films, including CuPc, have different optical characteristics. The relationship between refractive index (n), extinction coefficient (k), real and imaginary parts of the complex dielectric constant, and reflectivity (R) and energy (E) was addressed, and it was found that these values fluctuate significantly with E. The biggest energy gap (Eg) was found in CoPc and MnPc with 3.25 eV, while the lowest Eg was found in CuPc with 2.71 eV.

In (2012) , Sawanta S. Mali et al. [58] studied Copper phthalocyanine (CuPc) thin films of various thicknesses were produced on glass substrates . Grazing angle XRD diffraction was used to investigate structural characteristics. The metastable and stable polymorphic variants are the most common. Both variants have the same inter planar distance (3.4 A°). The angles of the molecules in regard to the vertical axis of the column are 26.50 for the α -form and 2500 for the β -form, respectively, while the lattice parameters are a = 23.9 and b = 3.8 A °for the α-form and a = 19.4 and b = 4.79 A° for the β -form. X-ray measurements were also performed on CuPc thin films with diameters of 27, 45, and 85 nm. Fourier transform infrared spectroscopy was used to investigate vibrations (FT-IR).

In(2013) , Jaehyun .L et al .[59] Zinc (Zn), copper (Cu), and cobalt (Co) were used to create new phthalocyanine (Pc) derivatives with an alkyl group in the ligand .UV-Visible (UV-Vis) spectroscopy and photoluminescence (PL) spectroscopy were used to explore the optical properties of the new phthalocyanine derivatives with a different core metal. 2H, Co, Cu, and Zn complexes had maximal UV-Vis values of 708 nm, 677 nm, 686 nm, and 684 nm, respectively.

In (2015), Ali H. Jalaukhan [60] studied Thin films of Copper Phthalocyanine (CuPc) with thicknesses of around 200 nm were formed on glass substrates using the thermal evaporation method at 303^0 K and 403^0 K substrate temperatures (Ts) and pressures more than 10^{-5} mbar. The effect of substrate temperature on several physical properties of CuPc thin films, such as optical qualities in the visible range, was the focus of this research. Optical characterization was performed at room temperature utilizing absorption spectra in the 200-900 nm band at normal incidence. Absorption and extinction coefficients vary with wavelength and they increase with increasing of substrate temperature. Refractive index in the range 325 – 425 nm increase with increasing substrate temperature. Increase in substrate temperature indicating better crystallinity of films deposited at higher substrate temperature. It is found that the optical band gap decreases from 3.29 eV for the film deposited at 303 ^{o}K to 3.23 eV for film deposited at 403 ^{o}K.

In (2016) , Haneen A. hussien[61] studied phthalocyanines thin films with the same thicknesses (100) nm were formed on glass at room temperature . The moidoactive sources Co-60 average energy(1.24 Mev) and Am-241 energy irradiated a Pc thin film with gamma rays (60keV). The Pc thin films have a direct energy gap (Eg) for all samples, according to UV-vis spectra. Also determined were optical constants including absorption coefficient, refractive index, extinction coefficient, and dielectric constant. The traps inside the energy gap play a vital role and have an effect on optical behavior, the average crystal size(354.22nm) was estimated by XRD while the roughness (1.0324nm) was determined by AFM (Co-60,1.25Mev). However, for low energy Gamma rays, the average crystal size of Pc thin films (405.525nm) was estimated by XRD and the roughness (0.9144nm) was determined by AFM (Am-241,60Kev)

In (2016), Ashok .D et al . [62] studied Copper phthalocyanine powder is made in the lab using a chemical technique that involves phthalic unhydride and urea. UV-Visible characterisation spectra are studied using spin coated Copper phthalocyanine films. UV-Vis spectra are used to calculate the energy band gap. The current findings demonstrate that the films before and after annealing have a direct allowable energy gap of 2.6 eV. The Soret band, which is a feature of metal phthalocyanines, is used to compute these values. For pristine film, the energy gap is projected to be 1.6 eV, whereas for annealed film, it is estimated to be 1.7 eV.

In (2017),Divya K. Nair et al .[63] used Copper phthalocyanine is produced and studied as a source material for γ-radiation dosimetry. Up to a certain point, the optical characteristics of copper phthalocyanine showed a linear response to γ-radiation. Both active channels have a thickness of around 200nm. XRD analysis revealed that both phthalocyanines are of β -form. Regarding the topological study, it provides that CuPc is crystalline in nature whereas ZnPc is amorphous in nature. From optical characterization, it is investigated that maximum absorption is at Q band (690nm) for both the films. Also activation energy is calibrated as 1.95eV for copper phthalocyanine whereas for ZnPc, it is found as 1.3eV. It is proposed that a linear relationship of absorbance for the various radiations can make ZnPc and CuPc a potential candidate for radiation dosimeter.

The presence of a diffraction peak at 6.70° in the CuPc spectra corresponds to the (100) diffraction of β-form crystal at the stable crystal form. The diffraction peak's lattice spacing is found to be $12.7A^0$, indicating that the distance between the planes of the copper atom in the subsequent layer is $12.7A^0$.The crystallite size obtained for a sample was around 42-52nm.

In (2018) , Sahar. N Rashid et al. [64] studied, Thin films were coated on glass substrates using the (Spin Coating) technique in a convection oven at (600°C) for one hour, and then subjected to beta radiation for various durations of time (15, 30, 45, 60, 75, and 90 minutes). To explore the influence of beta radiation on created thin films, the optical characteristics of thin films were tested before and after irradiation. The thin films' optical tests revealed that they have generally high transmittance, while their absorbance and reflectance decrease as the irradiation time increases. The results showed that extending the length of beta irradiation increased the energy gap values of these thin films. The optical constants were decreased, including refractive index, extinction coefficient, dielectric constant, and imaginary dielectric constant

In (2020),[Mohamed H. Eisa] [65] studied thin films, in which a Sr-90 radioisotope beta radiation was delivered for varied durations to the thin films. Furthermore, the optical absorption and transmission were studied using the UV–Visible technique before and after irradiation for 24, 72 and 120 h .The energy band gap (Eg) has a range of 2.51 to 3.41 eV, depending on the action of beta radiation. Absorption coefficients increased after irradiation and showed the highest value at 4 eV, after irradiation for 120 h, whereas optical band gaps decreased before irradiation is 3.41eV and after irradiation is 3.20eV, 2.77eV and 2.51eV for 24, 72 and 120 h, respectively.

In (2021), Reem R. Mohammed et al [55] studied Copper Phthalocyanine CuPc thin films of 150, 300, and 450 nm thickness. The optical absorption spectra of CuPc thin films reveal two bands of absorption, one in the visible range at roughly 635 nm, known as Q-band, and the other in the ultra-violet region at 330 nm, known as B-band. CuPc thin films exhibit a straight band gap of roughly (1.81 and

3.14) eV. Fourier transform infrared spectroscopy was used to carry out the vibrational studies (FT-IR)

In (2021),Laith .S et al [66] On soda glass substrates, thin films of copper phthalocyanine CuPC with various thicknesses (200,215,235,255 nanometers) were produced. The film was thermally treated (vacuum-annealed) with different annealing temperatures (300,373,473K^0) in order to evaluate the effect of the annealing temperature on the optical properties of this film, which has a thickness of 255 nm. As the thickness of the thin film increases, the value of the optical band gap decreases. Furthermore, at annealing temperatures of 300 and 373 K, the optical bandgap lowers and increases (473 K^0). The absorbance and extinction coefficients change with wavelength, increasing with thin film thickness and annealing temperature (300,373 K) and decreasing with wavelength (473 K). The optical band gap shrinks as the thickness of the films thickens and as the annealing temperature rises

1.6 Aim of the Work

1) Study the effect of nuclear Beta rays on the optical properties of copper Phthalocyanine (CuPc) Solutions and Thin Films
2) Distinguishing irradiation with plus and minus beta rays on CuPc material
3) Control in energy band gap of (CuPc) Thin films by using Beta irradiation

Chapter TWO

Theoretical part

2.1 Introduction

This chapter concentrate on the theoretical details about measurements technology of the thin films such as optical , surface morphology, structural properties

2.2 Beta ray

Electrons emitted from the nucleus of a decaying atom are known as beta particles. Beta particles can penetrate the dead skin layer and cause burns, even if they can be blocked by a thin sheet of aluminum.[67]

Beta decay is a form of radioactive decay in which β- or β+ particles are emitted.

Beta-radiation is unstable nucleus that may attain a more stable configuration by emitting a β-particle. In this process a neutron in the nucleus is transformed into a proton and an electron.[68]

The β-particle emission can be written:

$$^{A}_{Z}M \rightarrow {}_{Z+1}{}^{A}D + \beta + \nu \qquad (2.1)$$

M= original (parent) atom ,D = new (daughter) atom, β= beta particle

ν= neutrino,

Neutrinos and antineutrinos are neutral particles with a zero or very small mass. energy spectrum of β- radiation is continuous

2.2.1 Beta Minus Decay(β-)

An energetic electron makes up beta-minus (β) radiation. It is more ionizing than alpha, but not as much as gamma. A few centimeters of plastic or a few millimeters of metal can suppress beta rays from radioactive decay. When a neutron decays into a proton in a nucleus, the beta particle and an antineutrino are released. Natural beta radiation is significantly less energetic and penetrating

than beta radiation from linear particle accelerators. It is occasionally used to treat superficial cancers with radiation.[69]

When the neutron to proton ratio is too high, a neutron "transforms" into a proton and electron, with the electron being ejected from the nucleus. The ejected electron is called a “beta minus particle” or just "beta particle" The generalized atomic equation for beta decay is as follows: [69]

$$n = p + e^{-} + \bar{\nu} \qquad (2.2)$$

e=beta particle (electron) , $\bar{\nu}$ = anti neutrino

2.2.1.1 Radioactive Strontium (Sr-90)

Radioactive strontium-90 is formed by uranium and plutonium fission. The splitting up of the nucleus of a radionuclide into smaller pieces is known as fission[70]. Large quantities of radioactive strontium-90 were generated during atmospheric nuclear weapons testing. The eventual result of each Sr-90 decay is two betas. Because the daughter product, Y-90, has a much shorter half-life than the parent, Sr-90, These two beta decays are thought to be in secular equilibrium and occur at the same time. Sr-90 decays into Y-90 when it produces a beta particle with a maximum energy of 0.546 MeV and an average energy of 0.18 MeV. After Y-90 undergoes beta decay, zirconium-90 is produced, with a beta energy of 2.28 MeV and an average beta energy of 0.92 MeV as shown in Figure (2.1) [71]

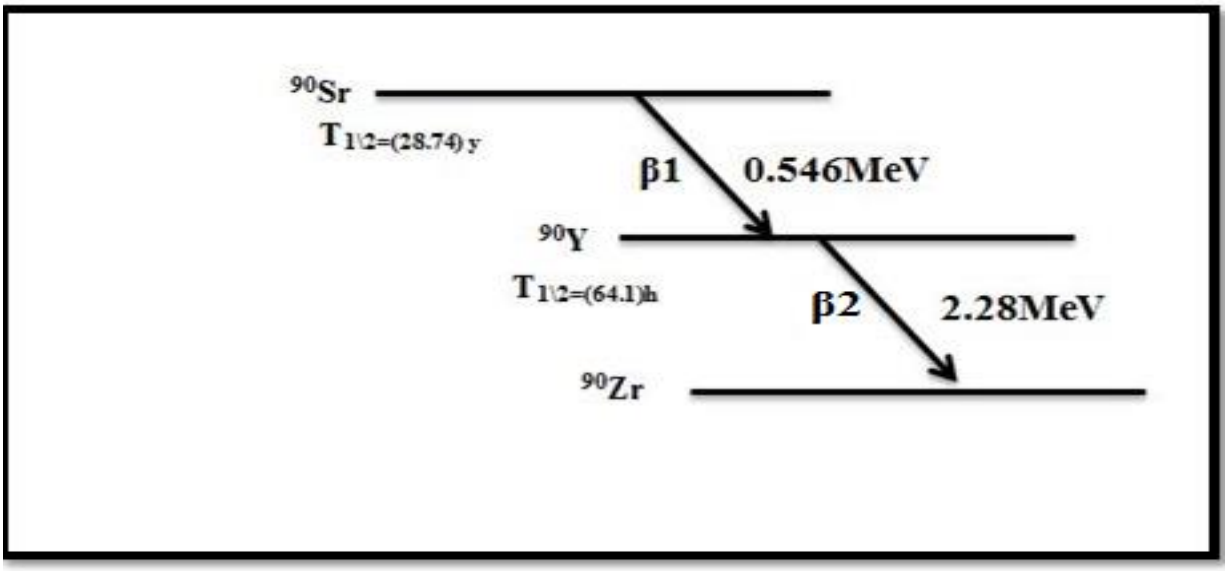

Figure (2.1): Scheme of Sr-90 decay[72]

2.2.2 Positron/Beta Plus Decay(β+)

The emission of positrons, the antiparticle form of electrons, is known as beta-plus (+) radiation. When a positron slows down to the same speed as electrons in a material, it will destroy an electron, generating two 511 keV gamma rays in the process.

When the neutron to proton ratio is too low, a proton transforms into a neutron and a positron (beta plus particle), and the positron is ejected from the atom.

A positron is an electron antiparticle with the same rest mass as an electron but the opposite electric charge sign.

The positron has an elementary particle that does not enter into the formation of ordinary matter and is not found free, nor in the nucleus of an atom and a neutron, the anti-electron particle or the anti-electron. It corresponds to the electron in all valid physical properties, except for the electric charge. The load of the positron carries a positive electrical charge equal to the charge of the electron, but unlike the electron it carries a negative electrical charge. In the

event of a positron collision with an electron, the annihilation of an electron-positron occurs, which means that they are transformed into two gamma rays. A body that converts to energy and appears in the form of two electromagnetic waves of the same frequency[73][74]

$$p \rightarrow n + e^{+} + \nu \qquad (2.3)$$

2.2.2.1 Radioactive Sodium (Na 22)

Na22 is a man-made isotope with a 2.6-year half-life. Its nuclide is produced by cosmic rays by spalling out argon, which is a component of the atmosphere (with a ratio of 0.93). It decays into stable neon-22 by generating a positron (β + decay). With a β + branching ratio of roughly 90 percent, Na22 decays to Ne-22* the excited state. After 3.7 ps, a γ- photon with a mass of 1274 keV emits, bringing Ne22 to its ground state. This photon arrives shortly after the positron emission, allowing it to be used to track the positron's birth. Because the β -decay reaction is a two-particle event, the positrons emitted by Na 22have a wide energy range, ranging from virtually zero to 545 keV [75], A simplest scheme of Na-22 decay shown in Fig. (2.2)

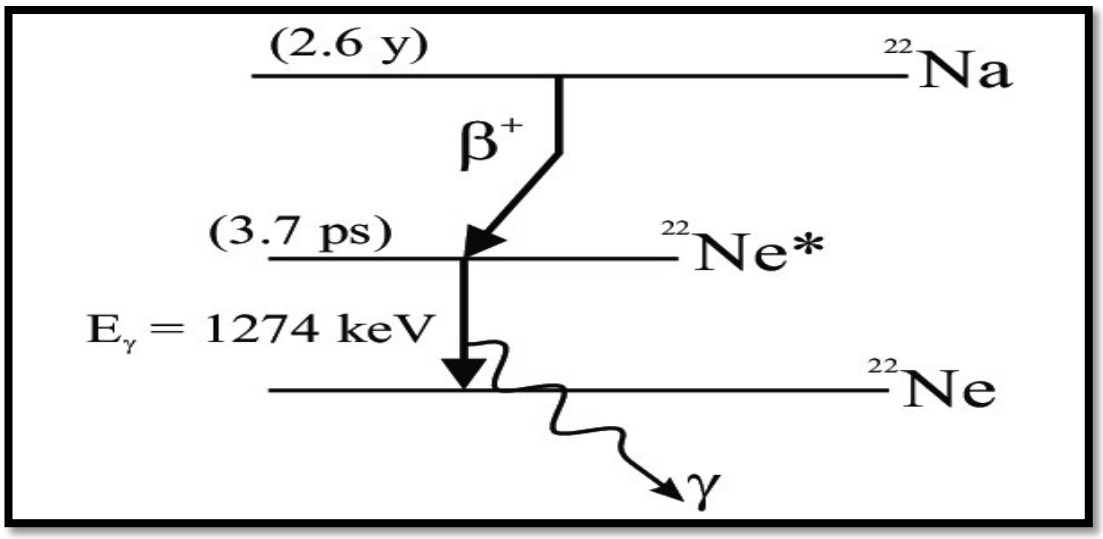

Figure (2.2): shows scheme of Na-22 decay

2.3 Optical Properties

Organic semiconductors are more suitable as a significant material in the fields of electronics and optoelectronics. Because of its optical uses in the field of organic light-emitting devices (OLEDs), phthalocyanines have gotten a lot of attention recently.[76]

for use with flat-panel displays One of the generality direct approaches to delve into the band structure of organic semiconductors is to analyze optical characteristics. Spectroscopic studies of metal-substituted phthalocyanines reveal important details regarding their electronic processes. Charge transfer transitions between the central metal ion and the phthalocyanine ligand reveal an electronic overlap between the centrally substituted metal ion and the phthalocyanine ring, indicating substantial interaction between the two electronic systems. Between 300 and 1000 nm, charge transfer transitions account for a large fraction of the measured spectra.[77]

2.3.1 FT-IR Emission

The wavelength and intensity of an object are measured using infrared spectroscopy. Infrared spectra, bending, turning, and vibrational motions of atoms in a molecule all twist. Two types of molecular vibrations can be used to characterize all of the motions. A stretch is one sort of vibration that causes a change in bond length. A stretch is a rhythmic movement along the atoms' line of contact.[78] .A bend, the second form of vibration, causes a change in bond angle. Stretches can be symmetrical or asymmetrical in nature. Bending can take place in the molecule's plane or out of it, as seen in Figure (2.3) . The intensity of light striking the detector is measured as a function of mirror position, then Fourier-transformed to give an intensity vs. mirror position diagram wave number is shown in figure (2.4).

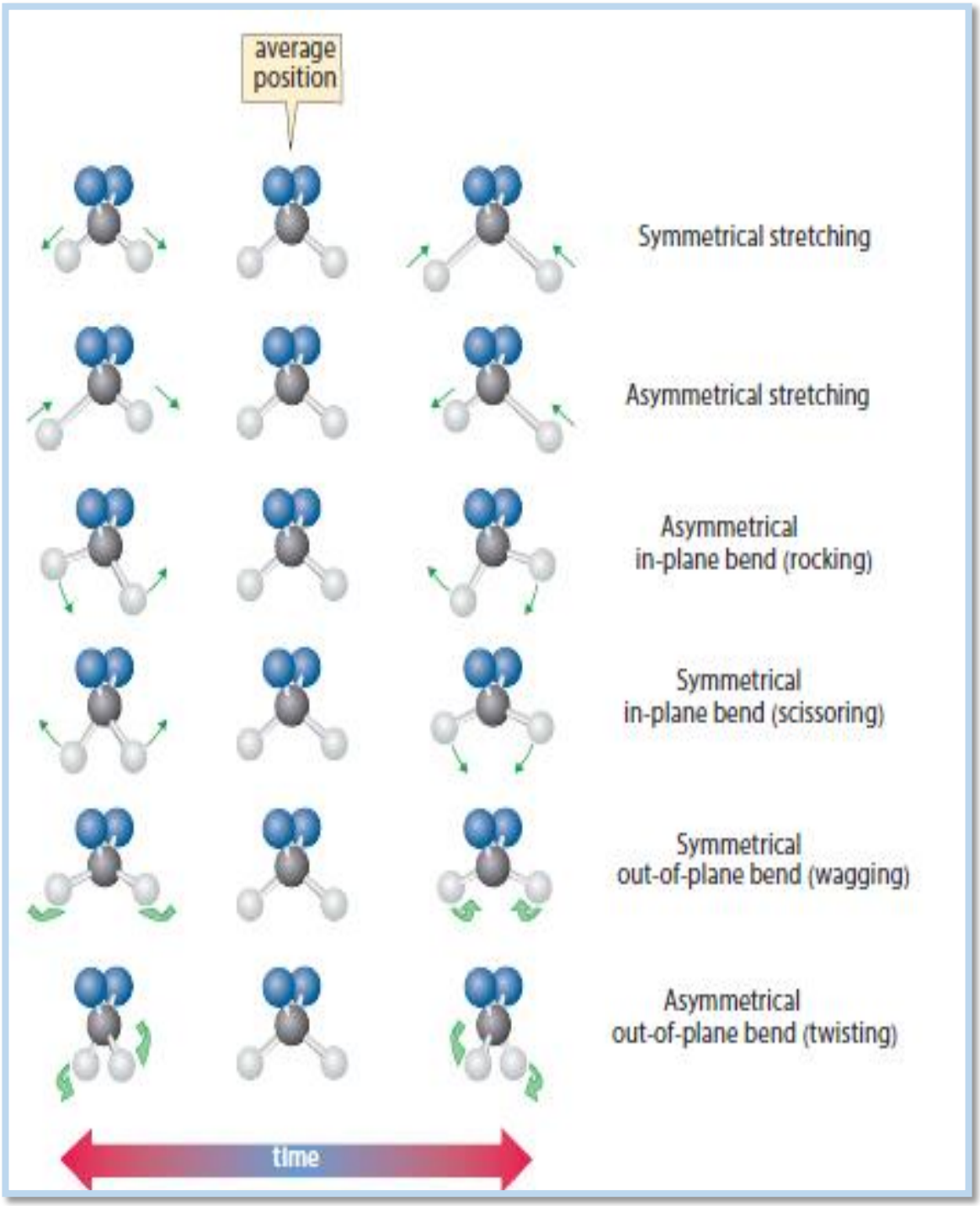

Figure (2.3): Oscillations observed in diatomic molecules[79]

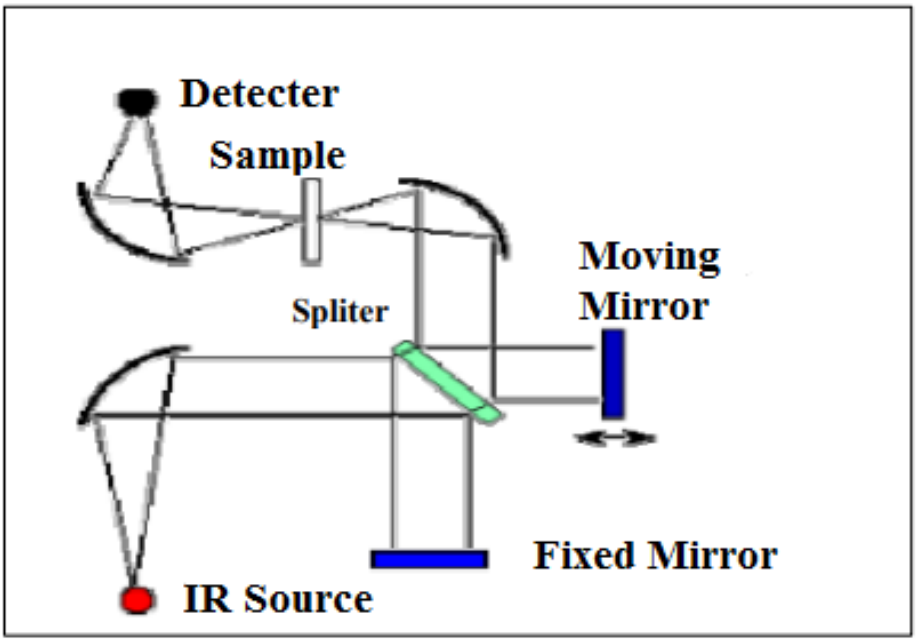

Figure (2.4): Schematic Representation of FT-IR Spectrometer[80]

2.3.2 Optical Properties of Semiconductors

Optical properties are significant because they give a useful method for identifying materials and are responsible for certain of their properties. The new occurrences and their implications for the photophysics of organic semiconductor materials packed in a solid, as well as molecular interaction. Except that the electronic and vibrational transitions occur at longer wavelengths, the absorption spectra is comparable to that of solitary molecules. The weak Van-Der-Waals forces that hold organic molecules together are the source of these optical features. [50] The most essential absorption process is fundamental absorption, which includes electrons transitioning from the valence to the conduction band [81] The absorption coefficient is between 10^5 and $10^6 cm^{-1}$. The band edge in semiconductors is caused by a rapid decline in the absorption coefficient on the high-energy side of the absorption band.

Absorption is a phenomenon of basic relevance because of its connection to the dynamics of the medium's electrons and ions under the impact of electromagnetic radiation. One of the advantages of organic semiconductor materials is their high absorption coefficient in the visible region of the electromagnetic spectrum, because this high absorption coefficient means that only a thin film is required to absorb the majority of incident light, which is an appealing feature for applications because it requires less material to manufacture them[82]

The frequency dependence of the absorption can be used to calculate the material's energy gap [18]. When the photon energy (hv) is equal to or greater than the energy gap (Eg), the photon can interact with a valence electron, elevating it into the C.B. and forming an electron–hole pair. The incident photon's maximal wavelength (λm) that forms the electron–hole pair is specified as[83] :

$$\lambda(\text{nm}) = \frac{hc}{E_g} = \frac{1240}{E_g(\text{eV})} \qquad (2.4)$$

Where λ is the wavelength of the incident radiation, h blank constant ,c light velocity in vacuum . The intensity of the photon flux decreases exponentially with distance through the semiconductor according to the Lampert equation[84]

$$I = I_0 e^{-\alpha t} \qquad (2.5)$$

Where α is the absorption coefficient I_o and I are the incident and the transmitted photon intensity respectively which is defined as the relative number of the photons absorbed per unit distance of semiconductor, and t is the thickness of the material[85] .

There are two types of the optical transitions, as illustrated in Fig.(2.5) and we will discuss them below:

2.3.2.1 Direct Transitions

When the incident photon's energy surpasses the material's band gap energy (Eg), one electron is stimulated from the valence band to the conduction band. Direct transitions include only photons, while indirect transitions involve both photons and phonons.

Figure (2.5a) shows a direct optical transition near the basic absorption edge of a semiconductor

At k = 0, the valence band maximum and the conduction band minimum emerge in the Brillouin zone at the same time. A vertical transition (also known as a direct transition) from the valence band's top state to the conduction band's k = 0 state includes the smallest energy difference and hence corresponds to the absorption edge**.**

The optical band gap can be determined using Tauc relation [86]

$$\alpha h\nu = B(h\nu \pm E_g)^{r} \qquad (2.6)$$

where h is Planck's constant, ν is frequency, B is constant which depends on the type of material while r depends on the type of transitions. The direct transition can be divided into allowed and forbidden transition[87]

2.3.2.1.1 Allowed Direct Transition

The transition which happens between the top of the valence band and bottom of the conduction band when the change in the wave vector equals zero $\Delta k = 0$. In this form of transition, the exponential value r in Equation (2.6) becomes 1/2 [87].

2.3.2.1.2 Forbidden Direct Transition

The forbidden direct transition happens between states of the same wave vector, but the wave vector does not equals zero. In this transition type, the exponential value r in Equation (2.6) becomes 3/2[87]

2.3.2.2 Indirect Transitions

In indirect transition there is a large momentum difference between the points to which the transition takes place in valence and conduction bands, this means that the conduction band minima are not at the same value of K as the valence band maxima, then, assistance of a phonon is necessary to conserve the momentum, therefore :[88]

$$h\nu = E_g \mp E_p \qquad (2.7)$$

Where E_p is the energy of an absorbed or emitted phonon. For an allowed indirect transition, the transition occurs from the top of the valence band to the bottom of the conduction band as shown in Figure.(2.5c)

While, the forbidden indirect transitions occur from any point near the top of V.B. to any point other than the bottom of the C.B., as shown in figure.(2-5d) [89]

Experimentally it is possible to differentiate between direct and indirect processes by the level of the absorption coefficient (α); α takes values from 10^4 to 10^5 cm^{-1} for direct transitions and 10 to 10^3 cm^{-1} for indirect transitions at the absorption edge[89]

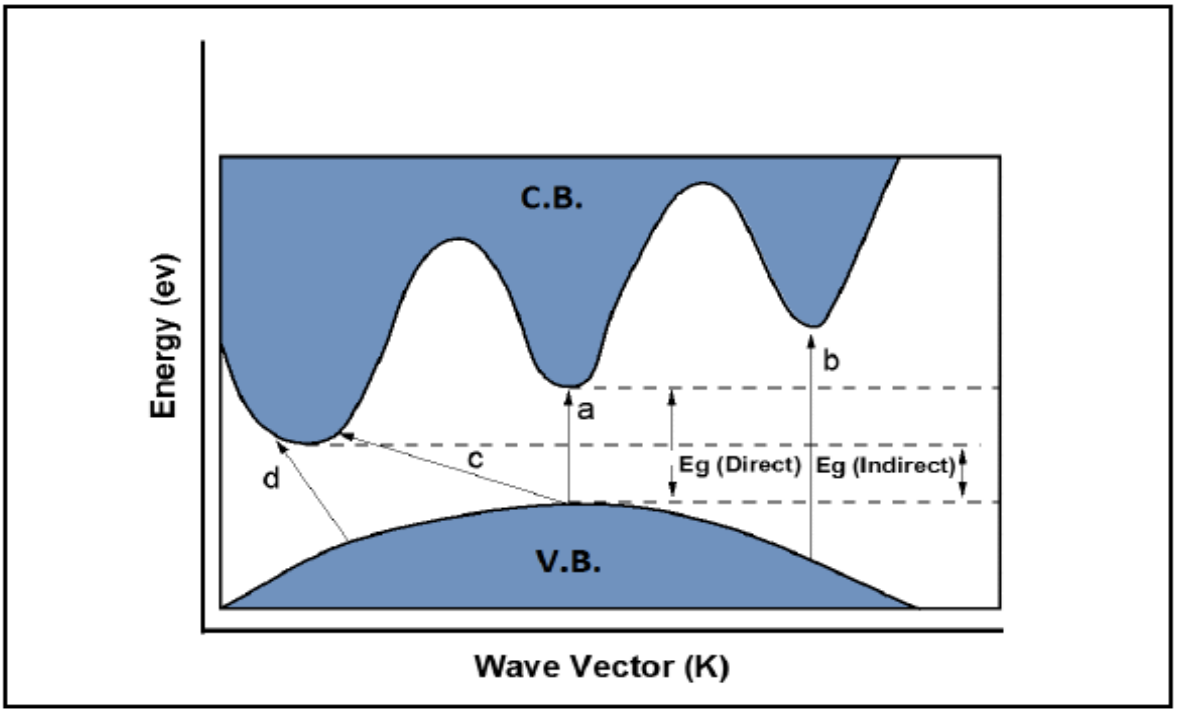

Figure (2.5)The Optical Transition (a) Allowed Direct Transition(b) The Forbidden Direct Transition ; (c) Allowed Indirect transition (d) The Forbidden Indirect Transition[90]

2.4 Optical Constants

Optical parameters are extremely essential since they characterize the optical behavior of materials. The absorbance and reflectance data can be used to calculate the optical constants of(CuPc) phthalocyanine thin films[91]. The material's absorption coefficient (α) is a significant function of photon energy and band gap energy, is given by [87]

$$\alpha = 2.303 \ \frac{A}{t} \qquad (2.8)$$

Where A is the absorbance and t is the sample thickness

Optical constants included refractive index (n), extinction coefficient (k), and real (εr) and imaginary parts (εi) of dielectric constant.

The extinction coefficient represents the attenuation of incident photon energy on the material for a unit thickness, and the absorbance processes are the

primary cause of this attenuation[92], which is connected to the exponential decay of the wave as it passes through the medium, is defined as the following [93]

$$k = \frac{\alpha\lambda}{4\pi} \quad (2.9)$$

The complex refractive index (N) is defined as[94]

$$N = n - iK \quad (2.10)$$

and it is related to the velocity of propagation in matter (v) and light velocity in space (c), as shown below:

$$N = c/v \quad (2.11)$$

The refractive index value can be calculated from the following equation [95]

$$n = \sqrt{\frac{4R}{(1-R)^2} - K^2} + \frac{1+R}{1-R} \quad (2.12)$$

Where R is the reflectance, and can be expressed by the relation[93]:

$$R = \frac{(n-1)^2 + k^2}{(n+1)^2 + k^2} \quad (2.13)$$

The real and imaginary part of dielectric constant can be calculated by using the following equations[96]

$$(n - ik)^2 = \varepsilon_r - i\varepsilon_i \quad (2.14)$$

Where

$$\varepsilon_r = n^2 - k^2 \quad (2.15)$$

And

$$\varepsilon_i = 2nk \quad (2.16)$$

The optical conductivity is calculated using the following equation:

$$\sigma_{op} = \frac{\alpha nc}{4\pi} \quad (2.17)$$

Where c is the speed of light.

2.5 Photoluminescence Spectrum

The direct electron transition from the lower vibrational of singlet excited state to lower energy level is called ”fluorescence” as shown in Figure(2.6)

Once a molecule is excited by absorption of a photon,it can return to the ground state with emission of fluorescence[97]. It involves using a beam of light, that excites the electrons in molecules of certain compounds and causes them to emit light; A complementary technique is absorption spectroscopy.

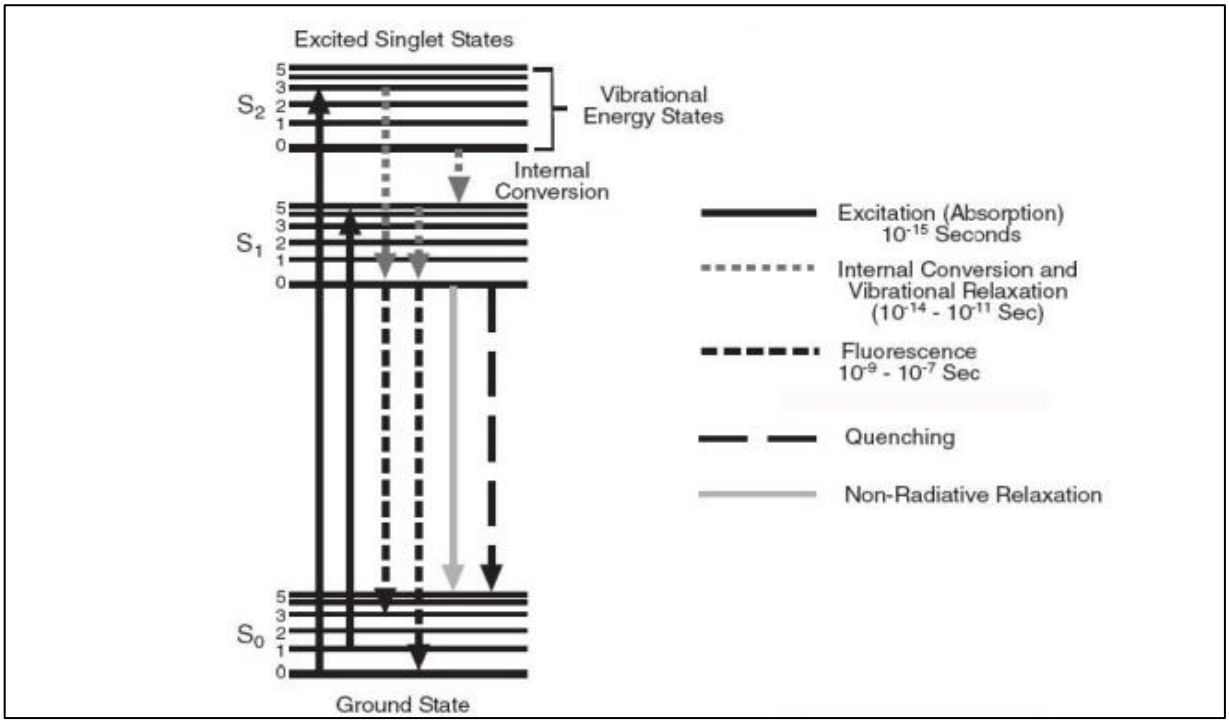

Figure (2.6) Representation of the energy transfer involved in the process of fluorescence (Jablonski diagram) [98]

Fluorescence in MPc is usually short lived, of the order 10^{-8} s. Pc fluorescence emission spectra are at longer wavelengths than the absorption spectra .Minimal rearrangement of the atomic coordinates of standard Pcs on photo excitation results in small Stokes shifts[99] . The fluorescence lifetimes of MPcs are usually of the order of a few nanoseconds. As a result of the lower energy emitted photon, Pc fluorescence emission spectra are at longer wavelengths than

the absorption spectra figure (2.7), where the difference in spectral position is known as the Stokes shift. Minimal rearrangement of the atomic coordinates of normal Pcs on photoexcitation results in small Stokes shifts . Two general types of instruments exist: filter fluorometers that use filters to isolate the incident light and fluorescent light and spectrofluorometers that use a diffraction grating monochromators to isolate the incident light and fluorescent ligh[100] Both types use the following scheme the light from an excitation source passes through a filter or monochromator, and strikes the sample. A proportion of the incident light is absorbed by the sample, and some of the molecules in the sample fluoresce. The fluorescent light is emitted in all directions. Some of this fluorescent light passes through a second filter or monochromator and reaches a detector, which is usually placed at 90° to the incident light beam to minimize the risk of transmitted or reflected incident light reaching the detector [101]

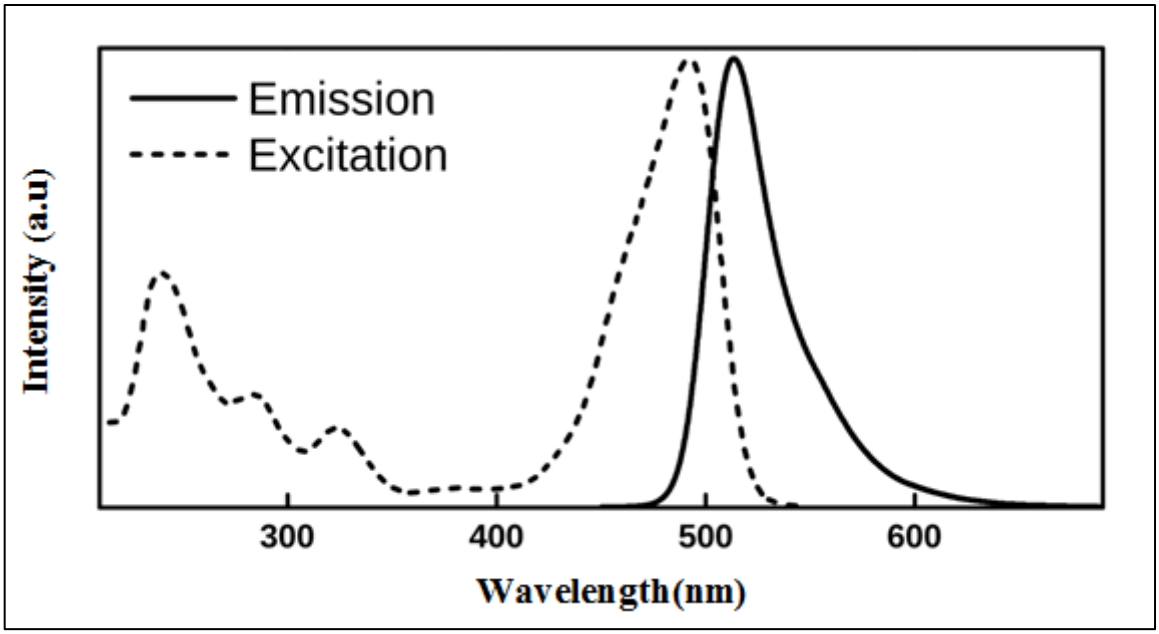

Figure (2.7): Typical (a) absorption and (b) fluorescence emission spectra of a symmetrical D_{4h} type MPc [102]

In fluorescence spectra recombination processes are observed with emission energies less than Eg. These processes include exciton recombination and

indirect transitions, which involve the trapping of electrons (or holes) by impurities Depending on the duration of the emission can distinguish photoluminescence in solids in which electronic states of solids are excited by light of particular energy and the excitation energy is released as light.[103]

The fluorescence life times of MPcs are usually of the order of a few nanoseconds (10^{-9} s) [104]

2.6 Structural Properties

2.6.1 X-ray Diffraction

X-ray diffraction, is a non-destructive rapid analytical technique used to characterize different materials. It is used for phase identification of a crystalline material and can provide information on the unit cell dimensions, crystal structure, orientation and average crystal size. It provides the researchers with a fast and very reliable tool to determine the material composition; however, it does not provide the qualitative compositional data as obtained from Scanning beam electroscopy.[105] X-rays can also be defined as electromagnetic waves that lie between gamma rays and ultraviolet rays

It has a relatively large energy and has a specific wavelength within the range (1.0 - 100)A^0, and the boundaries of the interatomic distance lie between its atoms, and that knowledge of the prevailing direction and the main crystal phases for the growth of the membranes under the preparatory conditions by the presence of characteristic peaks with crystalline directions

and Bragg diffraction angles (Angles Bragg) and it appears in the study the type of X-ray diffraction by Projection of a monochromatic X-ray beam, which has an angle (θ) on The levels of the membrane prepared in the laboratory as shown in Figure (2.7) [106]

The pattern of the X-rays diffracted is mathematically related to the structural arrangement of the atoms causing the scattering. The intensity of the diffracted beam also depends on the arrangement of the atoms in the repeated motif called unit cell . When an X-ray beam hits the sample and is Diffracted, the distance between the planes of the atoms can be measured using the Braggs law which states that[107]

$n\lambda=2d\sin\theta$ (2.18)

where n is the order of the Diffracted beam, d is the distance between the adjacent planes of the atoms and θ is the angle of incidence of the X-ray beam. The Diffraction pattern is a plot of Intensity versus 2θ

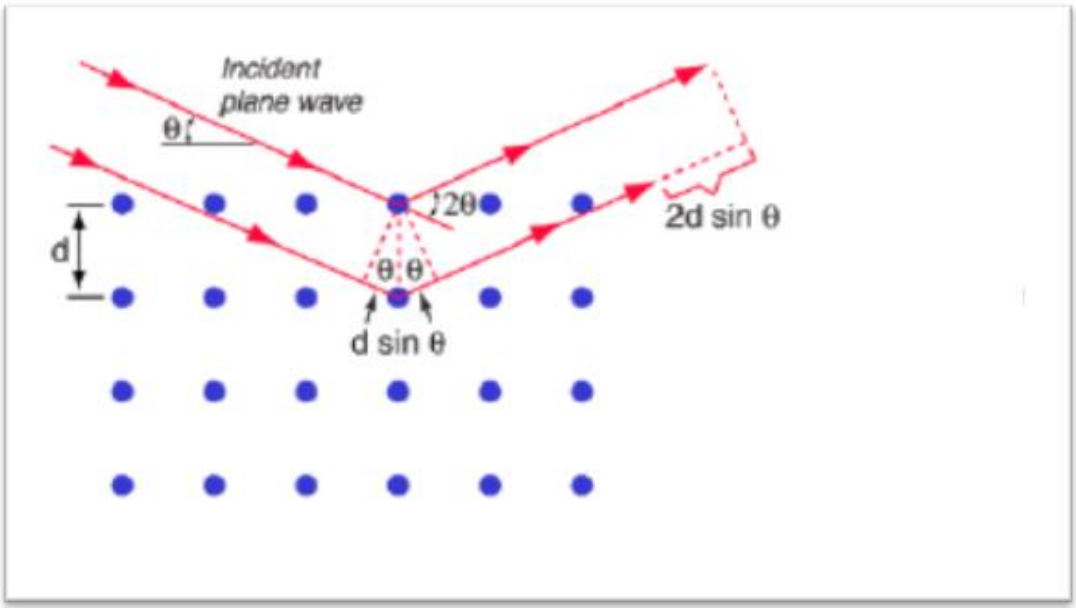

Figure (2.8): Reflection of X-ray beam of wavelength λ from a particular set of atomic planes separated by equal distances d. θ is the complement of the angle of incidence[105]

The intensity of the reflected beam has sharp peaks in the corresponding directions . They are called Bragg peaks. The Bragg peak can be found by varying the angle 2θ of the detector. This is the Bragg condition for diffraction[107].

The average crystal size of the films was studied form defractogram peaks using the Scherrer formula [108]].

$$D = \frac{k\lambda}{(FWHM)cos\theta} \quad (2.19)$$

Where D. is average crystal the size, k is a constant, (FWHM) is the Full Width at Half Maximum.,β angle and lattice parameters (a), (b) and (c) for monoclinic crystal can be calculated from X-ray d-spacing's according to equations:

$$\frac{1}{d^2} = \frac{1}{Sin^2(\beta)}\left(\frac{h^2}{a^2} + \frac{k^2 Sin^2(\beta)}{b^2} + \frac{l^2}{c^2} + \frac{2hl\,Cos(\beta)}{ac}\right) \quad (2.20)$$

$$\sin(\theta) = \frac{\lambda^2}{4Sin^2(\beta)}\left(\frac{h^2}{a^2} + \frac{K^2 Sin^2(\beta)}{b^2} + \frac{l^2}{c^2} + \frac{2hl\cos(\beta)}{ac}\right) \quad (2.21)$$

Where h, k, and l refer to the Miller indices of individual reflections and β is the angle between a and c.

2.7 Surface Morphology

Surface morphology and micro structural features control physical properties like the gas sensitivity, response recovery time, stability, reproducibility, and other sensing characteristics of thin films. Surface structure, polymorphic form and phase transition influence behaviors of the phthalocyanines .

2.7.1 Atomic Force Microscopy (AFM)

The atomic force microscope (AFM) (also known as the scanning force microscope – SFM) is a type of scanning probe microscopy that has been shown to have resolution on the order of a nanometer. An atomic force microscope can image features as fine as a carbon atom (0.25 nm) and as vast as the cross section of a human hair (80 m), allowing researchers to investigate sample

surface topography and morphology in unprecedented detail[109]. The scanning tunneling microscope (STM), created by Gerd Binnig and Heinrich Rohrer in the early 1980s, was a direct forerunner of the AFM. In 1986, they were awarded the Nobel Prize in Physics for this achievement. However, the STM had one important drawback: it could only be used with conducting specimens.[110] The first AFM was able to distinguish lateral features as small as 300 microns. However, after the introduction of microcantilevers, new modified Nano tips, and new optical beam deflection methods to assess tip movement and twist, significant progress in the AFM method application began. As a result of Alexander and colleagues' good work, the beam–bounce approach is now widely employed. [111]. Micro cantilevers and novel tips (the top of the tip can be produced from tens to hundreds of atoms) are commonly made of silicon or silicon nitride.. The Scheme of AFM device is shown in figure.(2.9).

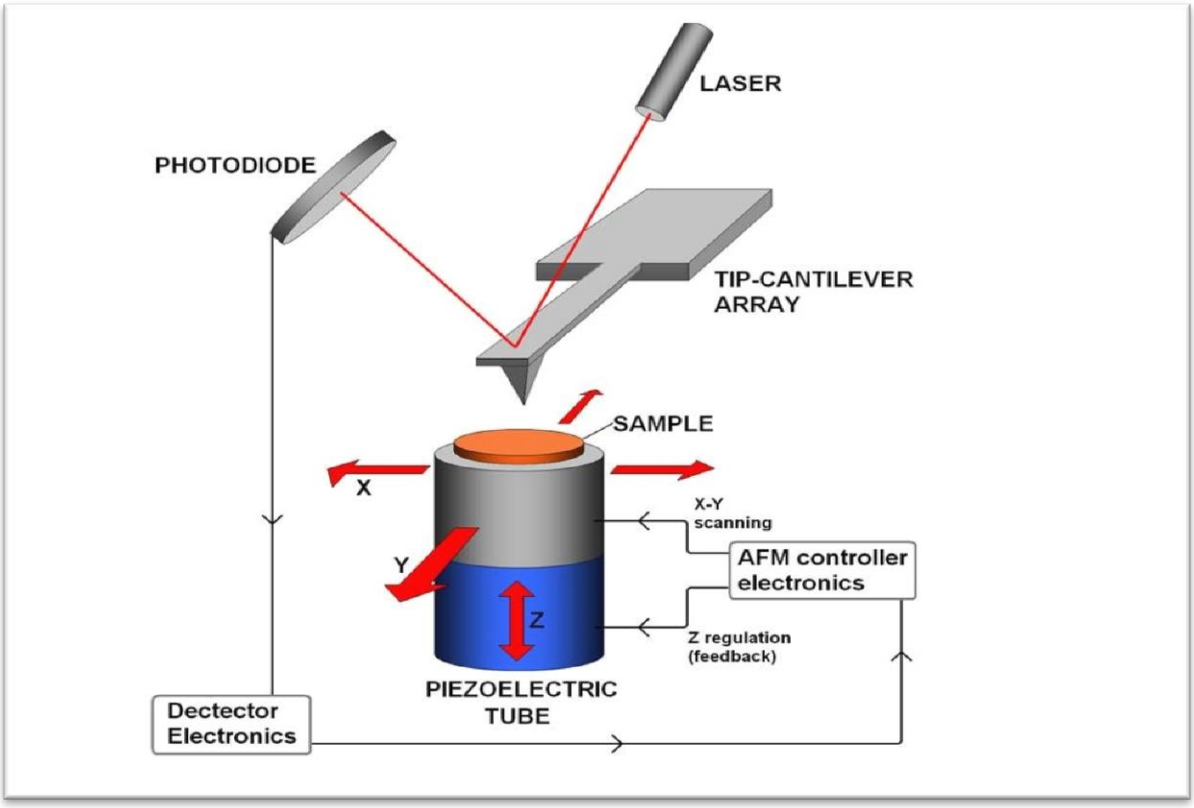

Figure (2.9): Scheme of AFM Device [49]

Chapter Three

Experiment Procedure and Measurements

3.1 Introduction

This chapter covers the materials and devices used in the study, as well as the thin-film deposition and thickness measurement techniques.

Optical qualities such as transmittance (T), absorbance (A), and structural properties such as XRD, AFM, FT-IR devices, and fluorescence are tested and measured using devices like XRD, AFM, FT-IR devices, and fluorescence. A schematic illustrating of the experimental work is shown in Fig (3-1).

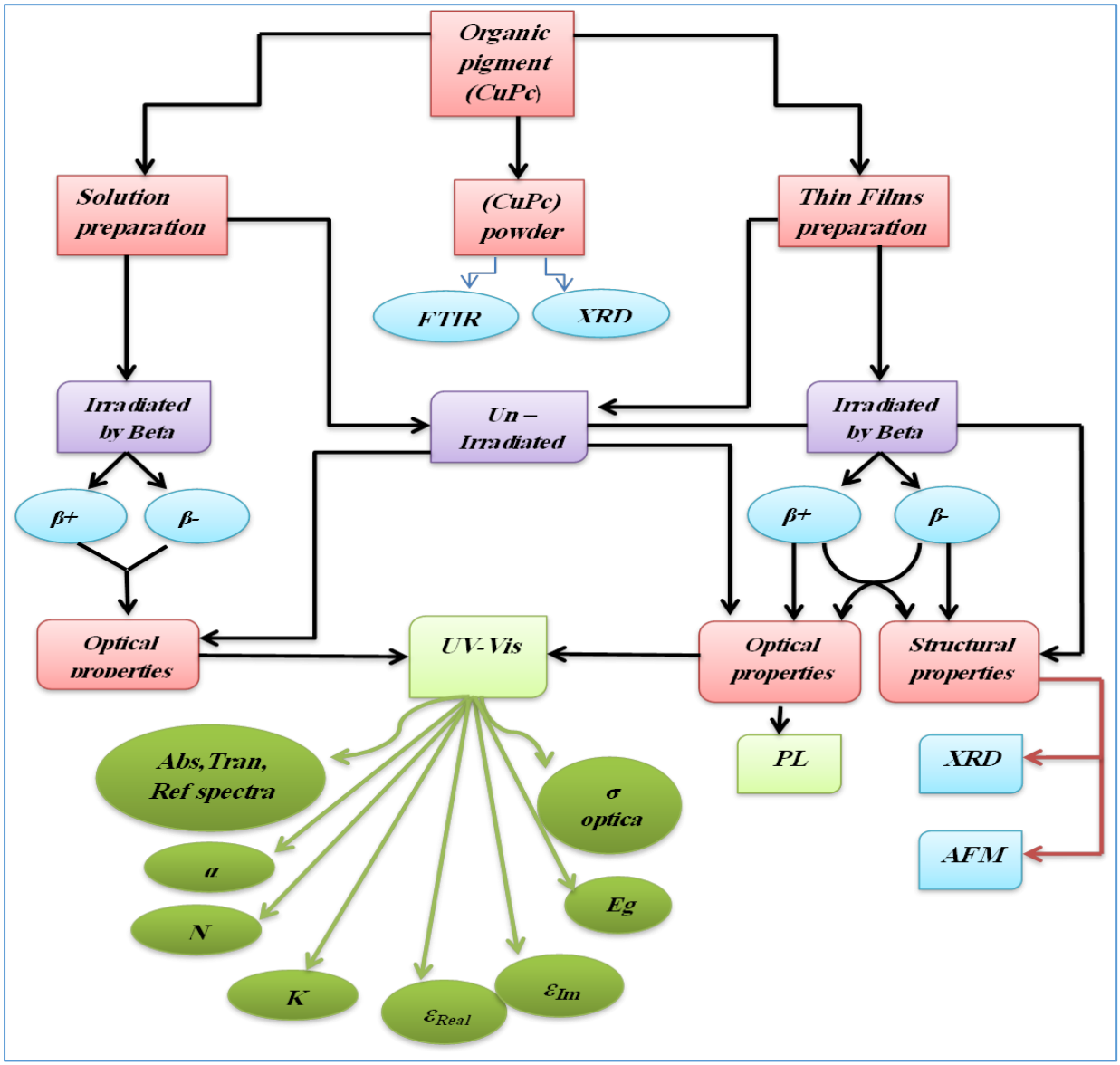

Figure (3.1) : Schematic diagram for the experimental work

3.2 Solutions Preparation

The solutions of CuPc molecules with a concentration of 0.15 gm/L was prepared using chloroform as a solvent.it was irradiated in pluse beta ray source in collage of science university of Karbala Na-22 (RE 402) and minis beta ray source Sr – 90(UB863) in time periods (1 , 2 , 3 days) , concentrations of (0.1,0.2,0.15) g/L was prepared then they were irradiated in pluse beta ray source Na-22 (RE 402) and minis beta ray source Sr-90(UB863) in constant time period (5 days) then the optical properties and energy band gap were measured before and after irradiation.

3.3 Preparation of blue CuPc Thin Films

The CuPc used as an active material, that obtained from VOXCO company, China. was prepared as thin films were made on a glass substrate by spin coating deposition of thickness (197, 214 nm) at room temperature. Spin coating is a method of covering flat objects with a thin layer of homogenous coatings. A small amount of coating material is usually placed in the center of the substrate and whirled gently or not at all. Using centrifugal force, the substrate is spun up to 1000 times per minute to disseminate the coating material. A spin coater, often known as a spinner, is a spin coating machine.[1] Figure (3.2) depicts the molecular structure of the CuPc employed as an active material, which was received from the VOXCO film (blue CuPc)

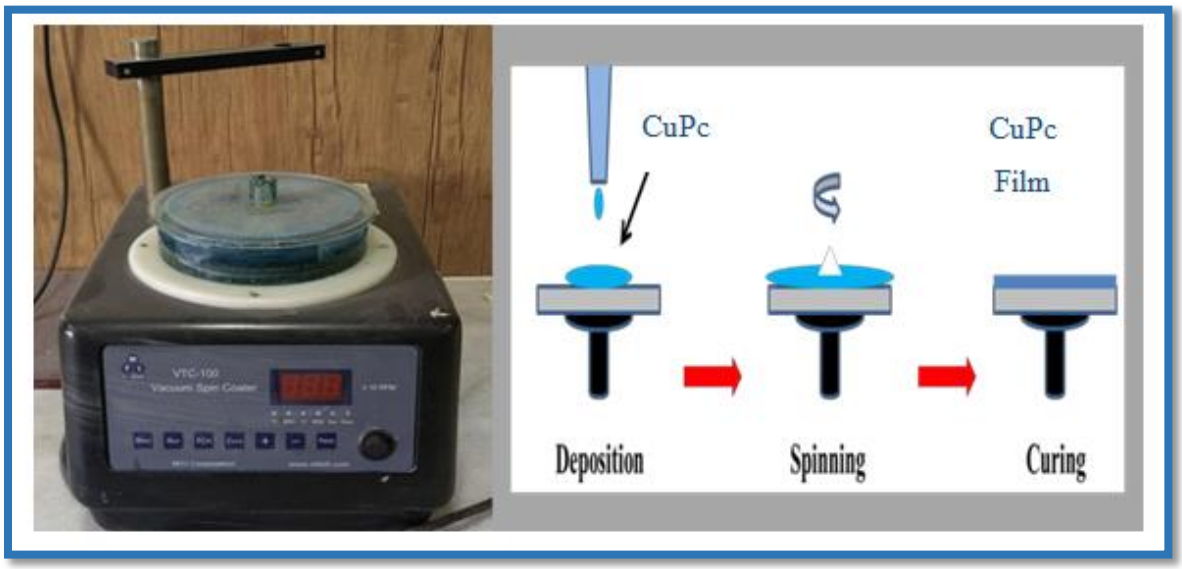

Figure (3.2) Represent The Spin Coating Method

3.4 Beta Particle Sources

The beta irradiation was carried out using two types of beta source (Na-22)(RE402) (Sr-90)(UB863) GSA GLOBAL company in university of Karbala college of science where the solution was irradiated at varied durations (0, 1, 2, and 3 day) for each concentration. Fig. (3.3) shows the beta source used for irradiation Table (3.1) shows Beta Source Isotopes

Figure (3.3) The Beta Sources

Table (3.1): Beta Source Isotopes

β Source	Charge type	Energy (MeV)	A_0	$T_{1/2}$ (y)	λ=(0.693/T)	Date now (mm)	Date now (yyyy)	man. Date (mm)	man. Date (YYYY)	time (Y)	$A=A_0 e^{-\lambda t}$
Sr-90	β^-	0.546	2	28.8	0.024063	1	2022	9	2012	9.333	1.597
Na-22	β^+	0.544	2	2.6	0.266538	1	2022	3	2009	12.833	0.065

3.5 Thickness Measurements

In the university of Babylon College of women science,the thickness of the produced thin film was measured using Ellipsometry HOLMARC company India as shown in Fig.(3.4) using a diode laser with an output power of (5mW) and a wavelength of (532 nm). It's a useful optical technique for estimating the thickness and surface density of reflective materials' across layers. Ellipsometers employ polarized light to examine a multi-layer or single-layer thin film material on a substrate non-invasively. It can also investigate the substrate's bulk. Single wavelength ellipsometers are typically employed for simple systems like a single layer non-absorbing material, although they are limited to only giving two parameters. There are two different variations of the approach that provide additional information. The ellipsometry technique is best for determining the thickness of a thin layer produced on glass using the spin coating method. [112]

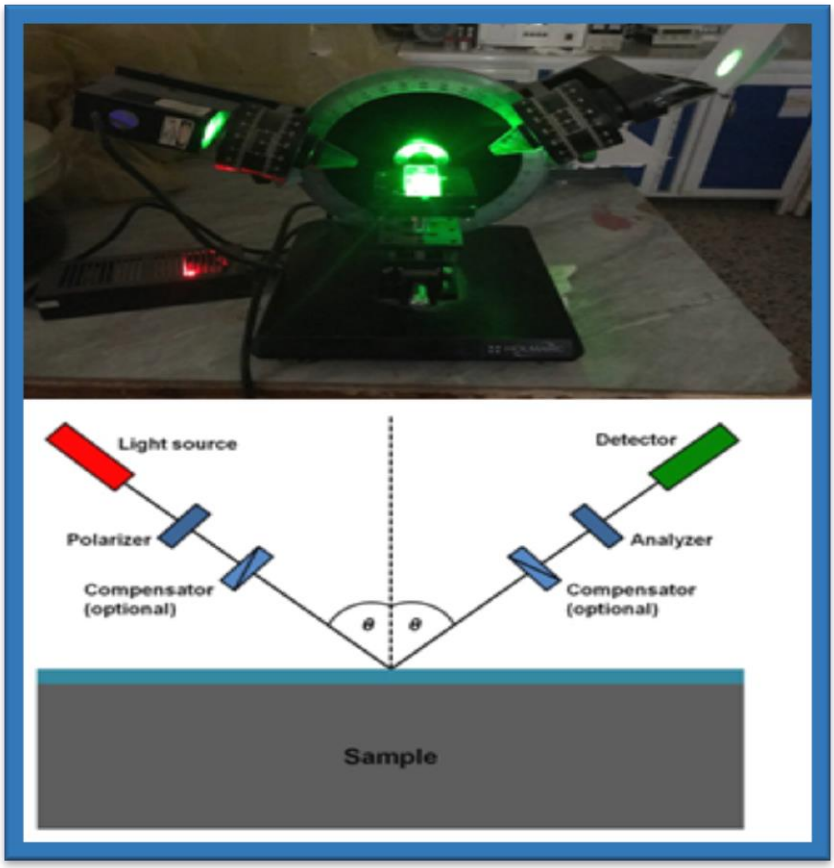

Figure (3.4) : Typical Configuration of Ellipsometer [113]

3.6 Optical Measurements

3.6.1 UV-Vis Measurements

CuPc thin films optical characteristics Using a UV/Vis (1900I) spectrophotometer (Shimadzu Company) Japanese made spectrophotometer, the time of beta ray irradiation by two beta ray sources Na-22and Sr-90 deposited at RT. these spectrometers contain two light sources: Deuterium and Tungsten lamp in the wavelength range 300-800 nm and 190–1100nm. The optical energy band gap, fundamental optical edge, and optical constants are determined.

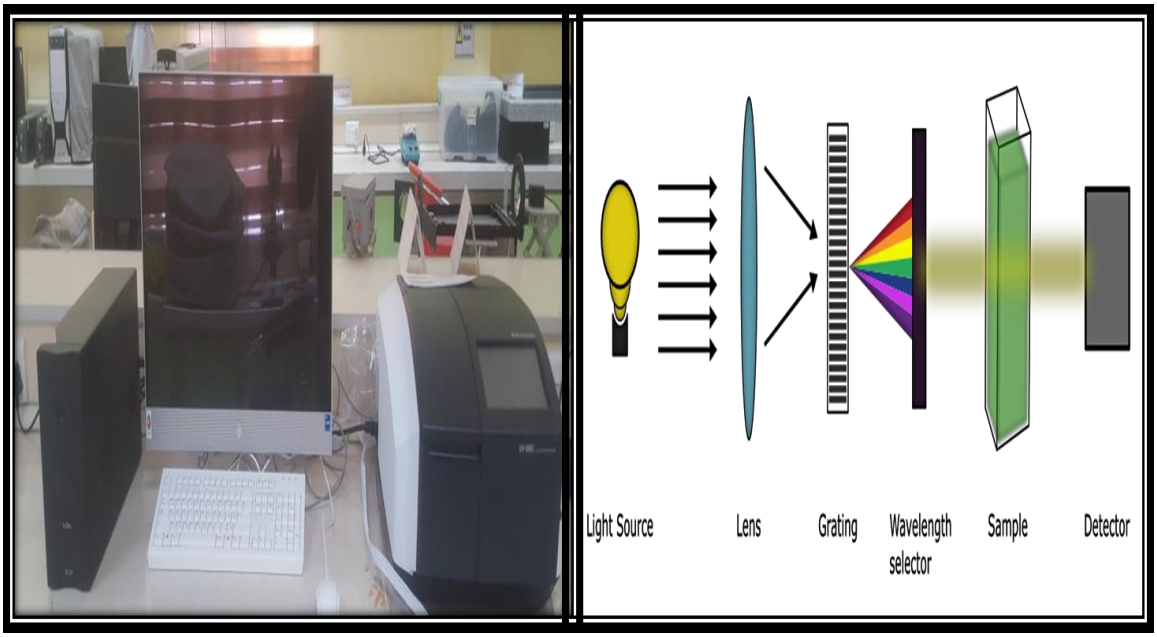

Figure (3.5) : UV-Vis Spectrophotometer

3.6.2 Photoluminescence Measurements

Photoluminescence measurements (Fluoro Mate Fs-2 spectrometer) registered by single beam spectrometer for CuPc thin films deposited with same thicknesses at RT. To show the role of traps PL measurements have been done at exciting wavelength 320 nm.

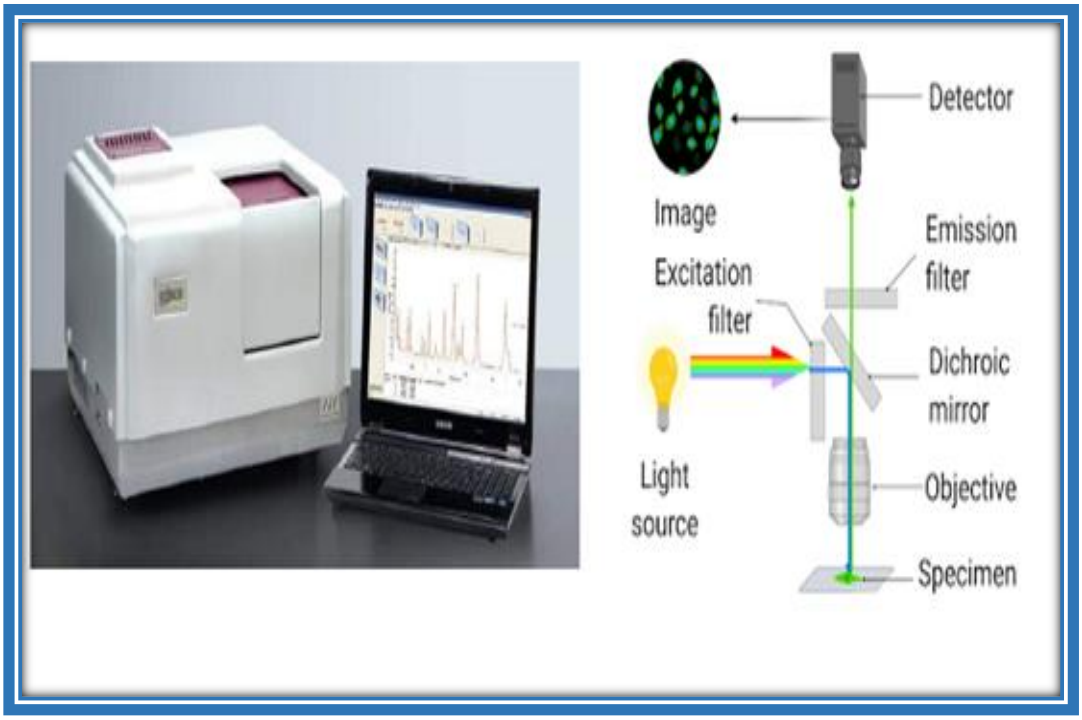

Figure (3.6) : Photoluminescence Spectrometer[114]

3.7 Structural Measurements

3.7.1 FT-IR Measurements

Shimadzu double-beam FTIR spectrometer recorded Fourier-transformed infrared spectra of CuPc powder after grinding with potassium bromide (KBr)

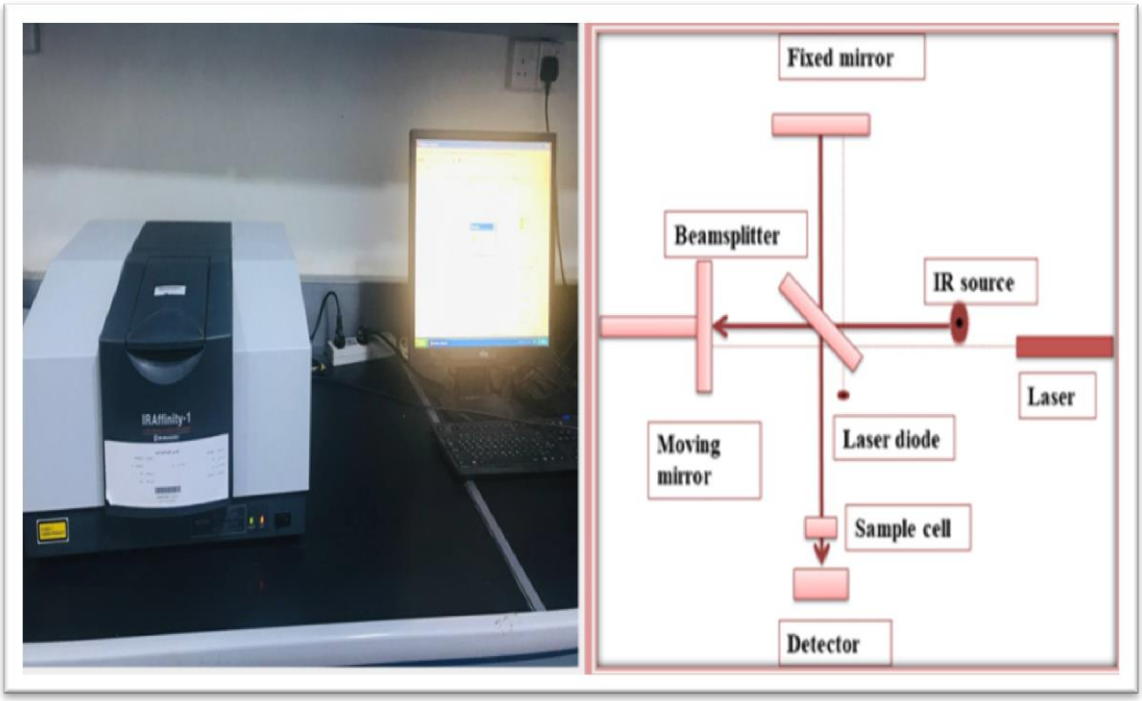

Figure (3.7) : FTIR Spectrophotometer[115]

3.7.2 X–Ray Diffraction

The structures of CuPc Powder and films were investigated using an X–ray diffractometer system (Shimadzu – XRD6000, Shimadzu Company /Japan) ,The intensity is calculated as a function of 2Θ. The radiation source was Cu (K) with a wavelength of λ=1.5405 nm, a current of (30 m Amp), and a voltage of (40 kV). With a speed of 2cm.min-1, the scanning angle 2θ was changed between (5–60) degrees. Using Bragg's law Eq.(2.17), Average crystal size was computed from the interpleader distance d(hkl) for different planes

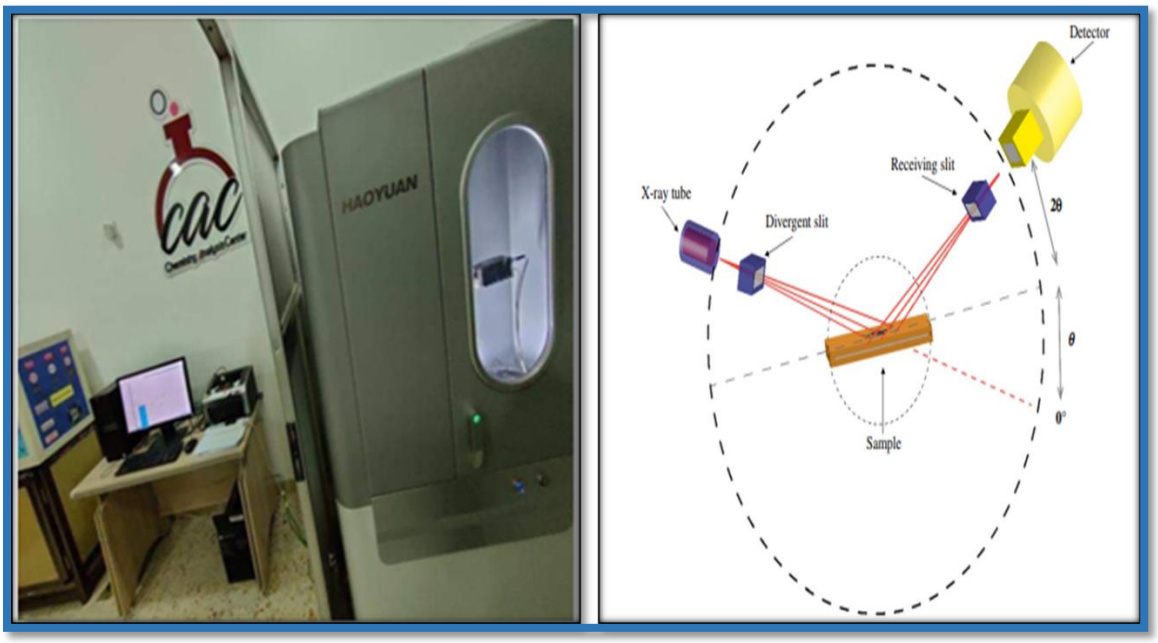

Figure (3.8) *:* Schematic illustration of X-ray diffraction instrument[116]

3.8 Measurements of Surface Morphology

3.8. 1 Measurements with an Atomic Force Microscope

The model TT-2 AFM workshop company in the United States performed surface morphological measurements for CuPc thin films with varying irradiating times of beta ray irradiated with energy Na -22 average energy 0.544 MeV and energy 0.546 MeV Sr-90. Roughness and diameter of grains were acquired computerized, also 2D and 3D images for all studied samples were get.

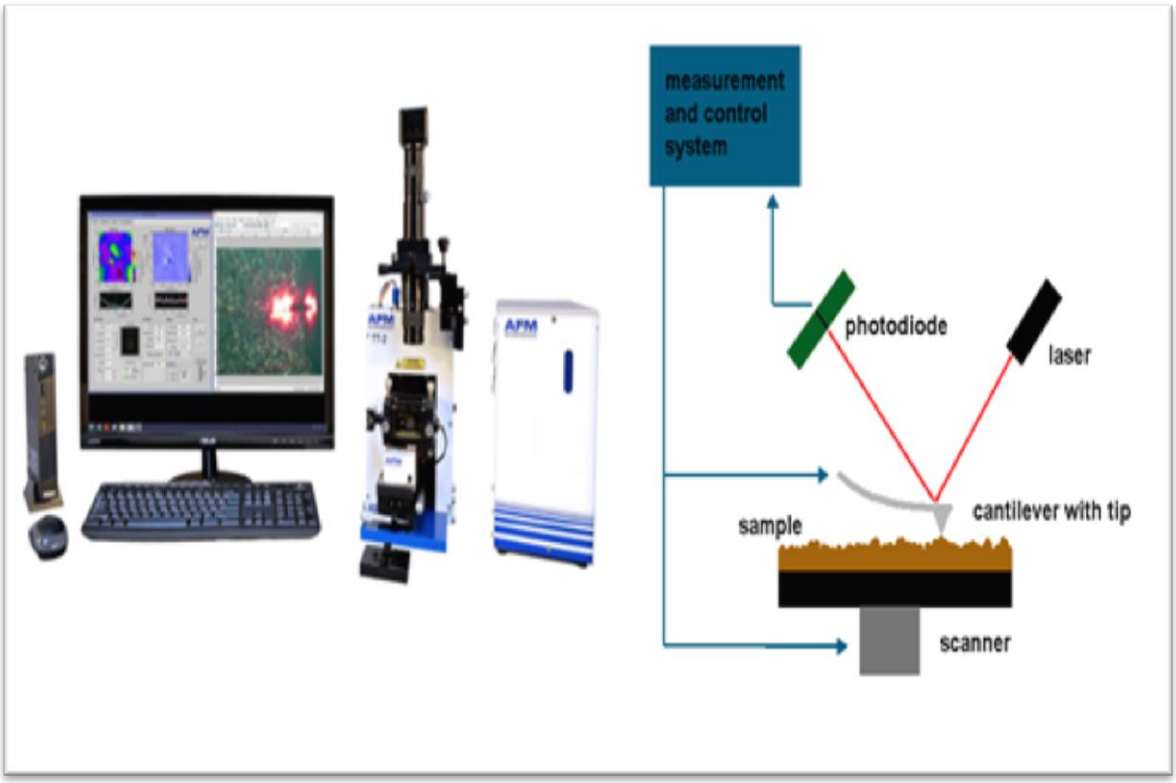

Figure (3.9) : ***AFM Device***[117]

Chapter Four

Results and Discussion

4.1 Introduction

This chapter contain the results and the analysis of the experimental measurements of the CuPc thin films with various irradiation time of Beta ray irradiation (Na-22)(RE 402) average energy 0.544Mev. and (Sr – 90)(UB863) energy (0.546Mev) the optical, structural, surface morphology properties of CuPc thin films prepared by Spin coating method which tested

4.2 FT-IR Transmittance Spectra

The FT-IR spectrum for CuPc Powder is measured at room temperature as shown in Figure (4.1) FT-IR for CuPc powder shows the bond bending represented by the range (400-2000) cm^{-1},while the bond stretching represented by the range (2000-4000) cm^{-1}. There is weak peak in the range (400-800) cm^{-1} which indicate the presence of (metal-Nitrogen) bond vibration. At (894) cm^{-1} have been assigned for (copper – Nitrogen) peak , At(1165) cm^{-1} is for bond of C-N, peak (1496) cm^{-1} for C=N and the peak (1620) cm^{-1} indicates C=C bond, peaks at 3047 indicates Alkene =C-H bond and 2862 cm^{-1} for alkan -C-H stretching , the range (2121-2245)cm^{-1} indicates Benzene ring band. This result agreements with reference [48]

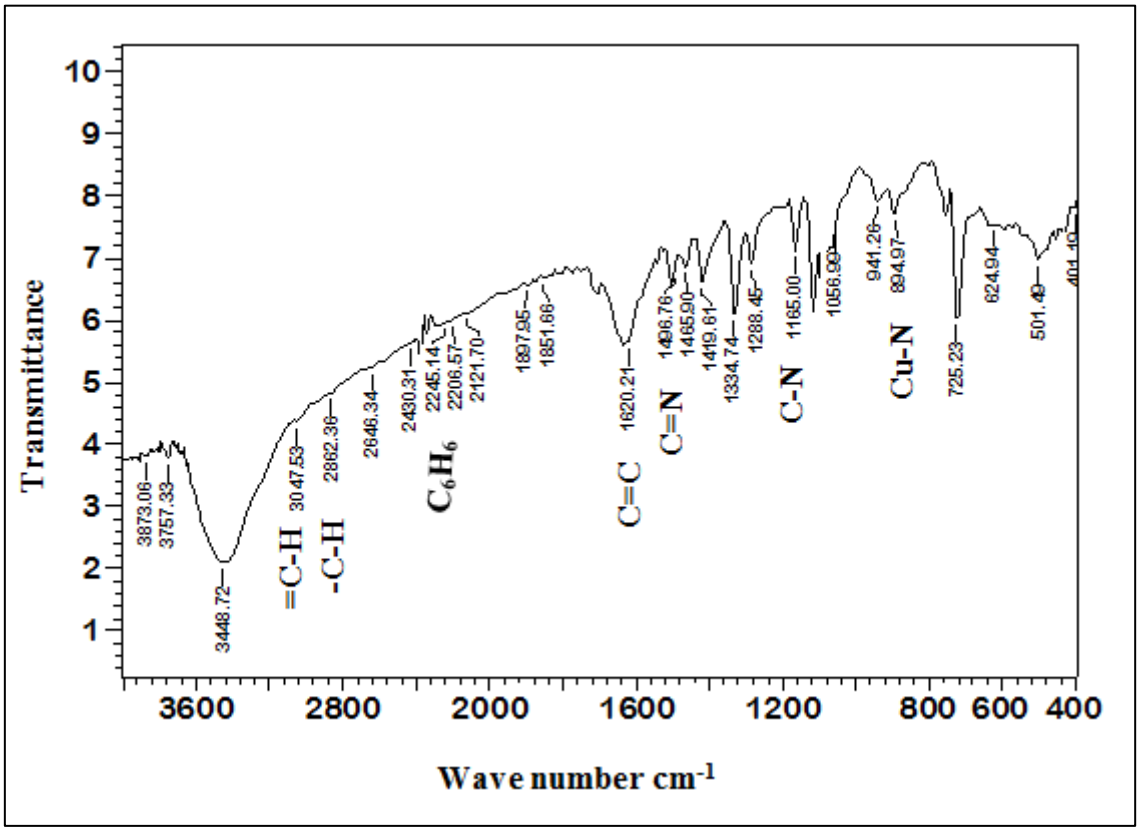

Figure (4.1) :FT-IR Spectra of CuPc Powder

4.3 Optical properties of CuPc

4.3.1 Effect of irradiation time on Optical properties of CuPc Solutions Irradiated by Beta ray

The results appeared for β-phase CuPc solutions when irradiated with plus and minus beta rays for several periods of time, as follows:

The results of UV-Vis for Beta rays with concentration(0.15) g/l are shown in Figs.(4.2a, 4.3a) which illustrate the absorbance spectra in the wavelength range (300-1100) nm. It can be seen that there are two bands for CuPc solutions. The first one is named as B-band (Soret) and appeared in the UV range in the region (300-400 nm) while the second one is obtained in the visible region and called Q-band with wavelength range (600-1100 nm) This suggests that the spectrum range is from (π- π^*) orbital's transition .The

increasing of the irradiating time leads to decrease the absorption of the solution since the rays broke at the bonds and the molecules lost their identity. The measurements are taken irradiating times (0,1,2, and 3 day) with Beta ray for concentration (0.15 g/l) the absorbance is higher at the non irradiated sample and decreased with increasing irradiation time (1 ,2 , and3) day as shown in Figs. (4.2b,4.3b)

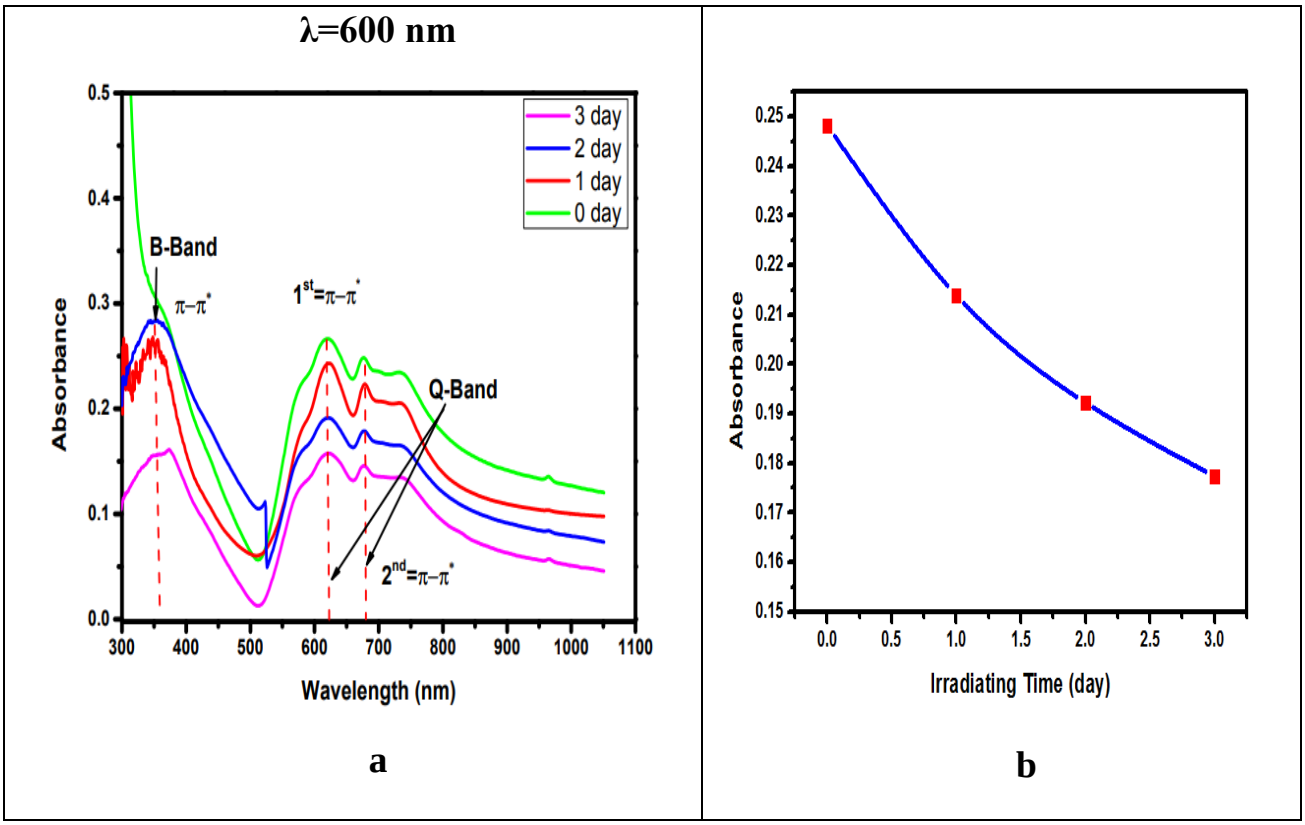

Figure(4.2) : a. Absorbance spectra with CuPc solutions concentration (0.15)g/l for β+ Irradiated samples in period time . b. The Maximum Absorption vs. the Irradiating time for β+ CuPc solutions at 600nm

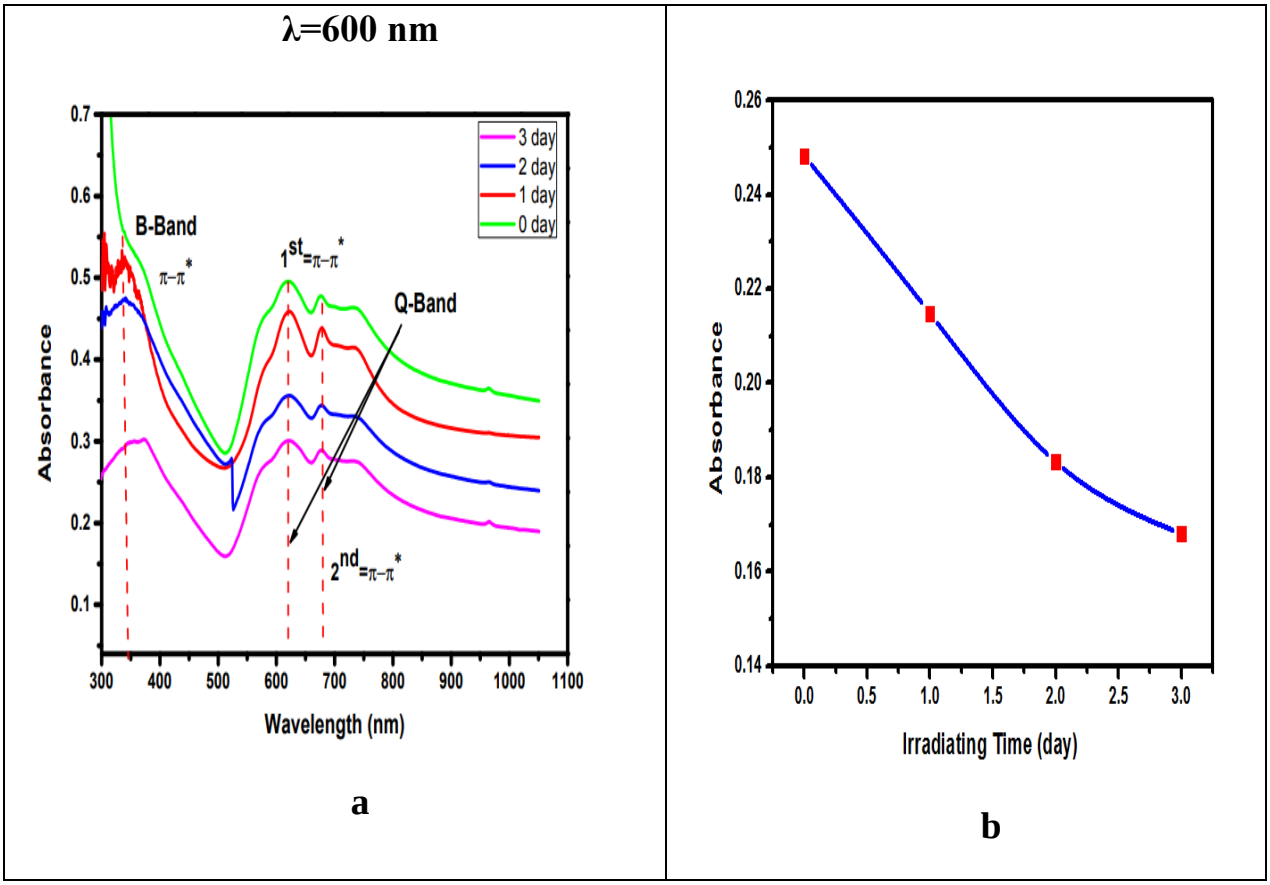

Figure(4.3*) :* a. Absorbance spectra *with* CuPc solutions concentration (0.15)g/l *for* β-Irradiated samples in period time. b. The Maximum Absorption vs. the Irradiating time for β- CuPc solutions at 600nm

The reflectance spectra with the solution concentration (0.15) g/l irradiated by Plus and minus Beta ray, simply it is shown that the reflectance spectra is higher in B band. The maximum reflectance appears at the highest non irradiated sample and decrease with increasing irradiation times (1 ,2 , and3 day) at wavelength (600) nm as shown in Figs. (4.4a ,4.5a). The maximum reflectance spectra against the irradiation time. Obviously, the reflectance is higher at irradiation time (0 day) for non-irradiated samples and decreases with increasing the irradiation time this behavior is similar to the absorbance behavior shown in Fig. (4.4b, 4.5b)

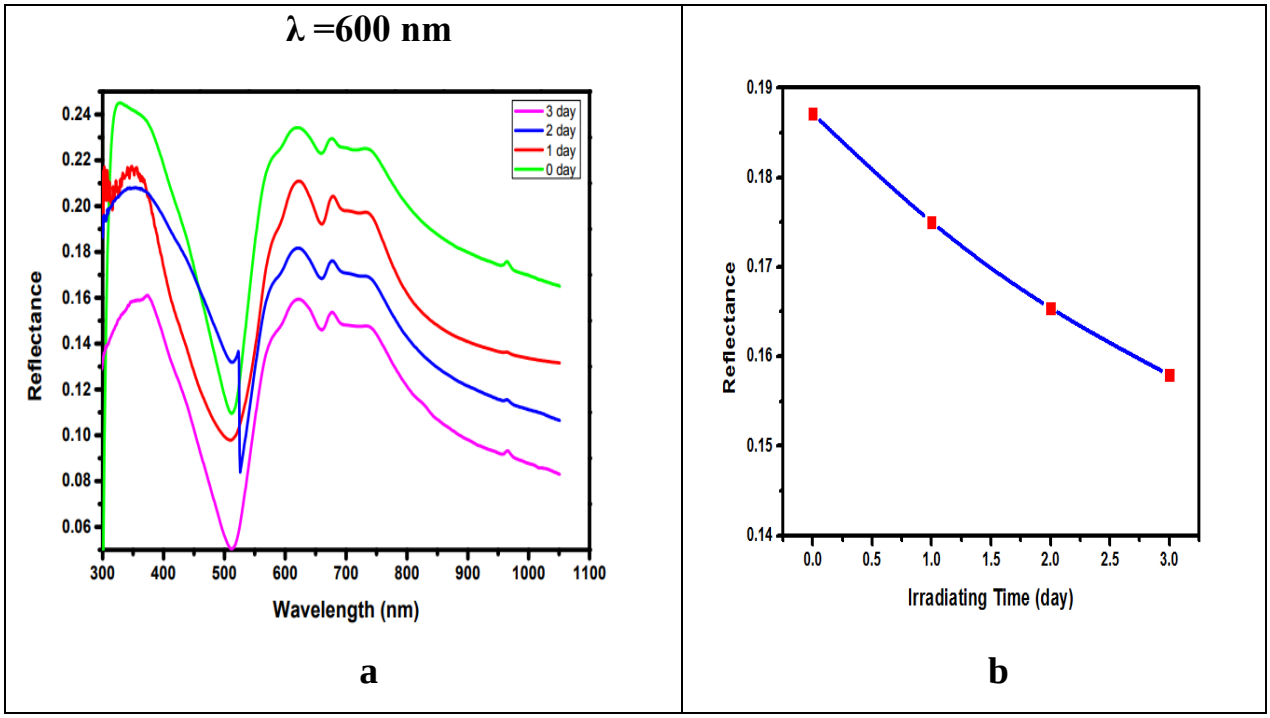

Figure (4.4) : a. Reflectance spectra with CuPc solutions concentration (0.15)g/l for β+Irradiated samples in period time . b. The Maximum Reflection vs. the Irradiating time for β+ CuPc solutions at 600nm

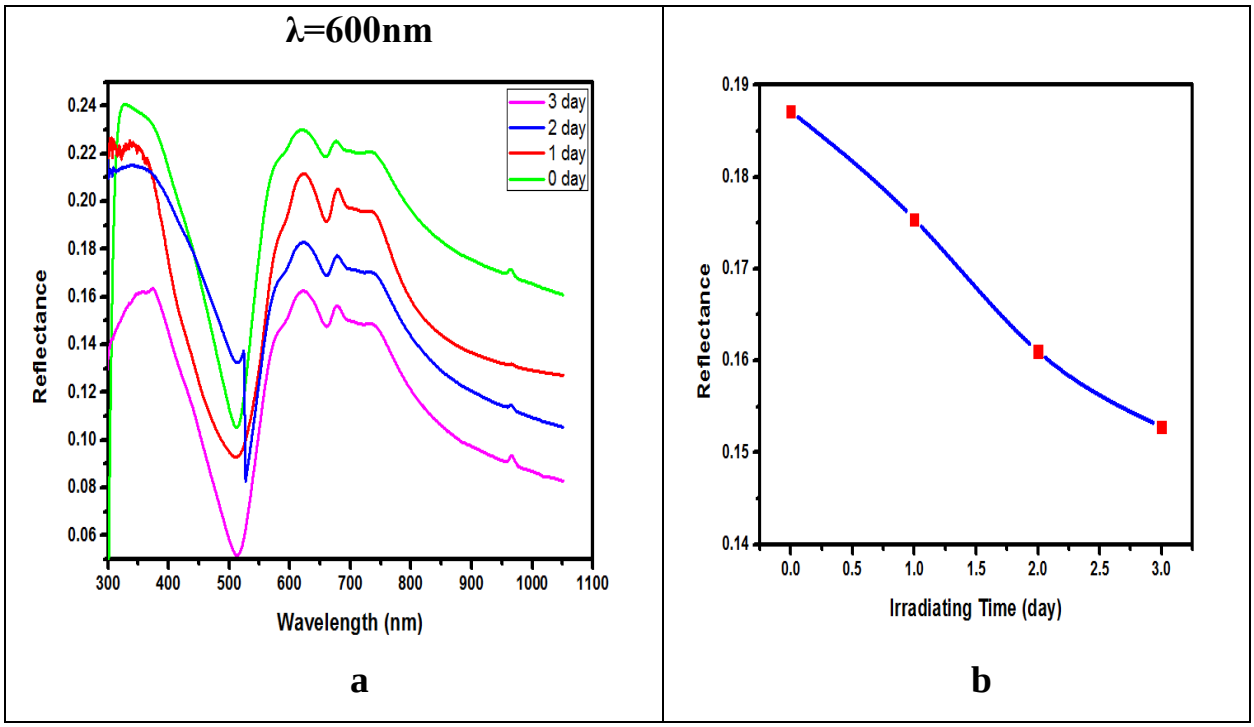

Figure (4.5) : a. Reflectance spectra with CuPc solutions concentration (0.15)g/l for Irradiated samples in period time . b. The Maximum Reflection vs. the Irradiating time for β- CuPc solutions at 600nm

The transmittance spectra of the solution concentration (0.15) g/l irradiated by Beta rays, simply it is shown in Figs. (4.6a,4.7a) the transmittance spectra is higher in Q band which increase with increasing wavelength from(700-1100)nm. the maximum transmittance spectra against the irradiation time(0,1,2 and 3 day). Obviously, the transmittance increases with increasing the irradiation time as shown in Figs. (4.6b to 4.7b)

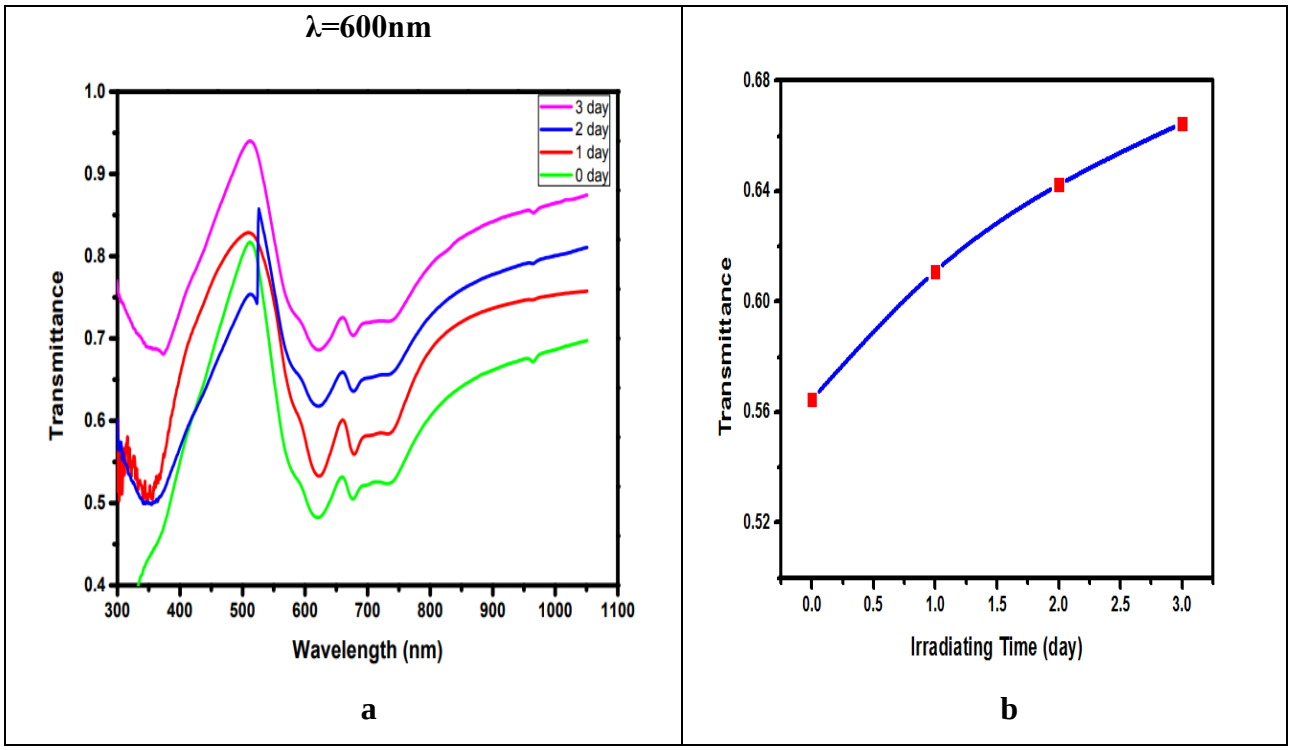

Figure (4.6) : a. Transmittance spectra with CuPc solutions concentration (0.15)g/l for β+Irradiated samples in period time . b. The Maximum Transmittance vs. the Irradiating time for β+ CuPc solutions at 600nm

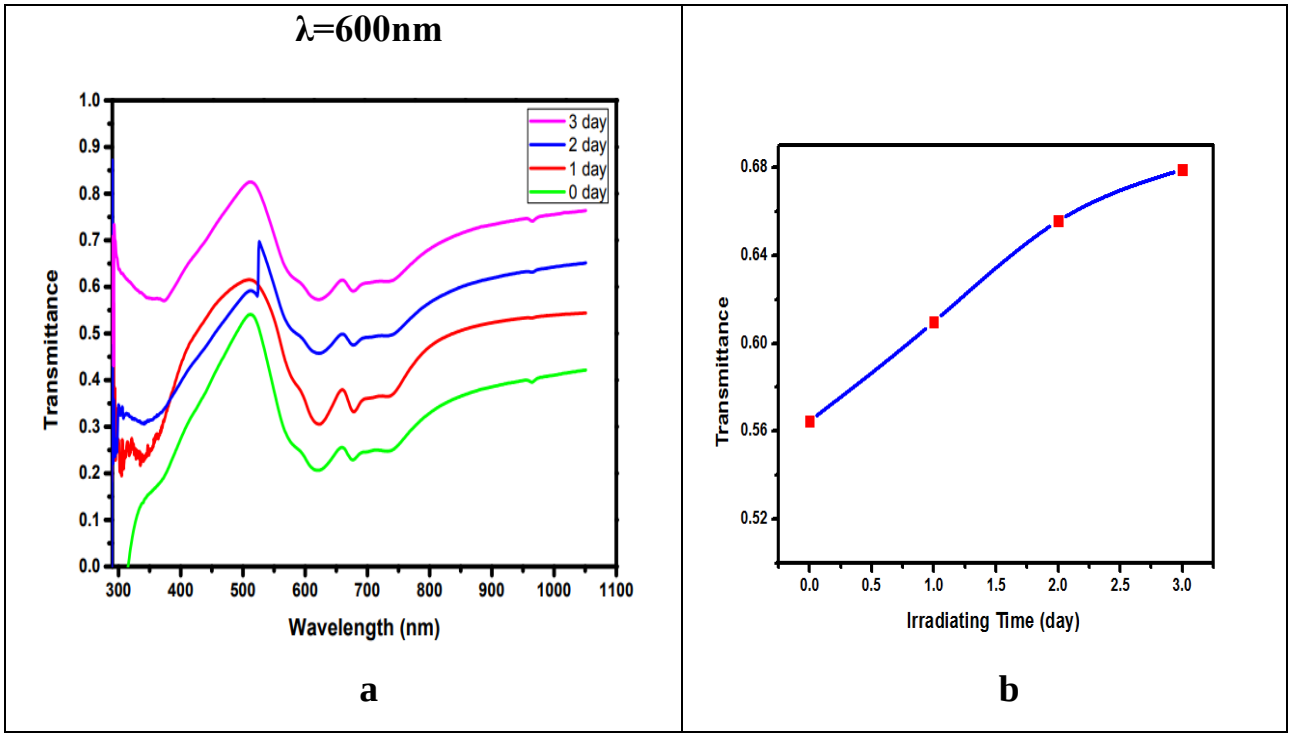

Figure (4.7) : a. Transmittance spectra with CuPc solutions concentration (0.15)g/l for β-irradiated samples in period time . b. The Maximum Transmittance vs. the Irradiating time for β-CuPc solutions at 600nm

The indirect energy band gap calculated from the equation (2.6) using Tauc method, the Figs. (4.8a , 4.9a) the tangent line intersect the energy axis with Eg values , the broken molecules lead to low absorbance and minimum defect in material as shown in Figs .(4.8b,4.9b)

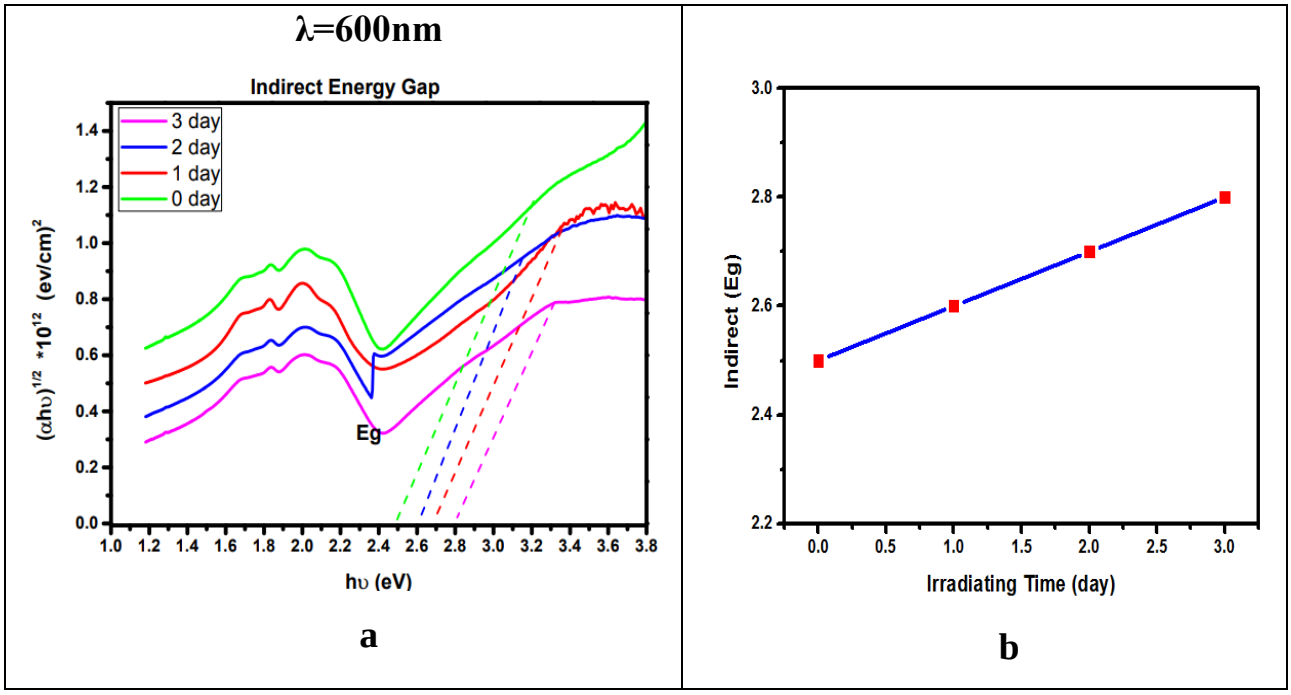

Figure (4.8) : a. Determined indirect energy band gap CuPc solutions concentration (0.15)g/l for β+ Irradiated samples in period times. b. The Maximum indirect energy band gap vs. irradiating time for β+CuPc solutions at 600 nm

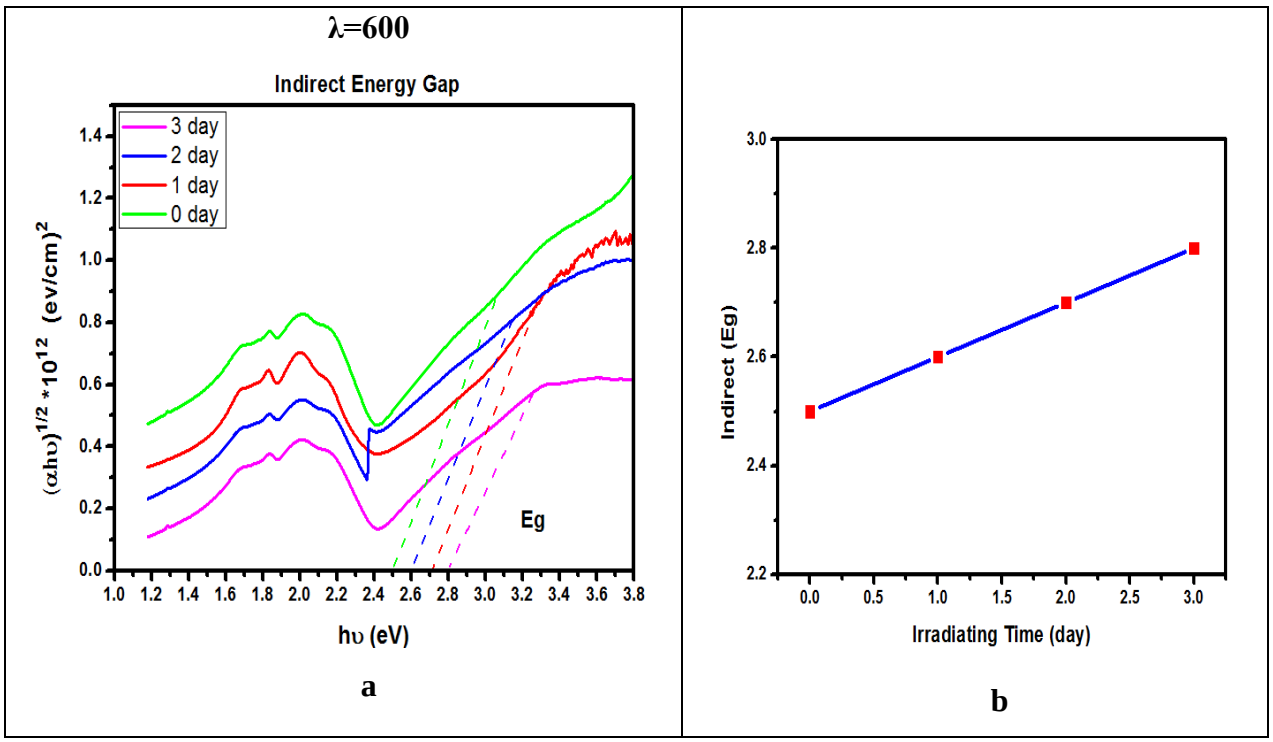

Figure (4.9) : a. Determined indirect energy band gap CuPc solutions concentration (0.15)g/l for β- Irradiated samples in period times. b. The Maximum indirect energy band gap vs. irradiating time for β-CuPc solutions at 600 nm

Optical parameters for solution concentration (0.15) g/l was irradiated by Plus, minis Beta ray as the Linear Absorption Coefficient (α) decreases due to a decrease in absorbance, since (α) less than 10^{-4} is indirect, The extinction coefficient (K) decreases due to the decrease in the number of dye molecules, and thus the attenuation of rays decreases, The refractive index (n) depends mainly on the reflectance , and the reflectance decreased with the increase in the irradiating time, The Real dielectric constant(ε_r); The dielectric of a substance decreases due to a decrease in the concentration of the substance upon its dissolution, The imaginary dielectric constant(ε_{img}) represents the loss in the electric field and its decrease is due to the decrease in the electric field stored in the insulating material and optical conductivity (σ) ; The decrease in the optical conductivity values is due to the decrease of its two main terms in the equation ($\sigma = \frac{\alpha n c}{4\pi}$) the refractive index and the absorption coefficient with an increase in the irradiation time as shown in Tables(4.1, 4.2)

Table (4. 1):Optical Constants of CuPc Solution irradiated byβ^+ - ray

at λ= 600 nm							
irradiating time (day)	**α *10^4 (cm^{-1})**	**(K)**	**(n)**	**(ε_{Real})**	**($\varepsilon_{Im.}$)**	**Eg (eV)**	**σ optical (s^{-1})**
0	0.223	1.067E-06	2.305	5.316	4.921E-06	1.9	1.230
1	0.194	9.290E-07	2.206	4.870	4.100E-06	2	0.102
2	0.192	9.183E-07	2.189	4.793	4.020E-06	2.1	0.100
3	0.177	8.475E-07	2.125	4.517	3.602E-06	2.2	` 0.090

Table(4.2): Optical Constants of CuPc Solution irradiated byβ^- - ray

at λ= 600 nm							
irradiating time (day)	α *10^4 (cm^{-1})	(K)	(n)	(ε_{Real})	($\varepsilon_{Im.}$)	Eg (eV)	σ optical (s^{-1})
0	0.223	1.067E-06	2.305	5.316	4.921E-06	1.9	0.123
1	0.214	1.026E-06	2.285	5.222	4.690E-06	2	0.117
2	0.183	8.756E-07	2.151	4.628	3.767E-06	2.1	0.094
3	0.168	8.027E-07	2.082	4.336	3.343E-06	2.2	0.083

4.3.2 Concentrations Effect on the Optical Properties for Cupc Solution Irradiated by Beta ray

The results of UV-Vis for Beta rays irradiated CuPc solution with concentrations(0.1, 0.15,0.2) g/l are shown in Figs. (4.10a , 4.11a) are examined .The absorbance spectra in the wavelength range (250-1100) nm. It can be seen that there are two bands for CuPc solutions. The first one is named as B-band (Soret) and appeared in the UV range in the region (300-500 nm) while the second one is obtained in the visible region and called Q-band with wavelength range (600-1100 nm).

The increasing of the irradiation time leads to increase the absorption of the solution obeying Beer Lambert law eq (2.5),The measurements are taken for irradiating times (5 day) with Beta ray with concentrations(0.1 ,0.15 ,0.2g/l), the absorbance is higher at the highest concentration sample (0.2 g/l)and decreased with decreasing the concentration. as shown in Figs. (4.10b , 4.11b)

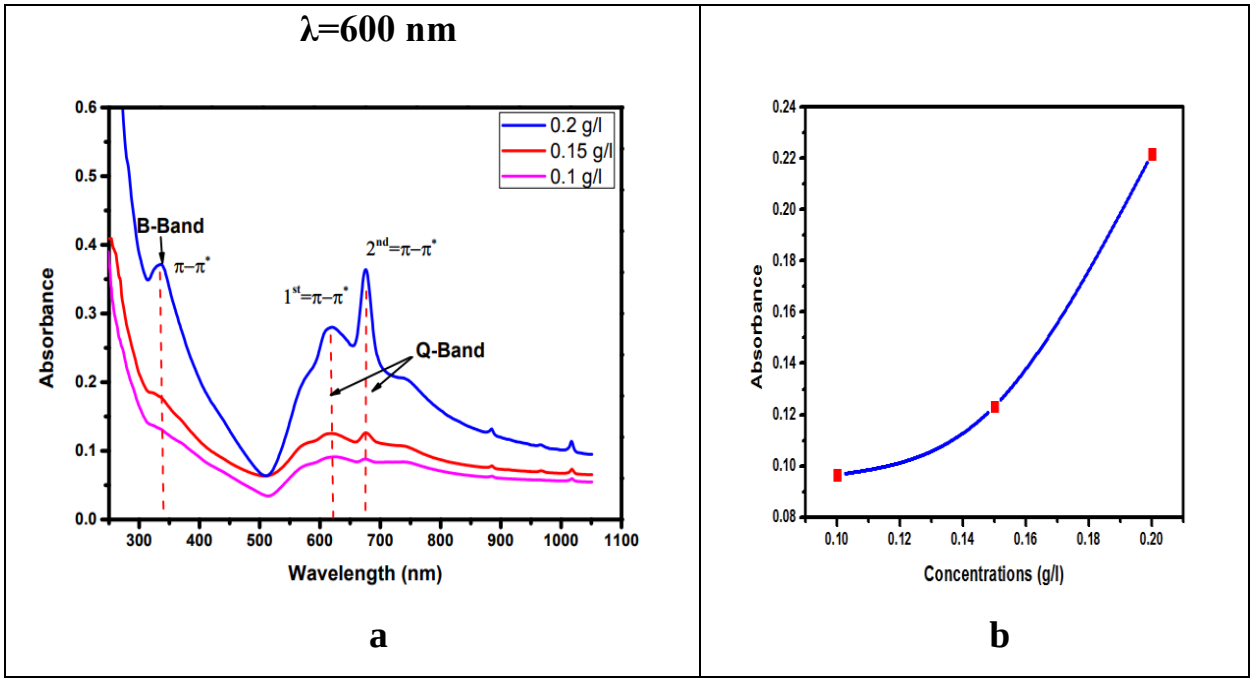

Figure(4.10): a. Absorbance spectra with CuPc solutions concentrations (0.1 ,0.15,0.2)g/l for β+Irradiated samples in (5 day) . b. The Maximum Absorbance vs. the concentrations for β+ CuPc solutions at 600nm

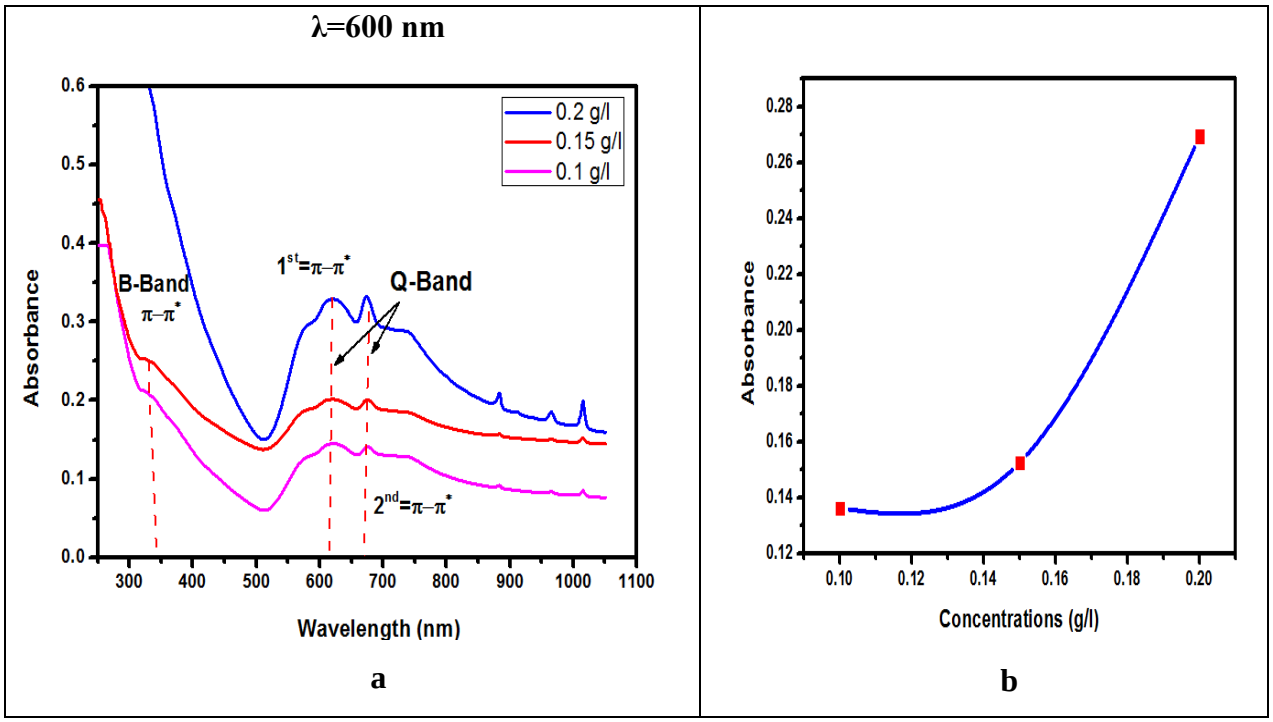

Figure(4.11): a. Absorbance spectra with CuPc solutions concentrations (0.1 ,0.15,0.2)g/l for β-Irradiated samples in (5 day) . b. The Maximum Absorbance vs. the Concentrations for β- CuPc solutions at 600nm

The reflectance spectra when varying the solution concentration (0.1, 0.15, 0.2) g/l, simply it is shown that the reflectance spectra is higher in B band as shown in Figs. (4.12a ,4.13a). Obviously, the reflectance is higher at the highest concentration sample(0.2g/l)and decreases with decreasing the concentration for the samples this behavior is like absorbance behavior shown in Figs. (4.12b , 4.13b)

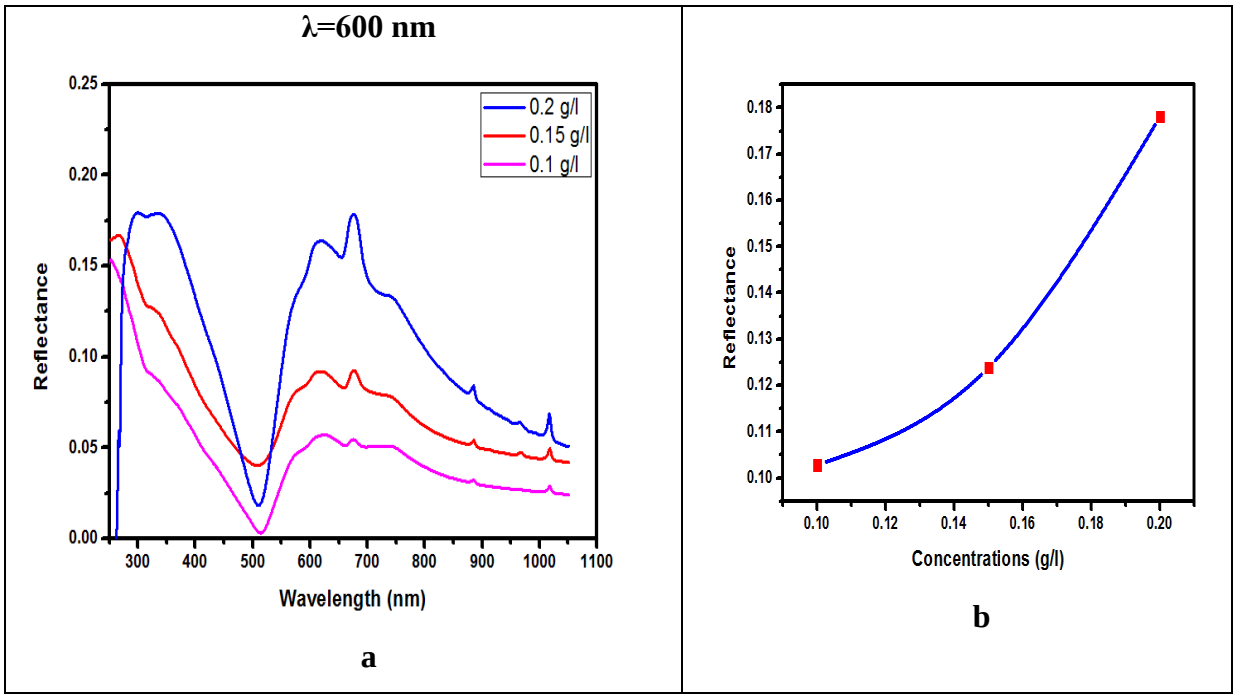

Figure(4.12) : a. Reflectance spectra with CuPc solutions concentrations (0.1 ,0.15,0.2)g/l for β+Irradiated samples in (5 day) . b. The Maximum Reflectance vs. the concentrations for β+ CuPc solutions at 600nm

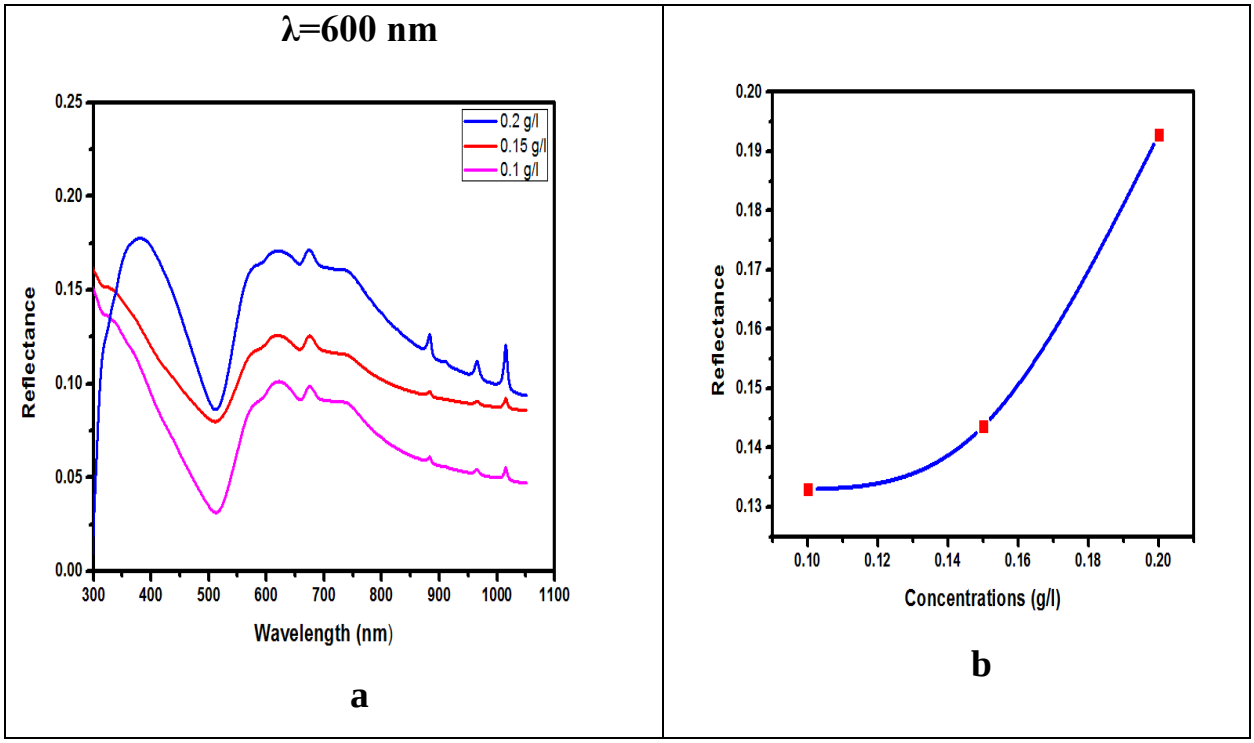

Figure(4.13) : a. Reflectance spectra with CuPc solutions concentrations (0.1 ,0.15,0.2)g/l for β-Irradiated samples in (5 day) . b. The Maximum Absorbance vs. the concentrations for β- CuPc solutions at 600nm

The transmittance spectra are measured for the solution concentrations (0.1 ,0.15 ,0.2) g/l was irradiated by Beta rays , simply it is shown in Figs. (4.14a, 4.15a) that the transmittance spectra is higher in concentration (0.1 g/l) and decrease with increasing the concentration(0.15 ,0.2 g/l).Obviously, the transmittance decreases with increasing the concentration as shown in Figs. (4.14b to 4.15b)

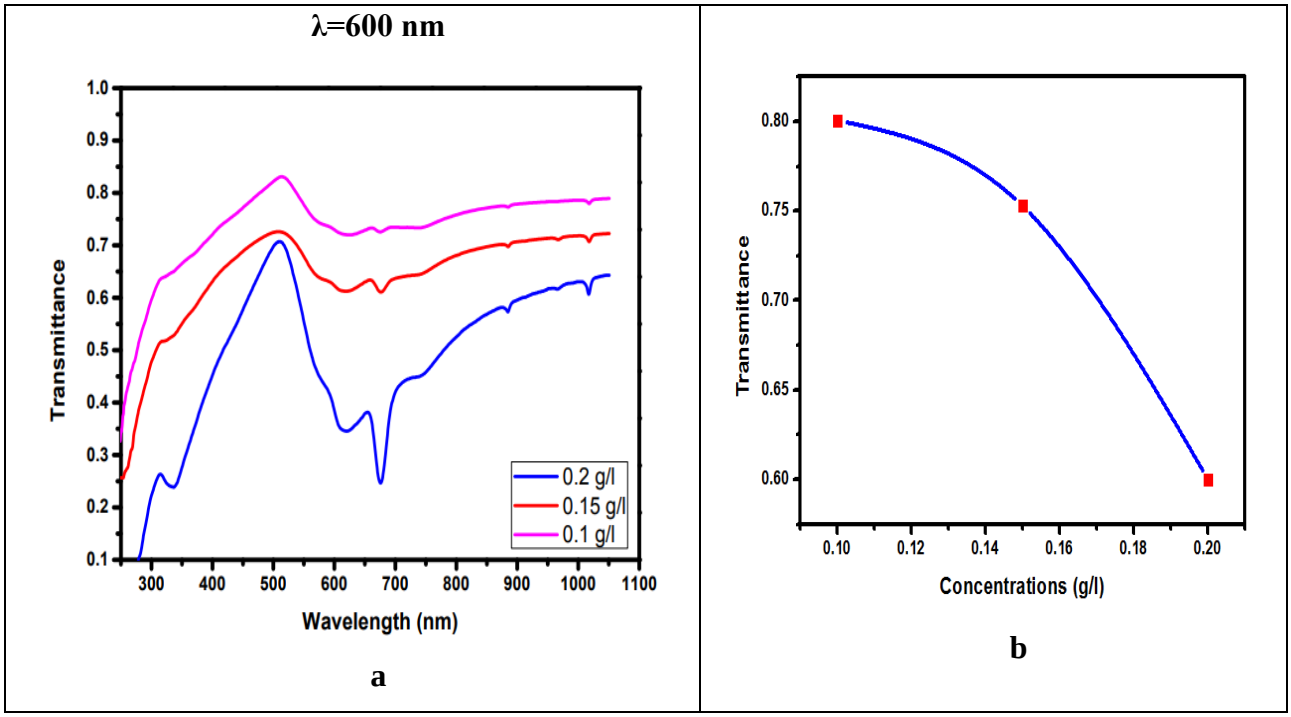

Figure(4.14): a. Transmittance spectra with CuPc solutions concentrations (0.1 ,0.15,0.2)g/l for β+Irradiated samples in (5 day) . b. The Maximum Transmittance vs. the concentrations for β+ CuPc solutions at 600nm

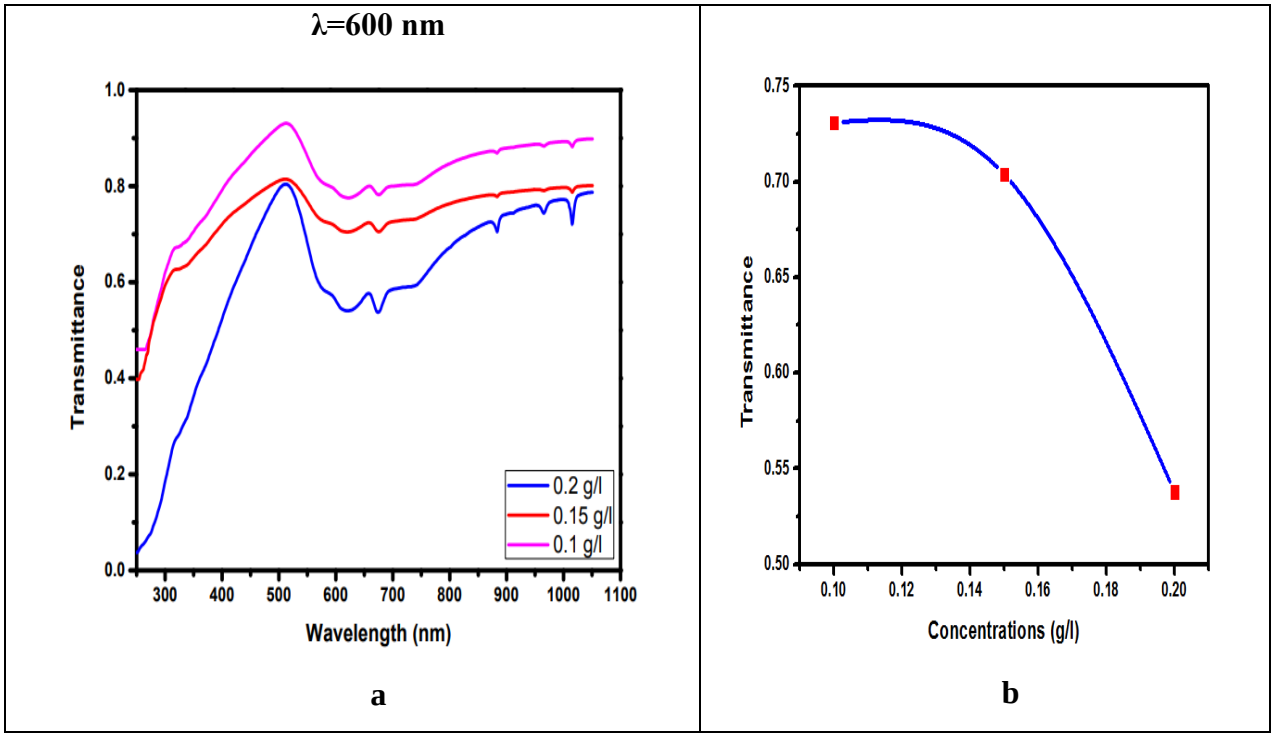

Figure (4.15): a. Transmittance spectra with CuPc solutions concentrations (0.1 ,0.15,0.2)g/l for β-Irradiated samples in (5day) . b. The Maximum Transmittance vs. the concentrations for β- CuPc solutions at 600nm

The indirect energy band gap calculated from the equation (2.6) using Tauc method ,the Figs. (4.16a , 4.17a) shows the tangent line intersect the energy axis with Eg values , increasing the number of molecules or increasing the ratio of the substance to the solution, ,which increases the number of local levels in the energy gap caused by the crystal defects as shown in Figs .(4.16b,4.17b)

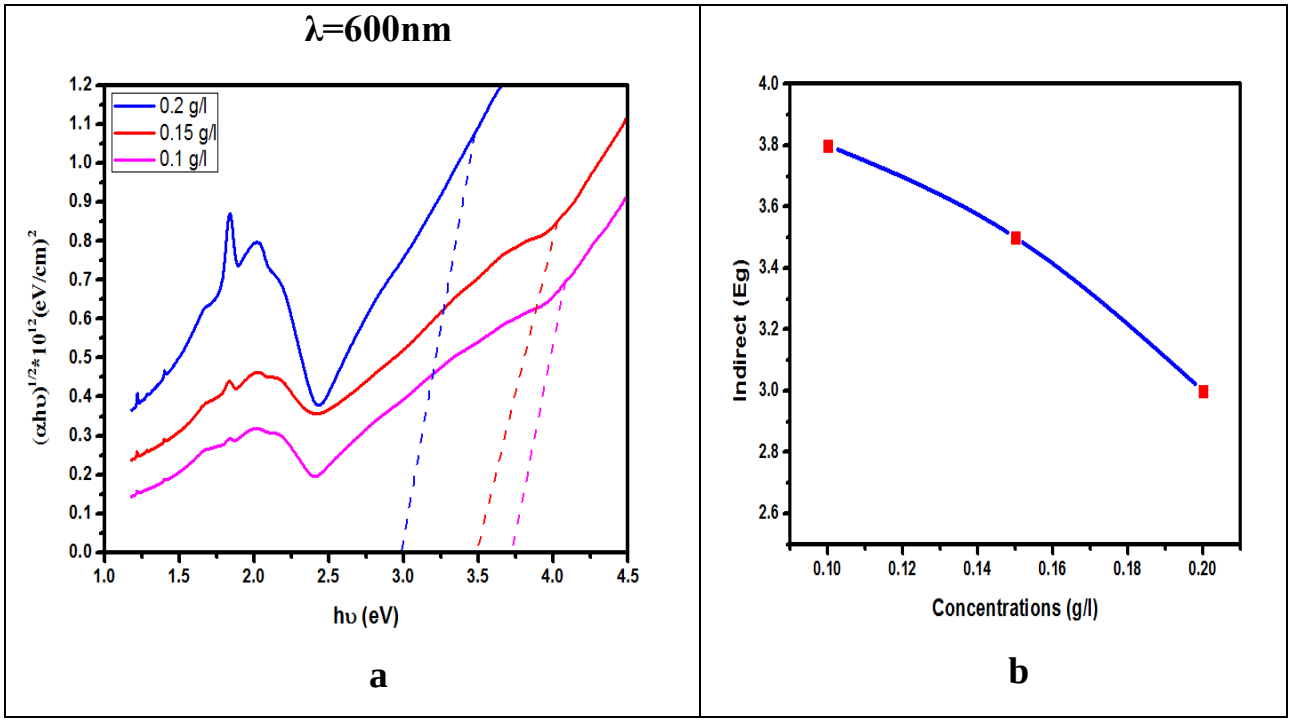

Figure (4.16): a. Determined indirect energy band gap for β+ ray CuPc solution with Concentrations (0.1,0.15,0.2) g/l. b. The Maximum indirect energy band gap vs.Concentrations at 600nm

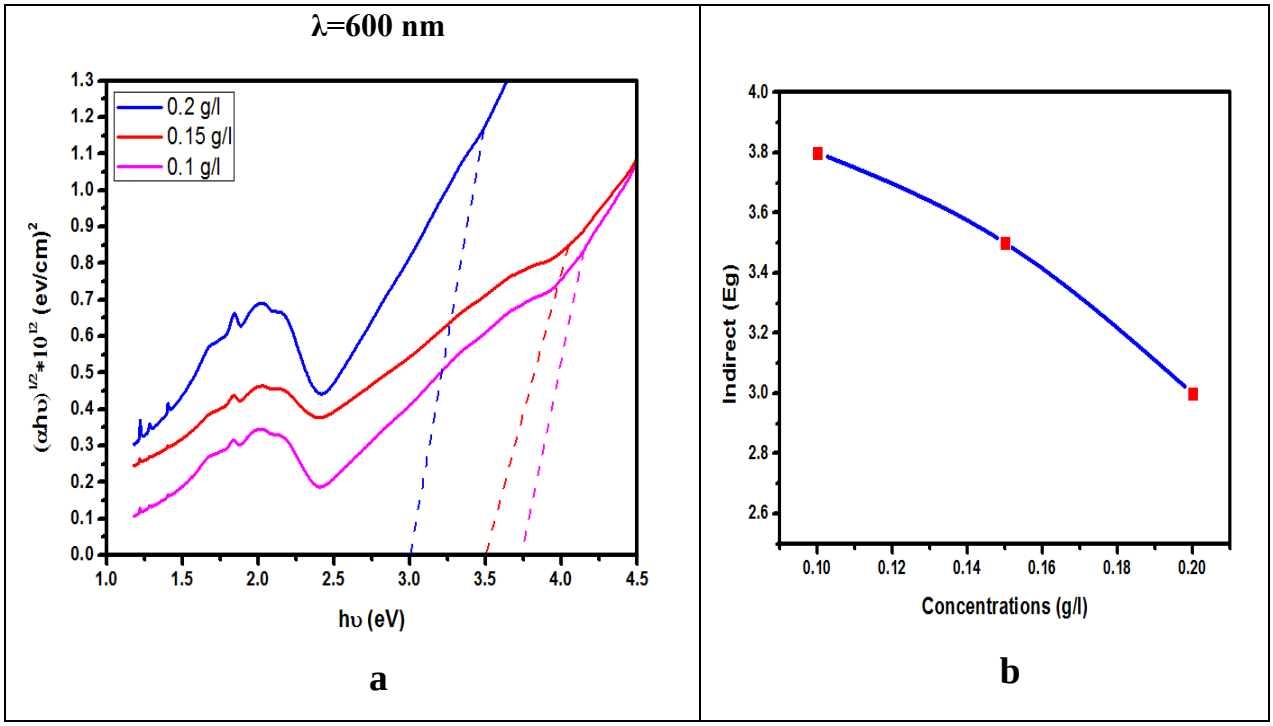

Figure (4.17): a. Determined indirect energy band gap for β- ray CuPc solution with Concentrations(0.1,0.15,0.2)g/l . b. The Maximum indirect energy band gap vs.Concentrations at 600nm

Optical parameters for CuPc solutions with concentration (0.15) g/l was irradiated by Plus and minus Beta ray as the Linear Absorption Coefficient (α) decreases due to a decrease in absorbance, since (α) less than 10^{-4}, it is indirect. The extinction coefficient (K) increases due to the increase in the number of molecules, and thus the attenuation of rays increases. The refractive index (n) depends mainly on the reflectance . The reflectance increased with the increase in the irradiating time. The Real dielectric constant(ε_r),The dielectric of a substance increases due to a decrease in the concentration of the substance upon its dissolution. The imaginary dielectric constant(ε_{img}) represents the loss in the electric field and its increase is due to the increase in the electric field stored in the insulating material and optical conductivity (σ) , The increase in the optical conductivity values is due to the increase of its two

main terms in the equation ($\sigma = \frac{\alpha nc}{4\pi}$) the refractive index and the absorption coefficient with an increase in the irradiation time as shown in Tables(4.3,4.4)

Table(4.3):Optical Constants for different Concentrations β+ CuPc Solutions

at λ= 600 nm							
Concentrations (g/L)	**α *10^4 (cm^{-1})**	**(K)**	**(n)**	**(ε_{Real})**	**($\varepsilon_{Im.}$)**	**Eg (eV)**	**σ optical (s^{-1})**
0.1	0.096	4.613 E-07	1.68	2.84	1.556E-06	2	0.038
0.15	0.123	5.891E-07	1.85	3.43	2.182E-06	1.9	0.054
0.2	0.22	1.059E-06	2.30	5.29	4.875E-06	1.7	0.121

Table(4.4):Optical Constants for different Concentrations β- CuPc Solutions

at λ= 600 nm							
Concentrations (g/l)	**α *10^4 (cm^{-1})**	**(K)**	**(n)**	**(ε_{Real})**	**($\varepsilon_{Im.}$)**	**Eg (eV)**	**σ optical (s^{-1})**
0.1	0.136	6.505E-07	1.92	3.687	2.498E-06	2	0.062
0.15	0.152	7.287E-07	2.00	4.038	2.928E-06	1.9	0.073
0.2	0.269	1.287E-06	2.43	5.921	6.263E-06	1.7	0.156

4.3.3 Effect of irradiation time on Optical properties for CuPc Thin Films Irradiated by Beta ray

The absorbance spectra for the wavelength range (300-1100 nm) are shown in Figures (4.18 a) to (4.21 a) for the UV-Vis results of CuPc thin films irradiated by Beta rays with a thickness of (197,214) nm. Increasing the duration of irradiation decreases the absorption of the solution in which the rays have broken the bonds and the molecules have lost their identity. As seen in Figs (4.18 b to 4.21 b). This result conforms with reference [65]

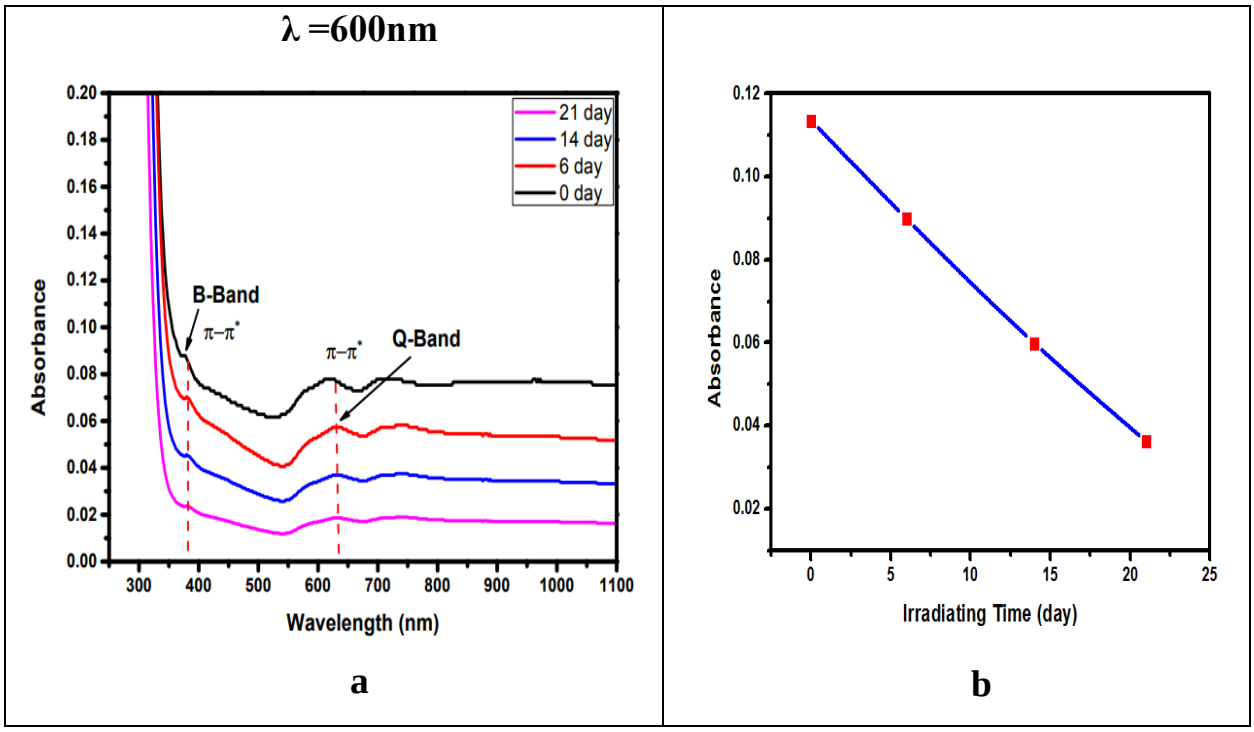

Figure(4.18): a.Absorbance spectra for β+ Cupc thin film with thickness (197) nm in period times . b. The Maximum Absorbance vs. irradating time for β+ Cupc thin film at 600 nm

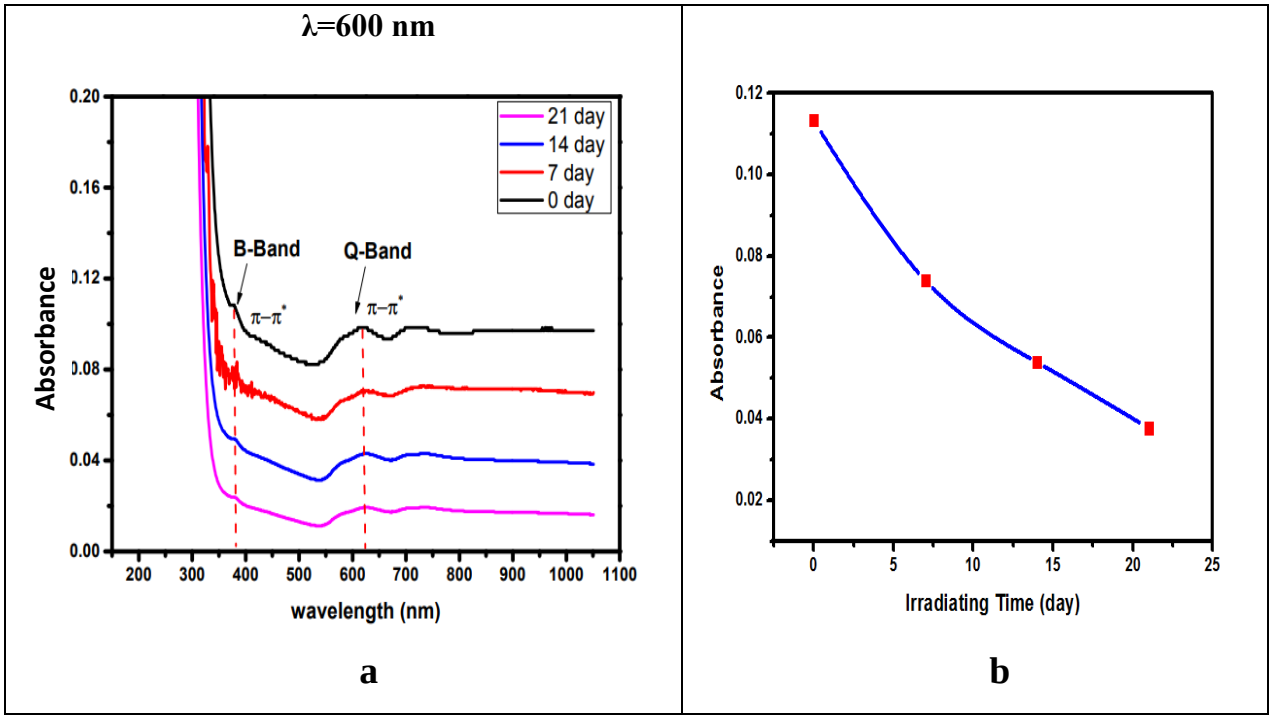

Figure(4.19): a.Absorbance spectra for β- Cupc thin film with thickness (197) nm in period times . b. The Maximum Absorbance vs. irradating time for β- Cupc thin film at 600 nm

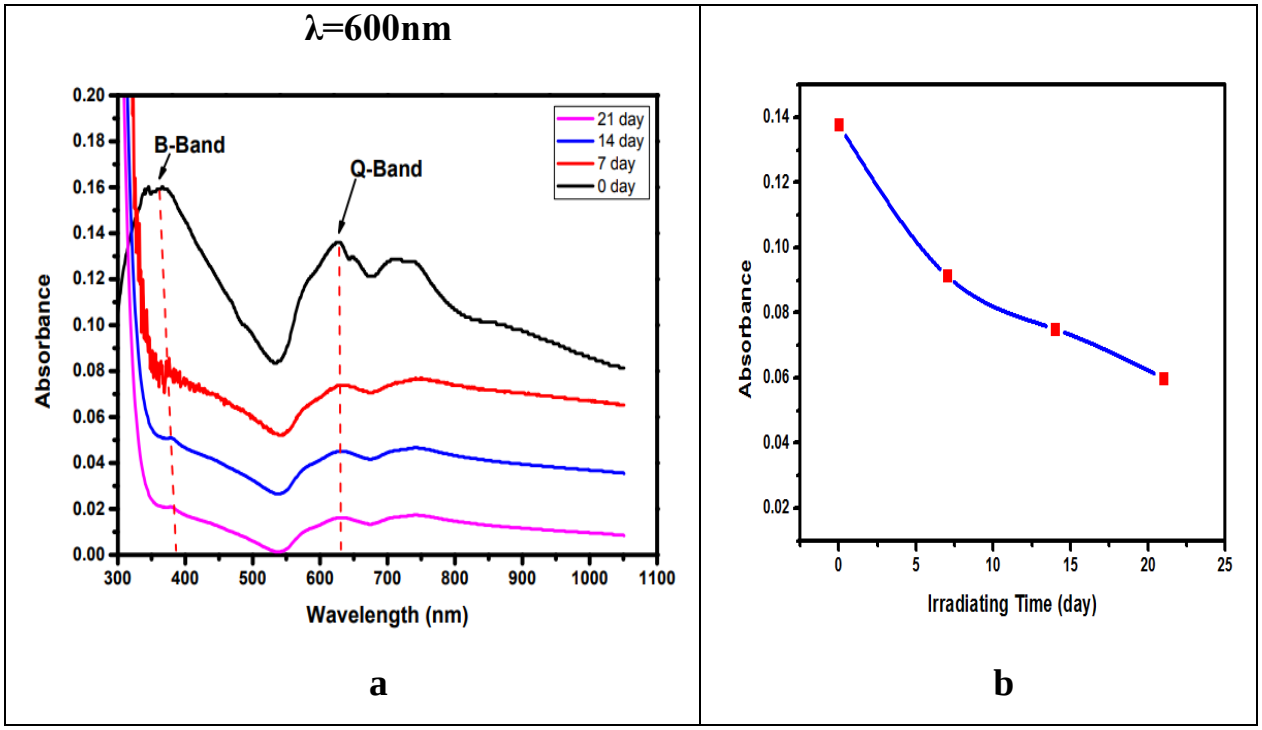

Figure(4.20): a.Absorbance spectra for β+ Cupc thin film with thickness (214) nm in period times . b. The Maximum Absorbance vs. irradating time for β+ Cupc thin film at 600 nm

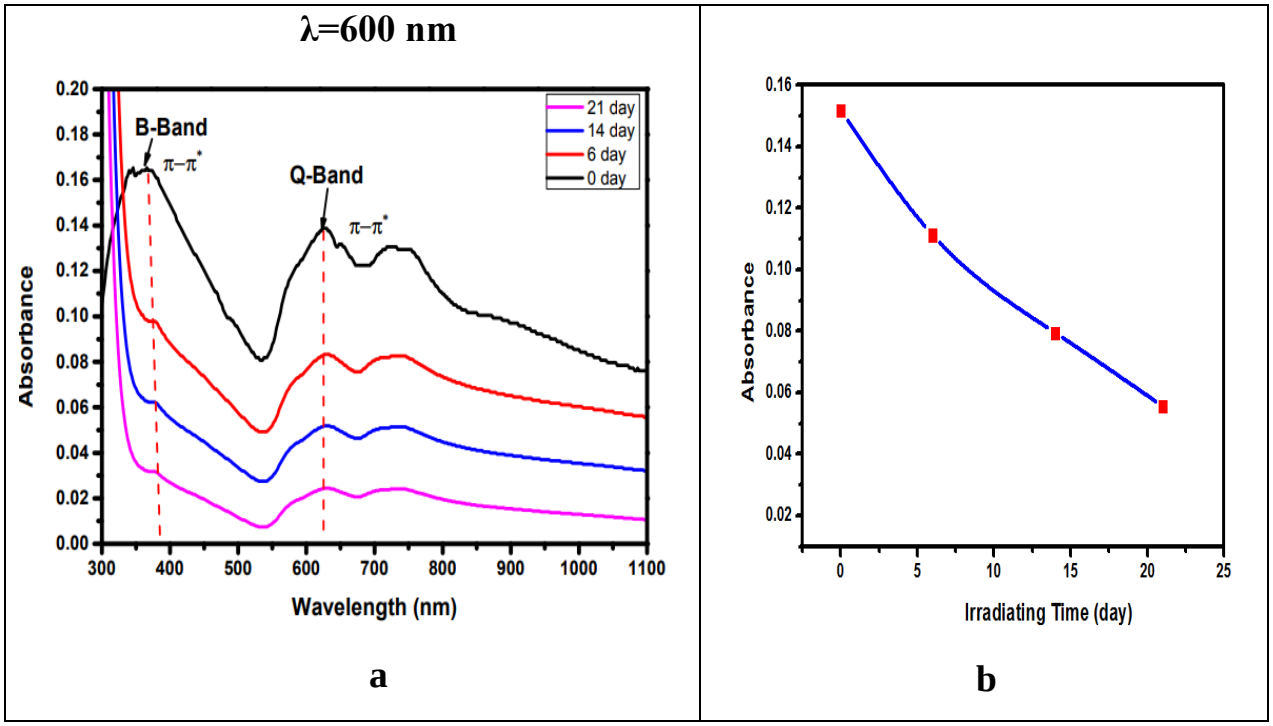

Figure(4.21): a. Absorbance spectra for β- Cupc thin film with thickness (214) nm in period times . b. The Maximum Absorbance vs. irradating time for β- Cupc thin film at 600 nm

Plus, minis Beta ray irradiation of the reflectance spectra with the thin films' thickness (197,214) nm simply demonstrates that the reflectance spectra is greater in the B band. As can be shown in Figs. 1 and 2, the maximum reflectance occurs at the greatest un radiated sample and decreases with increasing irradiation periods throughout a period of seven, fourteen, and twenty-one days at a wavelength of (600) nm (4.22a to 4.25a). The spectrum of maximum reflectance as a function of exposure time. As can be seen in Fig. 1, similar to the absorbance behaviour and discussion, the reflectance of unirradiated samples is highest at the beginning of the irradiation period (0 days) and falls as the irradiation period progresses (4.22b to 4.25b). The findings are consistent with the references [65]

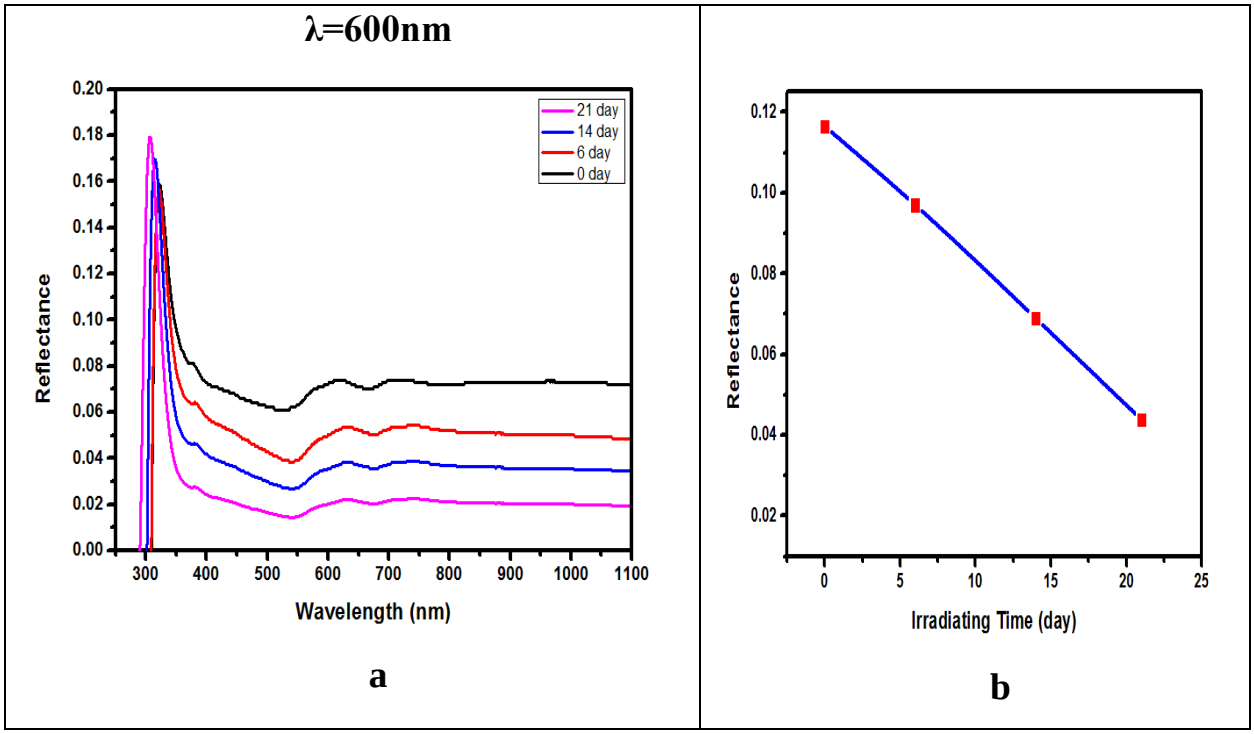

Figure(4.22): a.Reflectance spectra for β+ Cupc thin film with thickness (197) nm in period times . b. The Maximum Reflectance vs. irradating time for β+ Cupc thin film at 600 nm

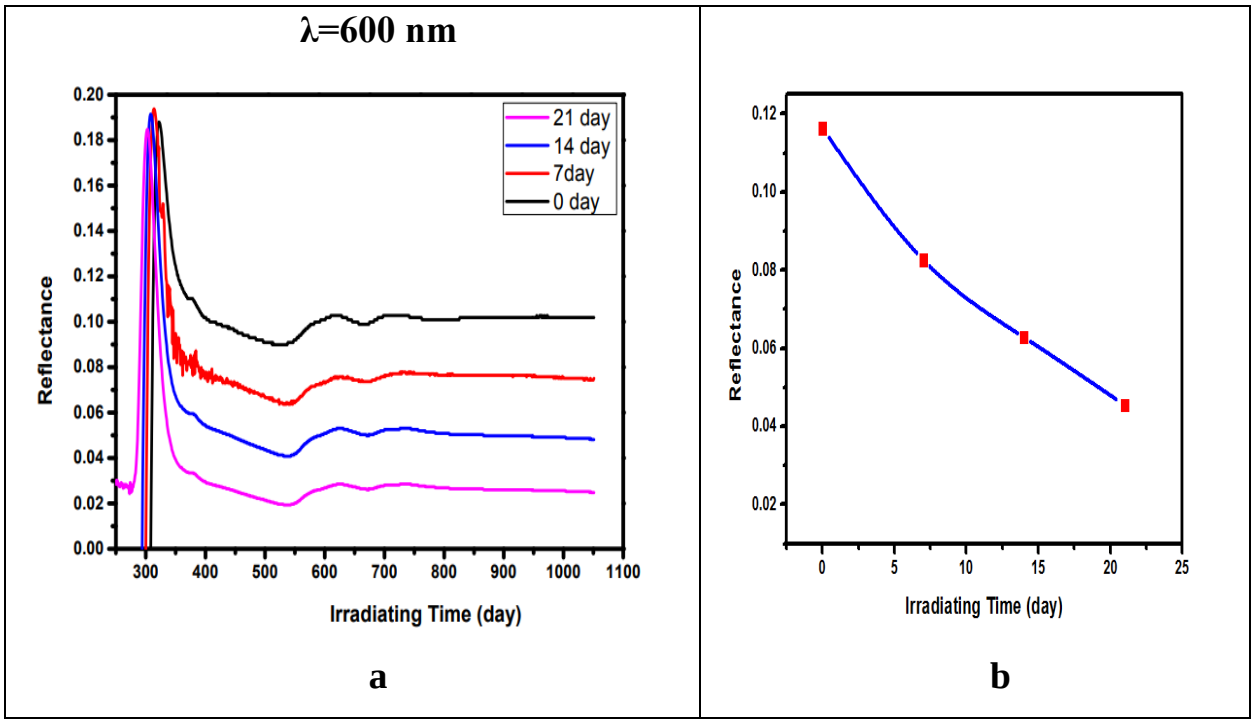

Figure(4.23): a.Reflectance spectra for β- Cupc thin film with thickness (197) nm in period times . b. The Maximum Reflectance vs. irradating time for β- Cupc thin film at 600 nm

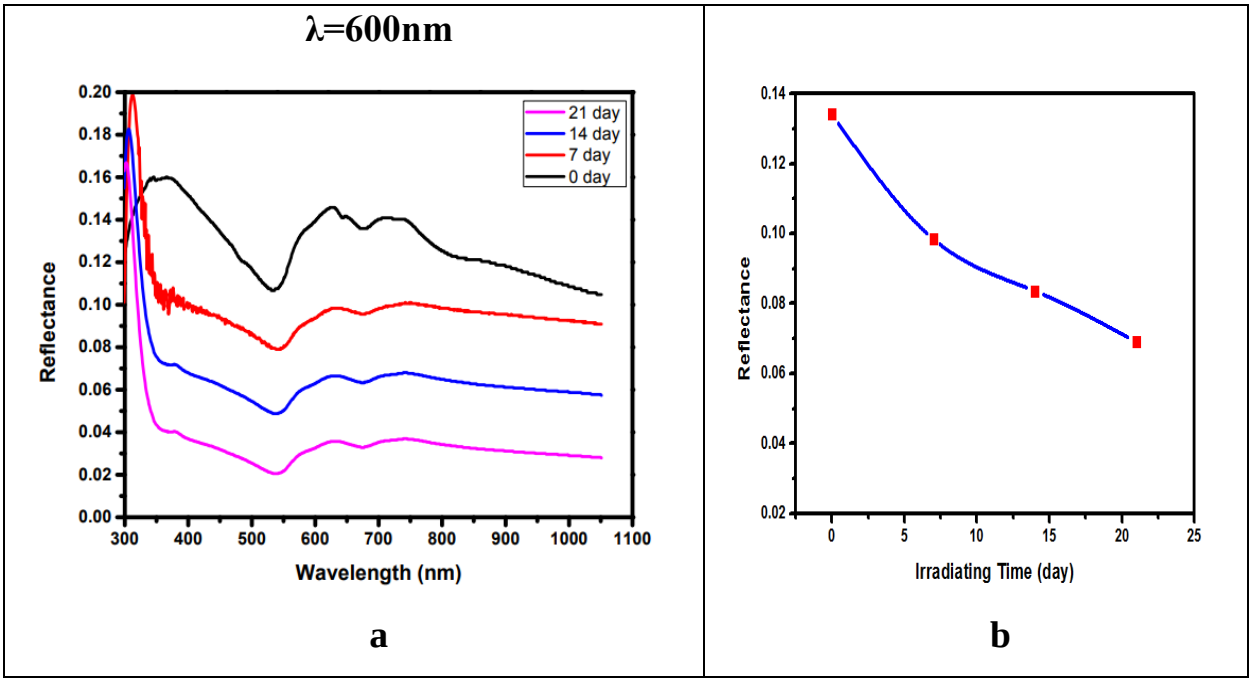

Figure(4.24): a.Reflectance spectra for β+ Cupc thin film with thickness (214) nm in period times . b. The Maximum Reflectance vs. irradating time for β+ Cupc thin film at 600 nm

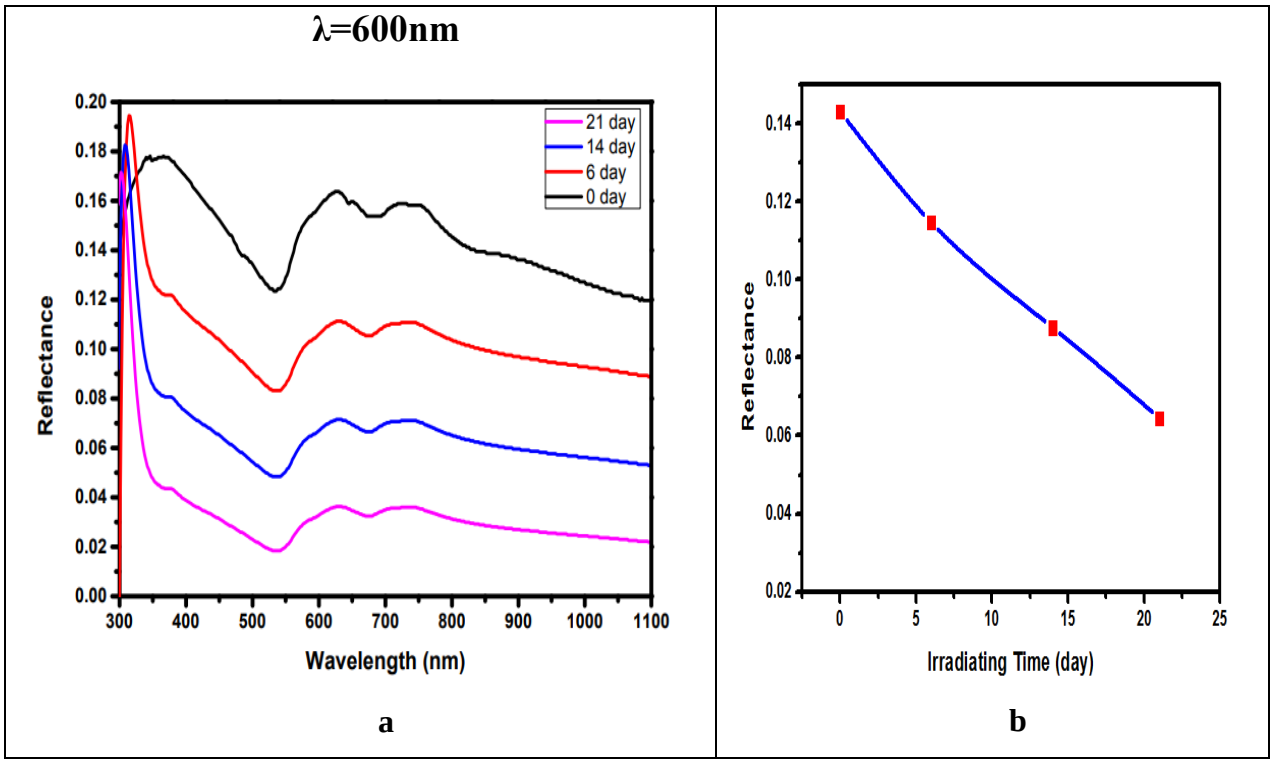

Figure(4.25): a.Reflectance spectra for β+ Cupc thin film with thickness (214) nm in period times . b. The Maximum Reflectance vs. irradating time for β+ Cupc thin film at 600 nm

Figures (4.26 a)–(4.29 a) indicate that the transmittance spectra is greater in the wavelength range(350-1100) nm, owing to the transmittance as opposed to absorbance, when the thin films of thickness (197,214)nm were irradiated by Beta rays. transmission spectra at their peak versus exposure time (0, 7 ,14 and 21 day). Figures (4.26 b) through (4.29 b) clearly demonstrate that when irradiation duration is extended, transmittance improves. The findings are consistent with the reference[65]

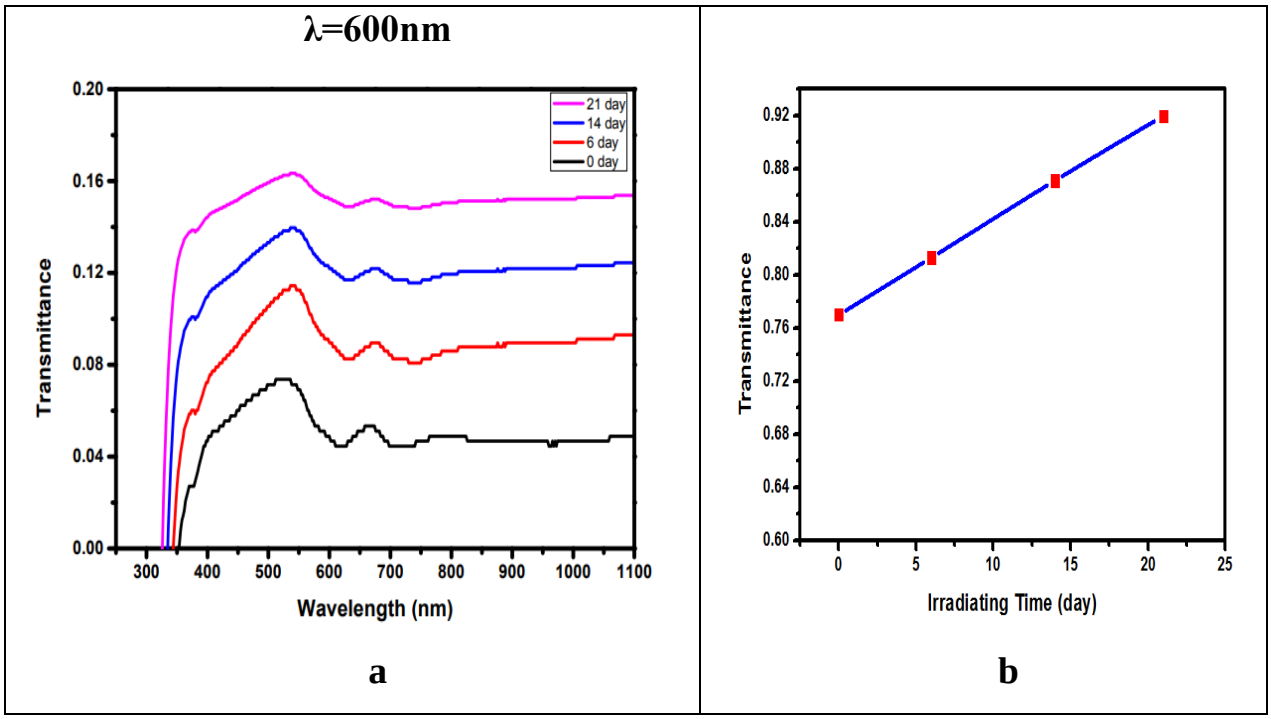

Figure(4.26): a.Transmittance spectra for β+ Cupc thin film with thickness (197) nm in period times . b. The Maximum Transmittance vs. irradating time for β+ Cupc thin film at 600 nm

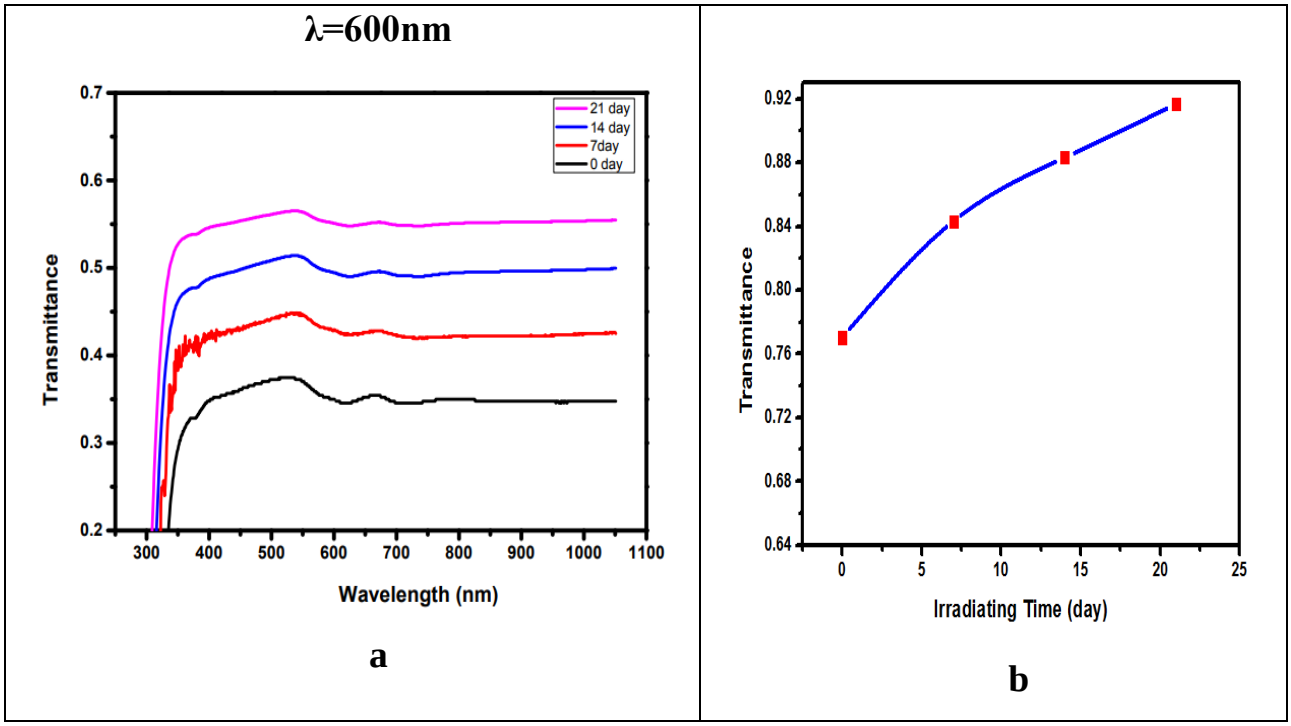

Figure (4.27): a.Transmittance spectra for β- Cupc thin film with thickness (197) nm in period times . b. The Maximum Transmittance vs. irradating time for β- Cupc thin film at 600 nm

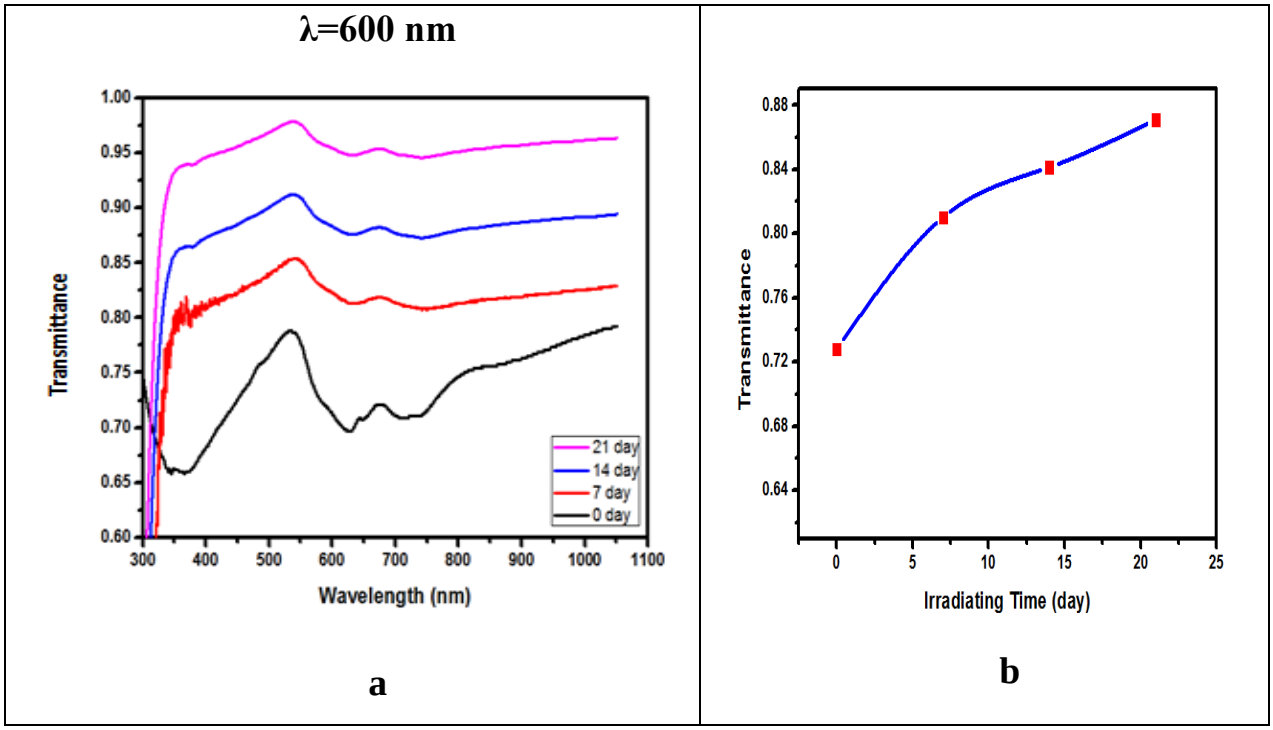

Figure(4.28): a.Transmittance spectra for β+ Cupc thin film with thickness (214) nm in period times . b. The Maximum Transmittance vs. irradating time for β+ Cupc thin film at 600 nm

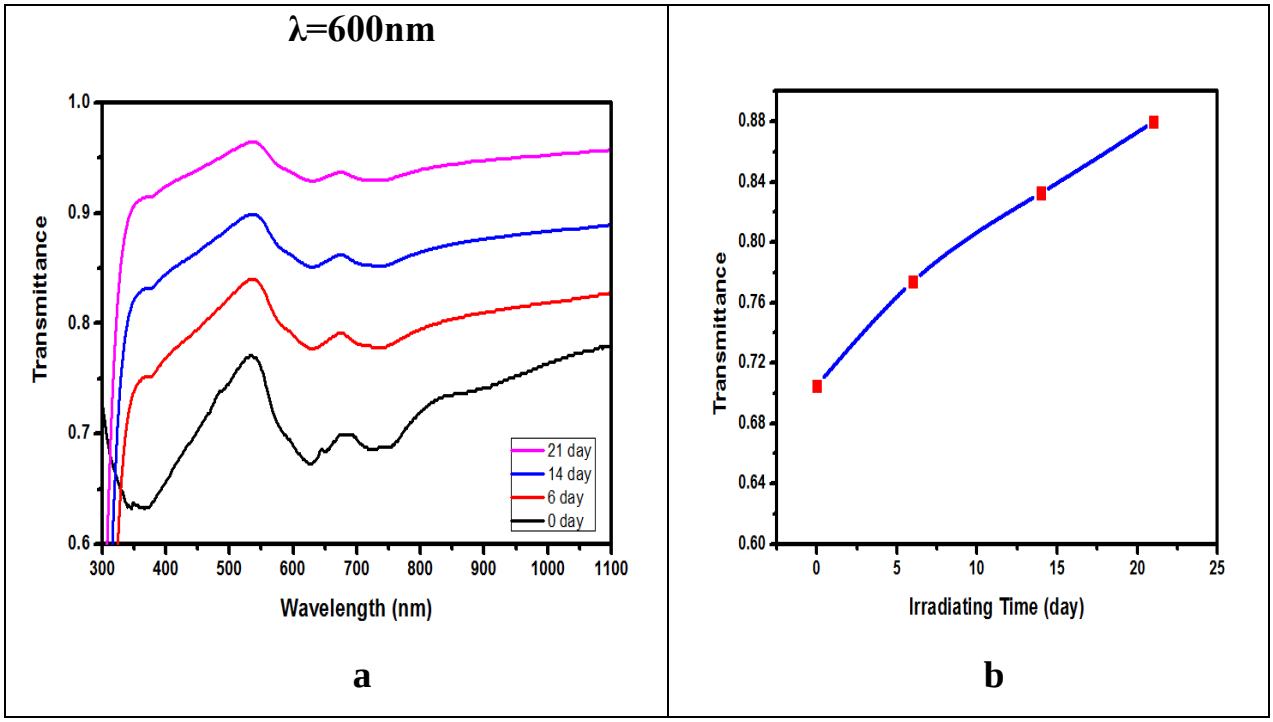

Figure(4.29): a.Transmittance spectra for β- Cupc thin film with thickness (214) nm in period times . b. The Maximum Transmittance vs. irradating time for β- Cupc thin film at 600 nm

The tangent line in Figs. (4.30 a) to (4.33 a) intersects the energy axis at Eg values, indicating that the broken molecules contribute to low absorbance and little defect in the material, as predicted by the indirect energy band gap obtained from equation (2.6) using the Tauc technique (4.30 b to 4.33 b). The findings are consistent with the references [118]

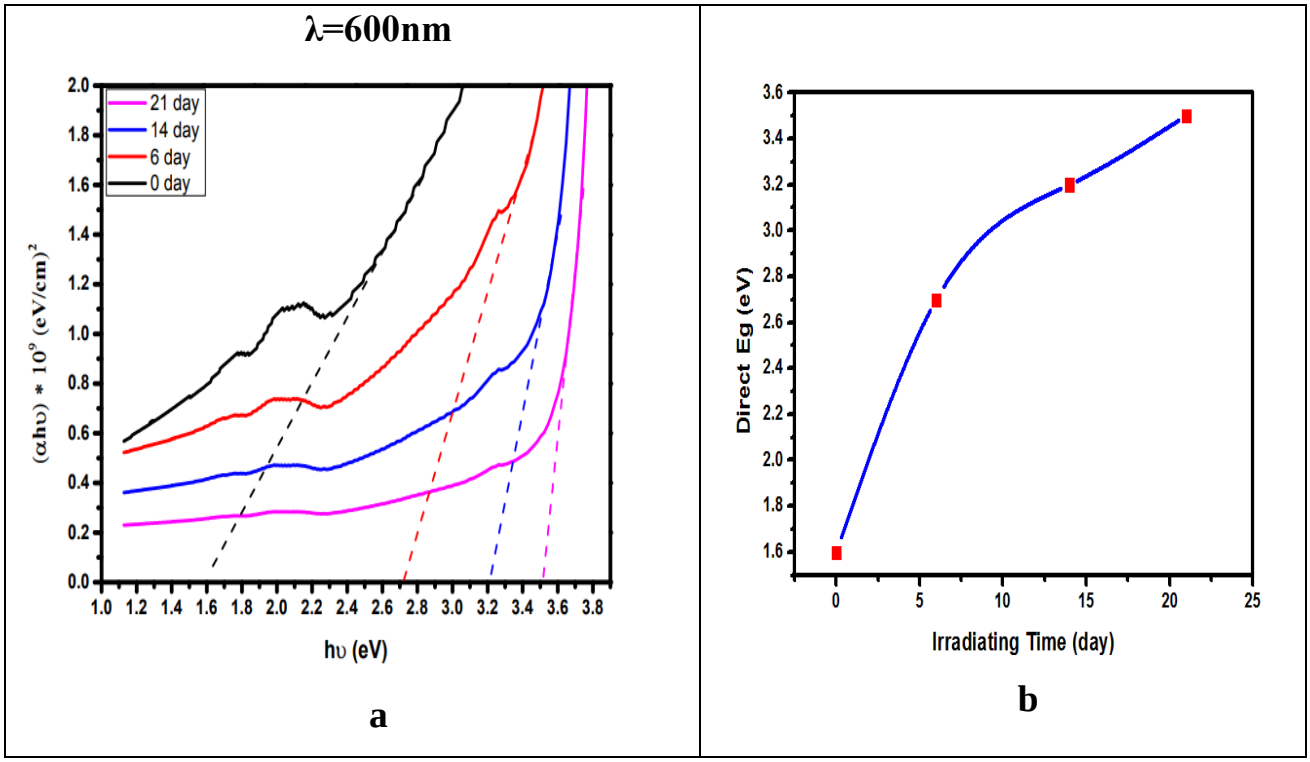

Figure (4.30): a. Determined Direct energy band gap for β+ ray CuPc Thin film with thickness(197)nm in period time b. The Maximum Direct energy band gap vs.Irradiating time at 600nm

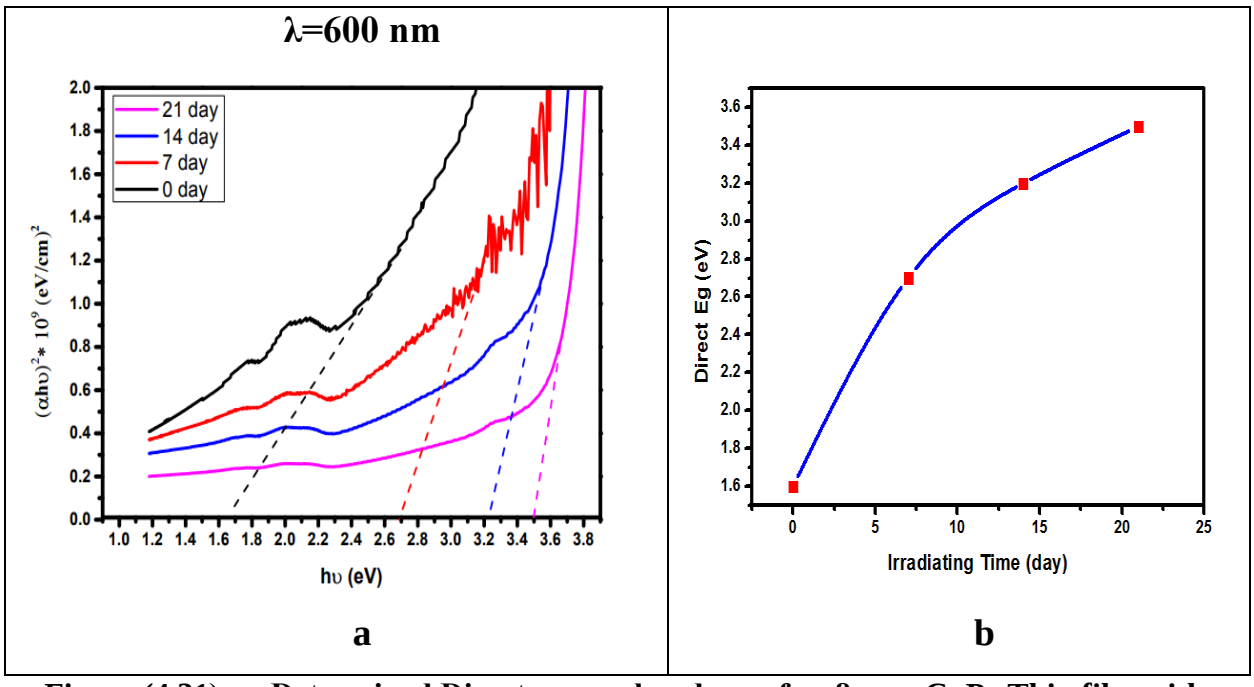

Figure (4.31): a. Determined Direct energy band gap for β- ray CuPc Thin film with thickness(197)nm b. The relation between Maximum Direct energy band gap and irradiating time at 600nm

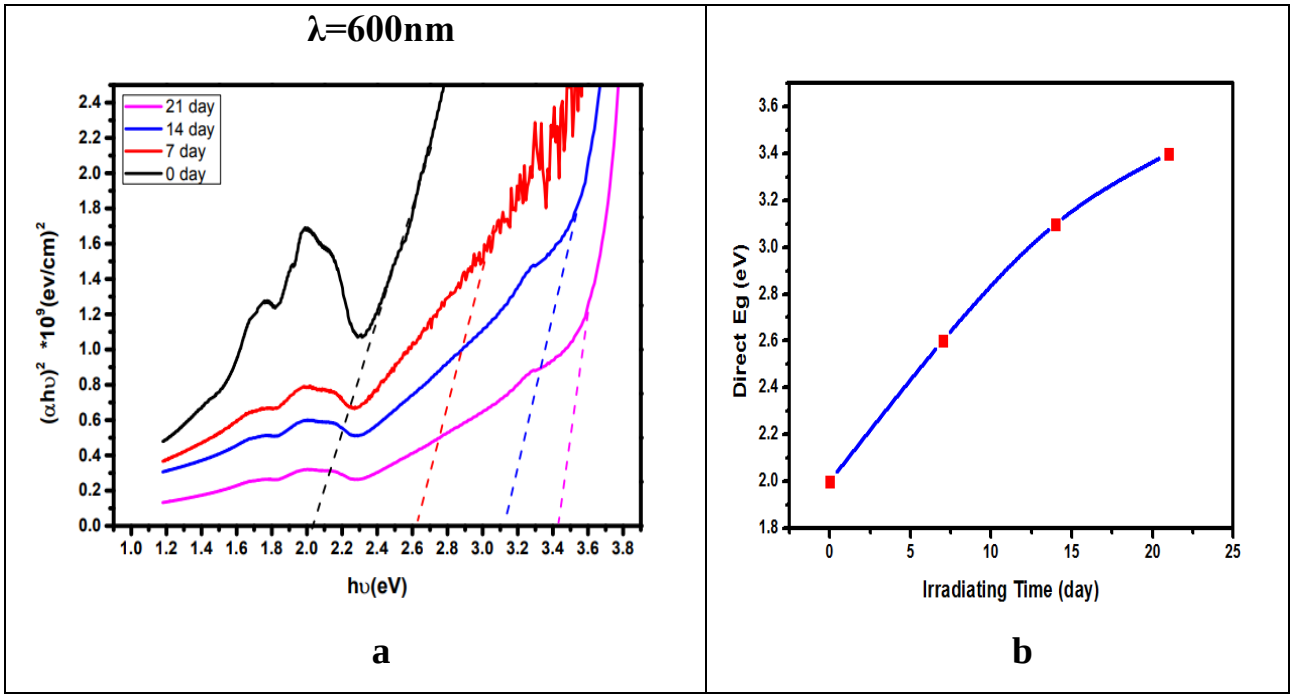

Figure (4.32): a. Determined Direct Energy Band Gap for β+ ray CuPc thin film with thickness(214)nm b. The Relation between Maximum Direct Energy Band Gap and irradiating time at 600nm

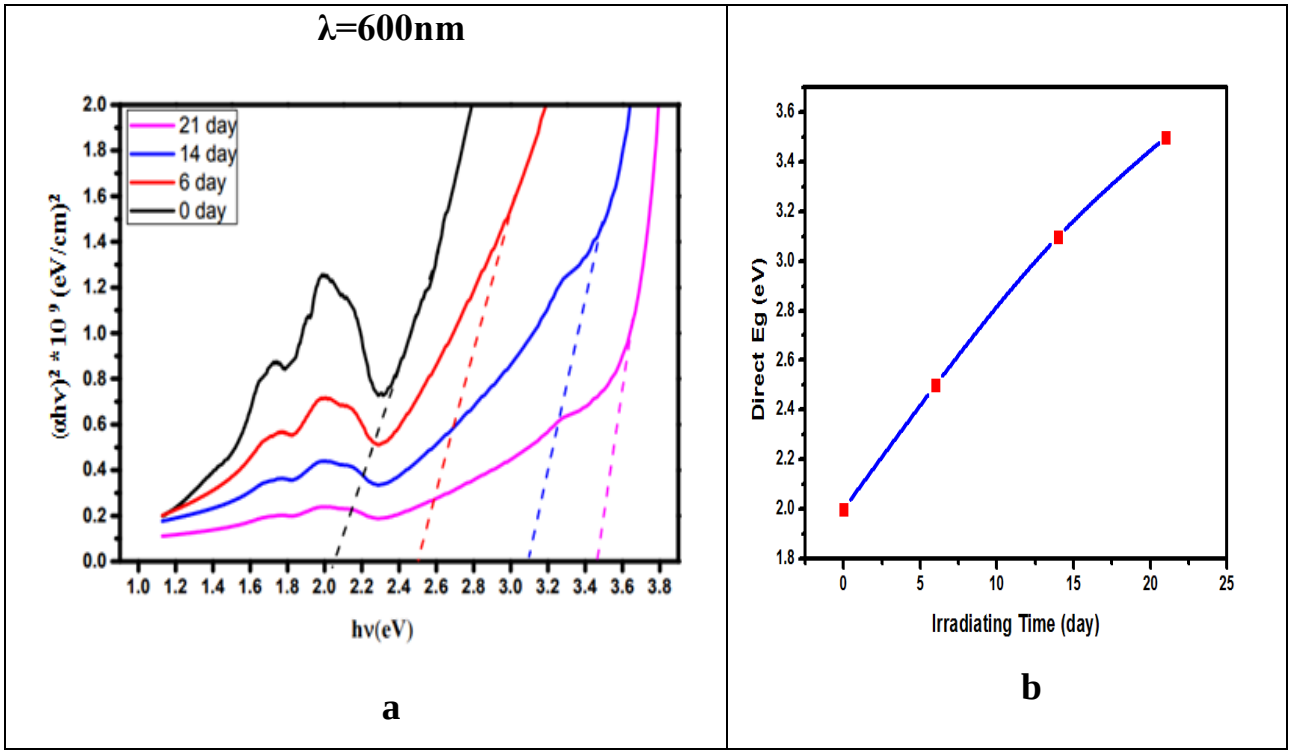

Figure (4.33): a. Determined Direct Energy Band Gap for β- ray CuPc thin film with thickness(214)nm b. The Relation between Maximum Direct Energy Band Gap and irradiating time at 600nm

Optical parameters for thin films at thicknesses(197,214)nm was irradiated by Plus, munis Beta ray as the Linear Absorption Coefficient (α) decreases due to a decrease in absorbance, since (α) less than 10^{-4} is indirect, The extinction coefficient (K) decreases due to the decrease in the number of dye molecules, and thus the attenuation of rays decreases, The refractive index (n) depends mainly on the reflectance , and the reflectance decreased with the increase in the irradiating time[118], The Real dielectric constant(ε_r); The dielectric of a substance decreases due to a decrease in the thickness of the thin film on the substance upon its dissolution, The imaginary dielectric constant(ε_{img}) represents the loss in the electric field and its decrease is due to the decrease in the electric field stored in the insulating material [118] and optical conductivity (σ) ; The decrease in the optical conductivity values is due to the decrease of its two main terms in the equation($\sigma = \frac{\alpha n c}{4\pi}$) the refractive index and the absorption coefficient with an increase in the irradiation time as shown in Tables(4.5 to 4.8)

Table(4.5): Optical constants for β+CuPc thin film at thickness 197 nm

at λ= 600 nm							
irradiating time (day)	**α *10^4 (cm^{-1})**	**(K)**	**(n)**	**(ε_{Real})**	**($\varepsilon_{Im.}$)**	**Eg (eV)**	**σ optical (s^{-1})**
0	2.178	0.104	1.794	3.210	0.373	1.6	0.934
6	1.723	0.082	1.646	2.703	0.271	2.7	0.677
14	1.149	0.054	1.444	2.083	0.158	3.2	0.396
21	0.696	0.033	1.257	1.625	0.084	3.5	0.212

Table(4.6): Optical constants for β-CuPc thin film at thickness 197 nm

at λ= 600 nm							
irradiating time (day)	α *10^4 (cm^{-1})	(K)	(n)	(ε_{Real})	($\varepsilon_{Im.}$)	Eg (eV)	σ optical (s^{-1})
0	2.175	0.103	1.793	3.206	0.372	1.6	0.931
7	1.419	0.067	1.541	2.371	0.209	2.5	0.522
14	1.034	0.049	1.402	1.964	0.138	3.1	0.346
21	0.724	0.034	1.286	1.652	0.088	3.5	0.222

Table(4.7): Optical constants for β+CuPc thin film at thickness 214 nm

at λ= 600 nm							
irradiating time (day)	α *10^4 (cm^{-1})	(K)	(n)	(ε_{Real})	($\varepsilon_{Im.}$)	Eg (eV)	σ optical (s^{-1})
0	1.484	0.070	1.931	3.726	0.273	2.1	0.684
7	0.984	0.047	1.655	2.739	0.155	2.6	0.389
14	0.807	0.038	1.547	2.394	0.119	3.1	0.298
21	0.645	0.030	1.445	2.087	0.089	3.4	0.222

Table(4.8): Optical constants for β-CuPc thin film at thickness 214 nm

at λ= 600 nm							
irradiating time (day)	α *10^4 (cm^{-1})	(K)	(n)	(ε_{Real})	($\varepsilon_{Im.}$)	Eg (eV)	σ optical (s^{-1})
0	1.633	0.078	2.005	4.015	0.313	2	0.782
7	1.197	0.057	1.778	3.160	0.203	2.5	0.508
14	0.855	0.040	1.577	2.486	0.128	3.1	0.322
21	0.598	0.028	1.414	1.999	0.080	3.4	0.202

4.4 Results of Photoluminescence Spectra for CuPc Thin Films

The photoluminescence spectrum, also known as the emission spectrum, is important because it provides information about the optical energy bandgap, and the energy gap value determined using the photoluminescence spectrum is more accurate than that computed using the Tauce equation. The photoluminescence spectra of CuPc thin films at various irradiation times are shown in Figs. (4.34-4.36), and the optical energy gap values are presented in Tables (4.9,4.10), and they are compared to Eg calculated using the Tauce equation, and all Eg values reported by PL spectra are identical to those derived by Tauce equation approach for all irradiating times.

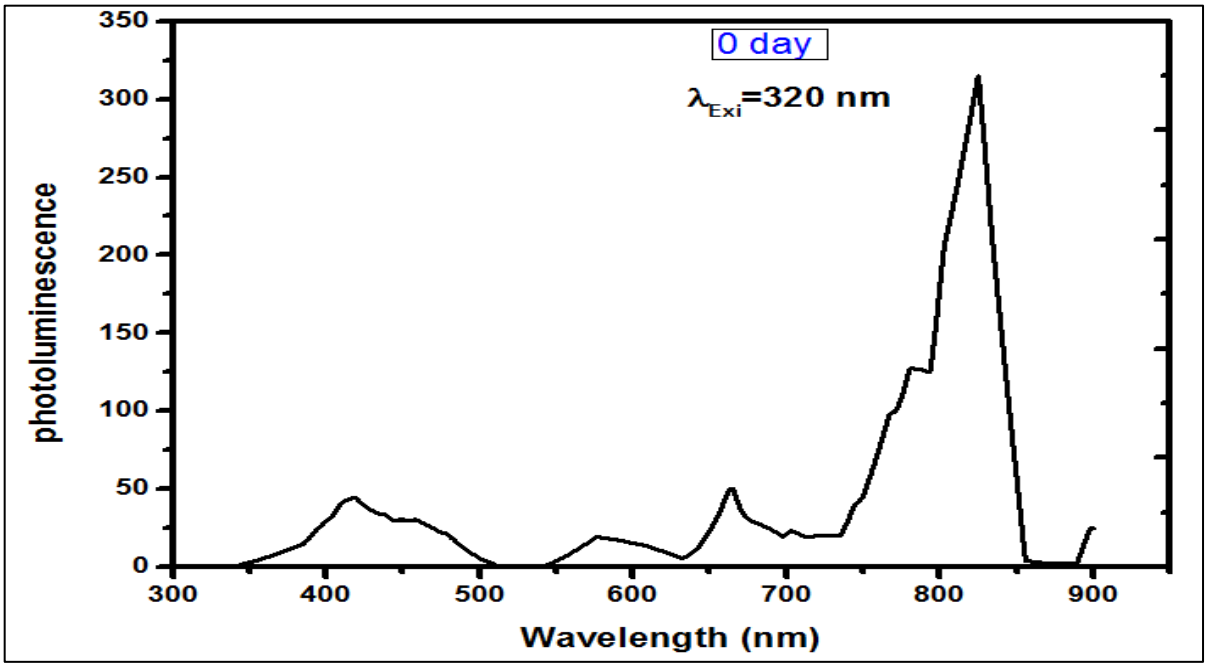

Figure (4.34): Photoluminescence Spectra For un Radiation Cupc Thin Films

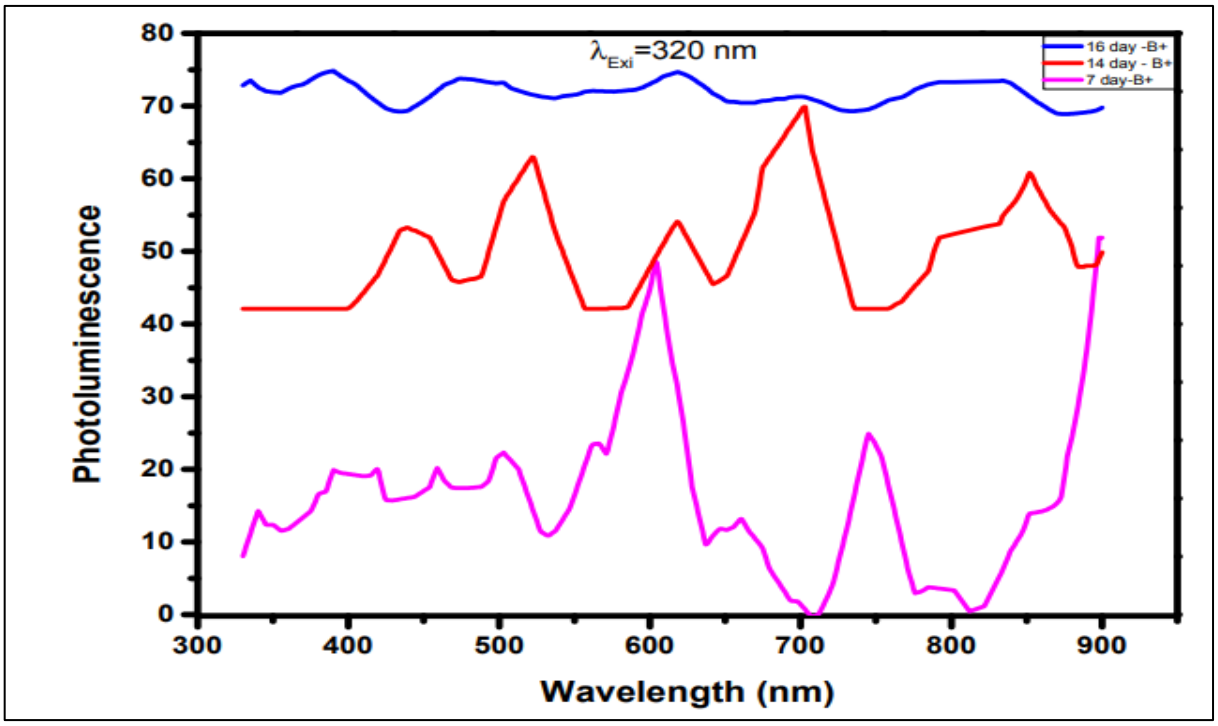

Figure (4.35): Photoluminescence spectra for CuPc thin films at different irradiating time of Beta ray source (β+)

Table (4.9): Energy gap obtained by Photoluminescence and Tauce method at different irradiating time of Beta ray source (β+)

Irradiating Time (day)	Eg (Tauce) (eV)	Eg (PL) (eV)	Mistake percentage %
0	2	2.1	0.9
7	2.6	2.4	1.4
14	3.1	2.8	1.7
16	-	3.17	-
21	3.5	-	-

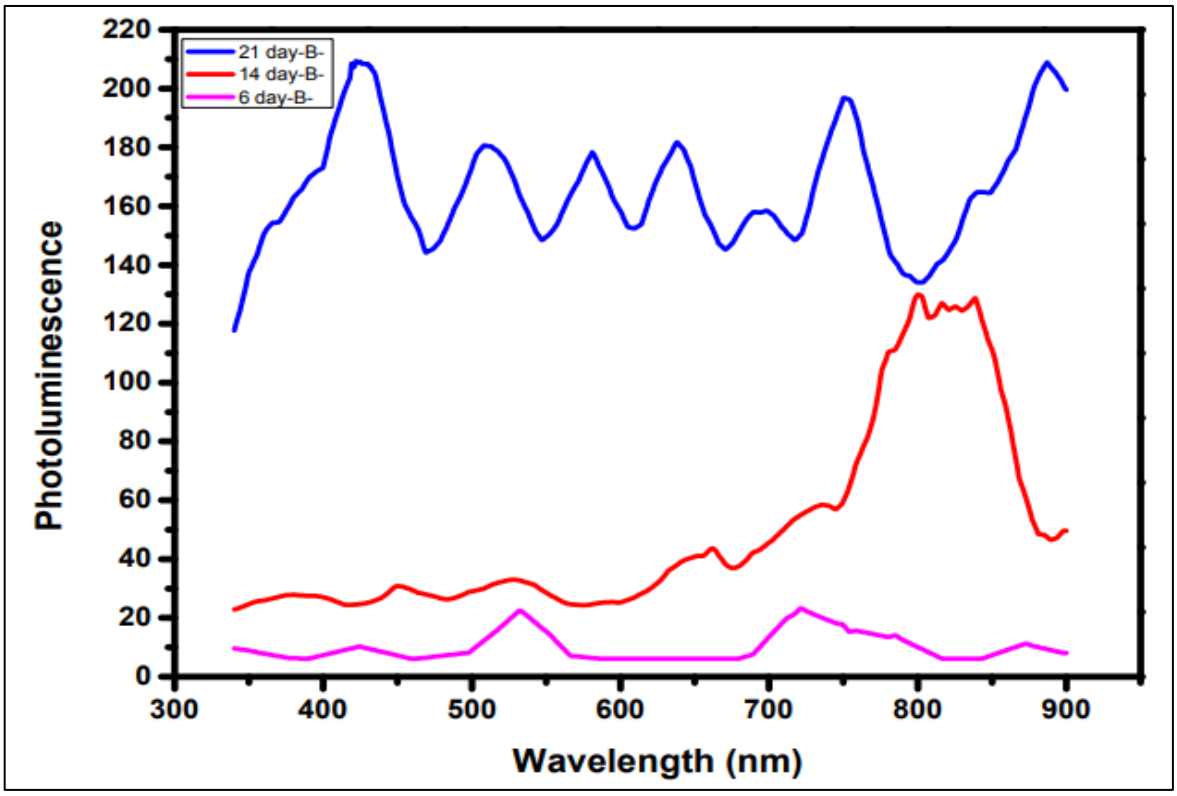

Figure (4.36): Photoluminescence Spectra for CuPc thin films at different irradiation time of Beta ray source (β-)

Table (4.10) :Energy gap obtained by Photoluminescence and Tauce method at irradiating time Minis beta ray(β-)

Irradiating Time (day)	Eg (Tauce) (eV)	Eg (PL) (eV)	Mistake percentage %
0	2	2.1	1.2
6	2.5	2.3	1.5
14	3.1	2.9	1.6
21	3.5	3.02	1.9

4.5 Results of Structural properties and Surface Morphology

4.5.1 XRD Results of CuPc

4.5.1.1 XRD Results of CuPc Powder

The X-Ray diffraction spectra for CuPc powder material, were recorded as illustrated in Figure (4.37). The crystal system is triclinic (anorthic),and lattice constants (a,b,c), and the lattice angles(α, β,γ)and d were calculated and Compared with the standard values in the card (JCPDS :96-210-3884), illustrated in Table (4.11).we can see the X-ray diffraction for CuPc powder is polycrystlaine , similar data have been also obtained by other researchers. Also, the average crystal size was calculated by plotting full width at half maximum against inverse of Cos(θ) according to Shirrer equation ($D = \frac{0.9\lambda}{\beta cos\theta}$). as shown in figure (4.37)

.

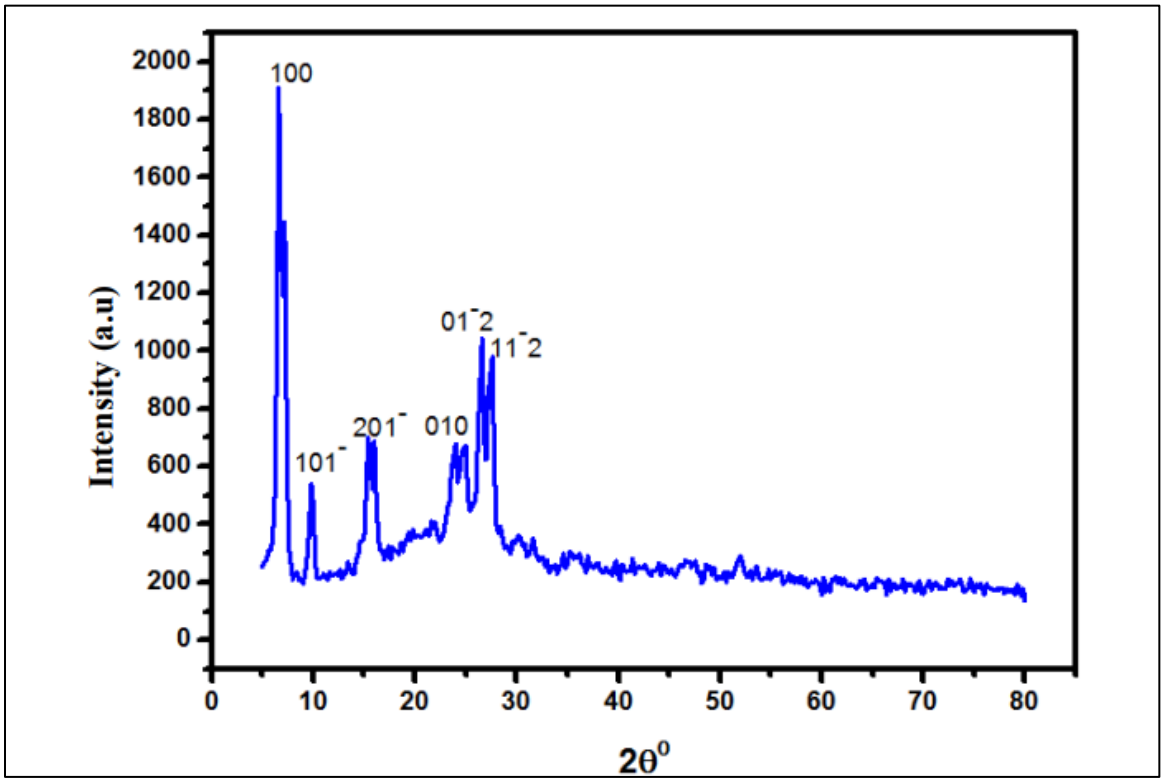

Figure (4.37): The XRD Spectrum for CuPc Powder

Table (4.11) :The Lattices Constants and Crystalline Angle of Cupc Powder Parameter

A (A^0)= 12.88	**α = 96.22^0**
B (A^0)= 3.76	**β= 90.62^0**
C(A^0)= 12.06	**γ= 90.32^0**

The structural parameters for CuPc polycrystalline structural powder were investigated as shown in Table (4.12).

Table (4.12): The structural parameters of CuPc polycrystalline structural powder.

2θ	d(nm)	I%	hkl	FHWM	D(nm)
6.688	1.32058	100	100	0.45	17
9.81	0.90088	21.8	$10^{-}1$	0.47	17
15.46	0.57267	28.4	201^{-}	0.74	10
21.628	0.41055	9.3	$1^{-}12$	1.27	6
23.988	0.37067	26.9	010	1.56	5
26.571	0.33519	50.7	$0^{-}12$	0.95	8

4.5.1.2 XRD for CuPc thin films for plus Beta ray (β+)

X-ray diffraction pattern of CuPc thin films with different irradiating time of β+ shown in the figure (4.16). XRD pattern indicates that all the samples are poly crystalline and that it has a β-crystalline phase [4-8]. Well-defined diffraction peaks by (100) gives the direction of the preferential orientation as deposited film (JCPDS, File No. 11-0744).

Table (4.13) shows the structure parameters of CuPc films, The full width at half maximum (FWHM) of preferential orientation, shows that the FWHM are reduced with increasing irradiating time , which represents better lattice quality ,The average crystal size D of the film which calculated using the Scherer eq.(2.18) Crystal angles decrease, the distance between planes increases and crystal size increases with increasing irradiating time at (7,14 and 21) day , thus crystal defects increases.

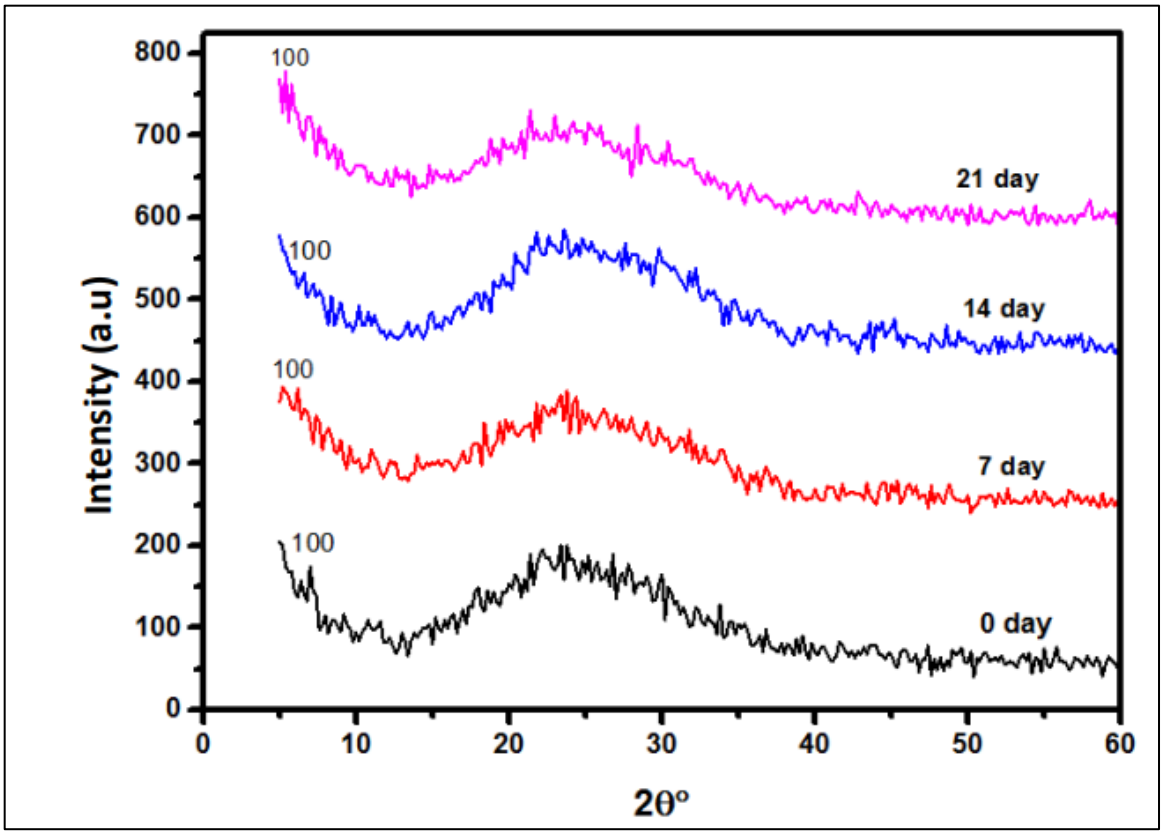

Figure (4.38): XRD Pattern For Cupc Thin Films irradiated by Beta ray Source (β+) at different irradiating time

Table(4.13): Structure Parameters of CuPc Thin Films Irradiated β+ Ray Source

0 day				7 day - β+				14 day - β+				21 day - β+			
2θ (deg)	d (nm)	FWHM (deg)	D (nm)	2θ (deg)	d (nm)	FWHM (deg)	D (nm)	2θ (deg)	d (nm)	FWHM (deg)	D (nm)	2θ (deg)	d (nm)	FWHM (deg)	D (nm)
9.2	0.95	0.74	10	7.4	1.45	0.73	12	6.6	4.88	0.6	13	5.4	0.99	0.59	14

4.5.1.3 XRD for CuPc thin films for Beta Ray source (β-)

The XRD pattern for CuPc thin films irradiated by Minus Beta ray source (Sr-90) at different irradiating time (6 ,14 and 21)days , were recorded and structure parameters were calculated as shown in Fig.(4.39) and the Table (4.14).

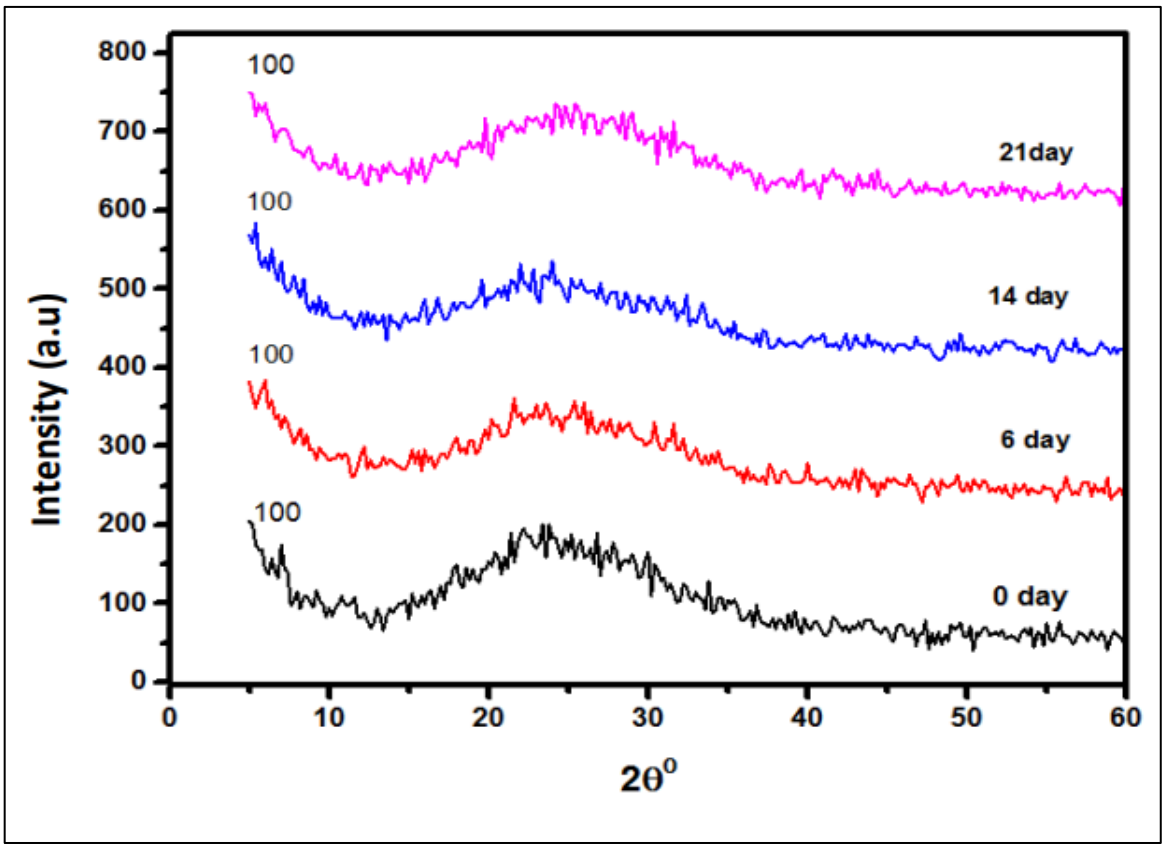

Figure (4.39): XRD pattern for CuPc thin films irradiated by Minus Beta ray source (β-) at different irradiation time

Table (4.14): Structure Parameters of Cupc Thin Films Irradiated β- Ray Source

0 day				6 day – β-				14 day – β-				21 day – β-			
2θ (deg)	d (nm)	FWHM (deg)	D (nm)	2θ (deg)	d (nm)	FWHM (deg)	D (nm)	2θ (deg)	d (nm)	FWHM (deg)	D (nm)	2θ (deg)	d (nm)	FWHM (deg)	D (nm)
9.2	0.95	0.74	10	6.00	1.47	0.67	11	6.4	1.36	0.59	13	5.9	1.47	0.58	13

4.5.2 Results of Surface Morphology for CuPc Thin Films

4.5.2.1 Atomic Force Microscope Measurements

The morphology and surface morphology of CuPc thin films of positive and negative beta rays with a thickness of 214 nm were studied using atomic force microscopy (AFM), which is characterized by a high analytical power of (1.0-0.1) nm and a magnification power of($5*10^2$-10^8) to examine the nature of the surface and its high potential in giving statistical values about the rate of grain size and how it is distributed on the surface, as well as the degree of surface roughness of the prepared films based on the square root mean of the roughness (RMS)), as well as giving three-dimensional pictures of the examination.

Figures (4.40, 4.42) show the three-dimensional surface topography of CuPc thin films at thickness(214 nm) irradiated with (β+), which was prepared with different irradiating times (0, 7, 14and 21) day , and(β-) with irradiating time (0, 6, 14and 21) days .

Figures (4.41,4.43) show granular distribution diagrams of a surface CuPc thin films with a thickness of 214 nm and irradiated with plus and Minus beta rays at different irradiation times), these diagrams show the number of grains as a function of their diameters.

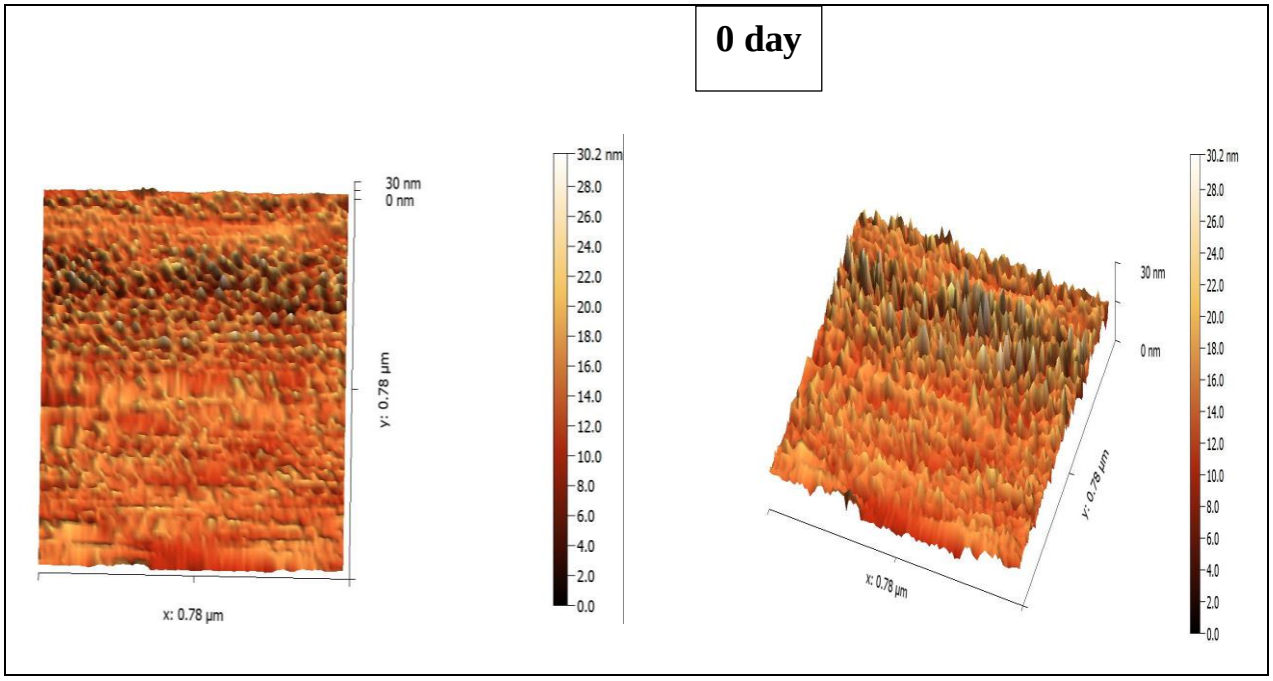

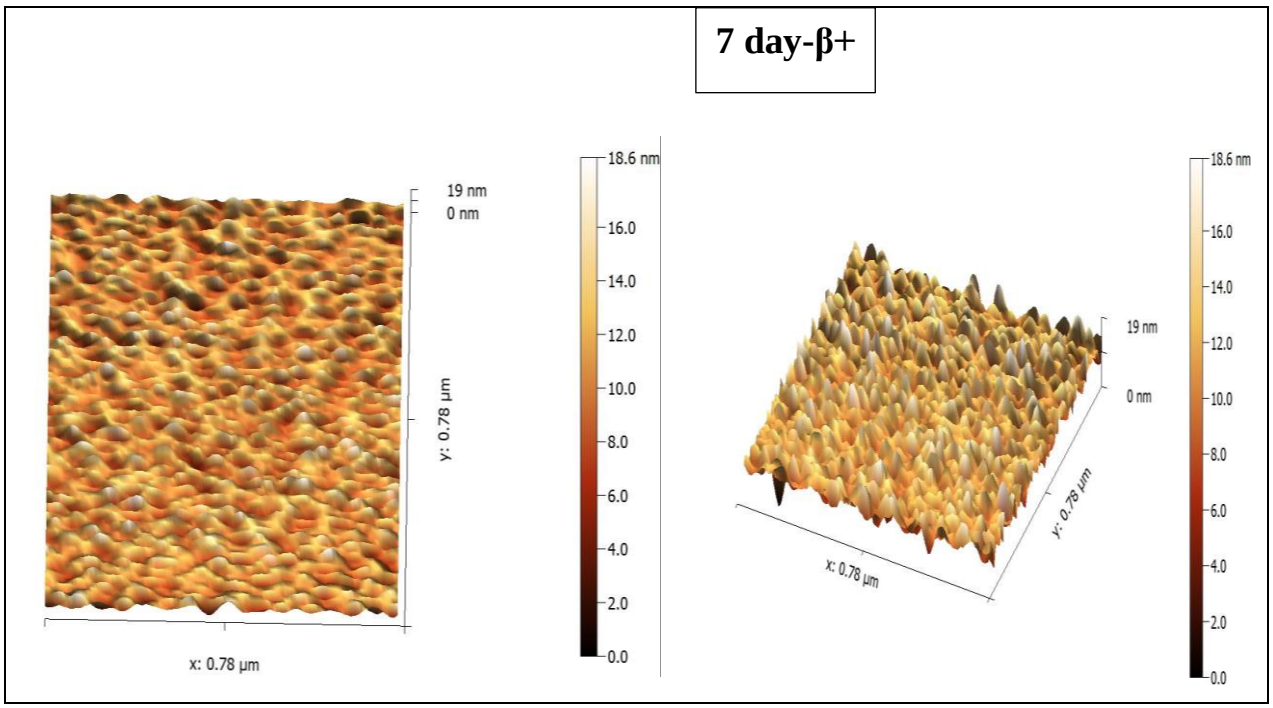

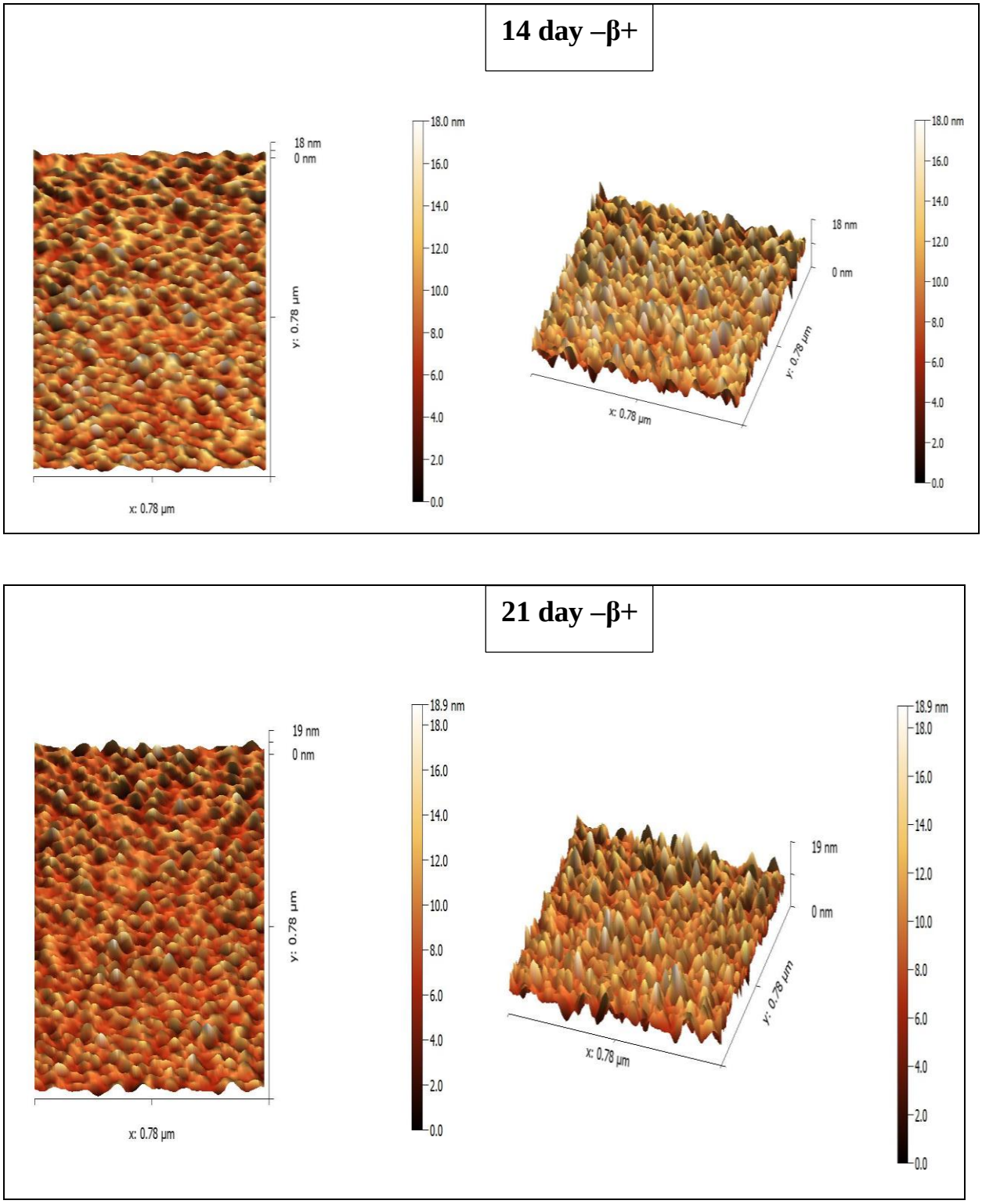

Figure (4.40) : 2D and 3D AFM images of CuPc thin films Irradiated by(β^+) with different irradiating times

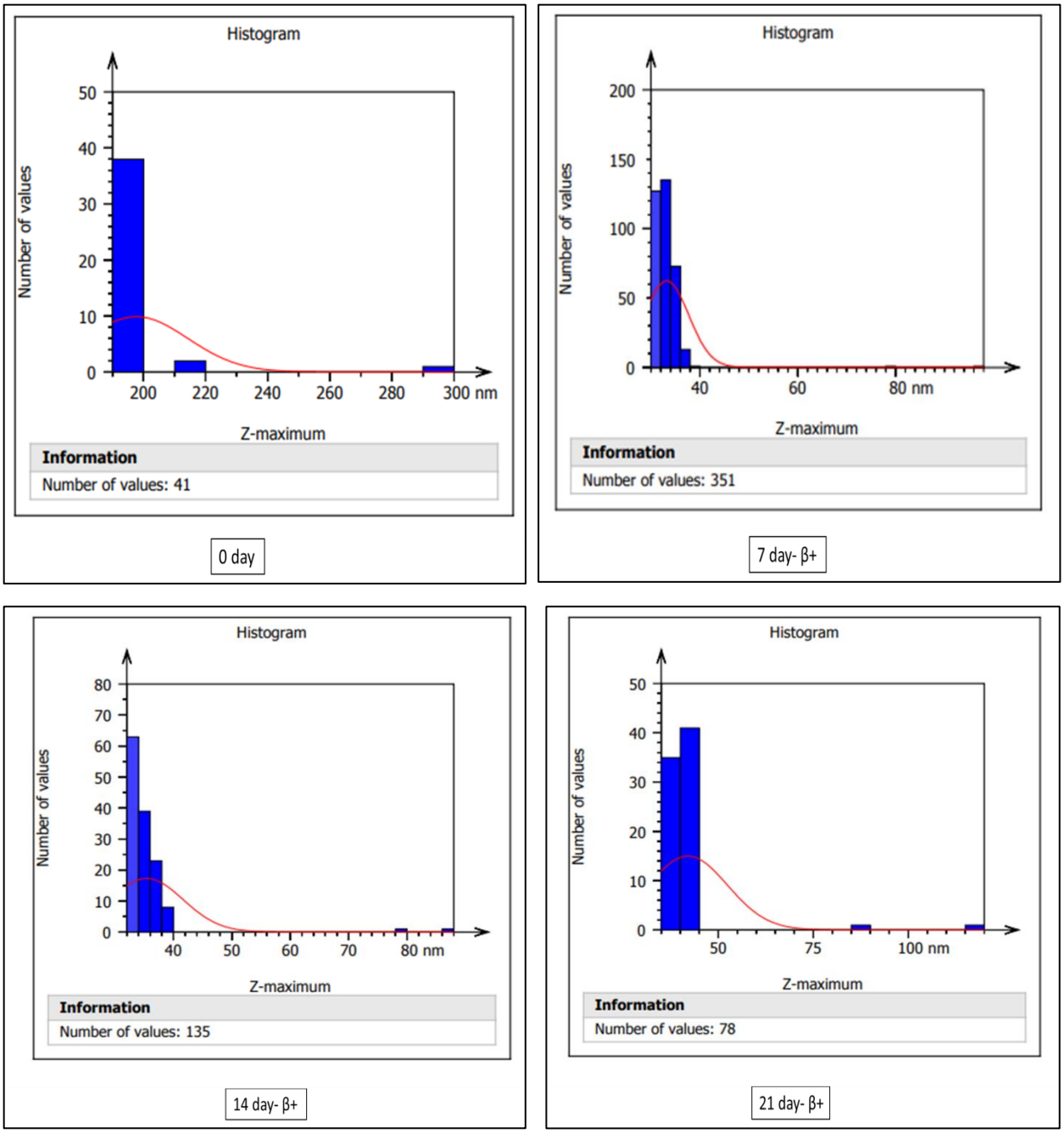

Figure (4.41): show granular distribution diagrams of a surface CuPc thin films with a thickness of 214 nm and irradiated with β+ at different irradiating times

Table (4.15) : AFM Measurements for CuPc irradiated with Plus Beta ray(β+)

irradiating time (day)	Grain size (nm)	Roughness (nm)	Diameter (nm)	RMS (nm)
0	13.61	11.66	197.7	2.21
7	10.86	3.873	33.23	2.24
14	10.06	3.794	35.38	2.59
21	10.15	1.94	42.02	2.44

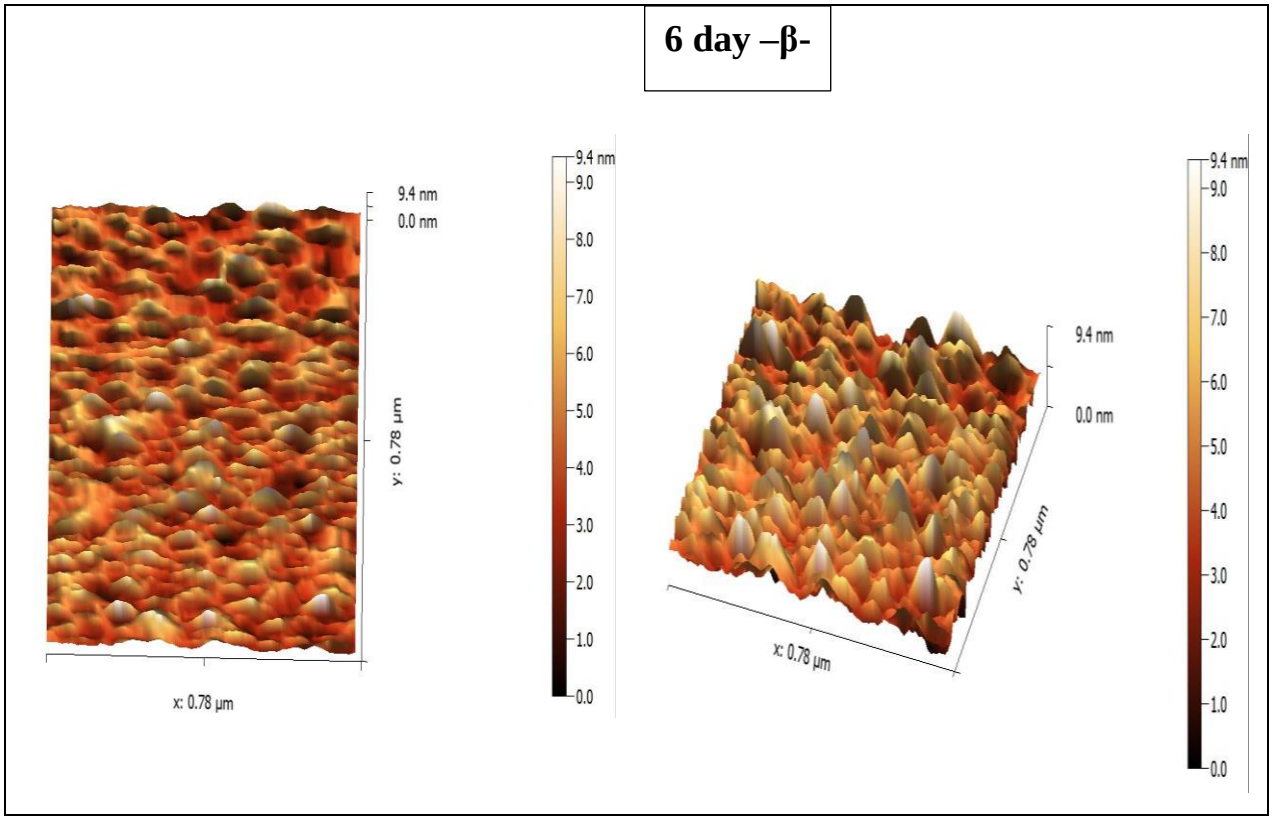

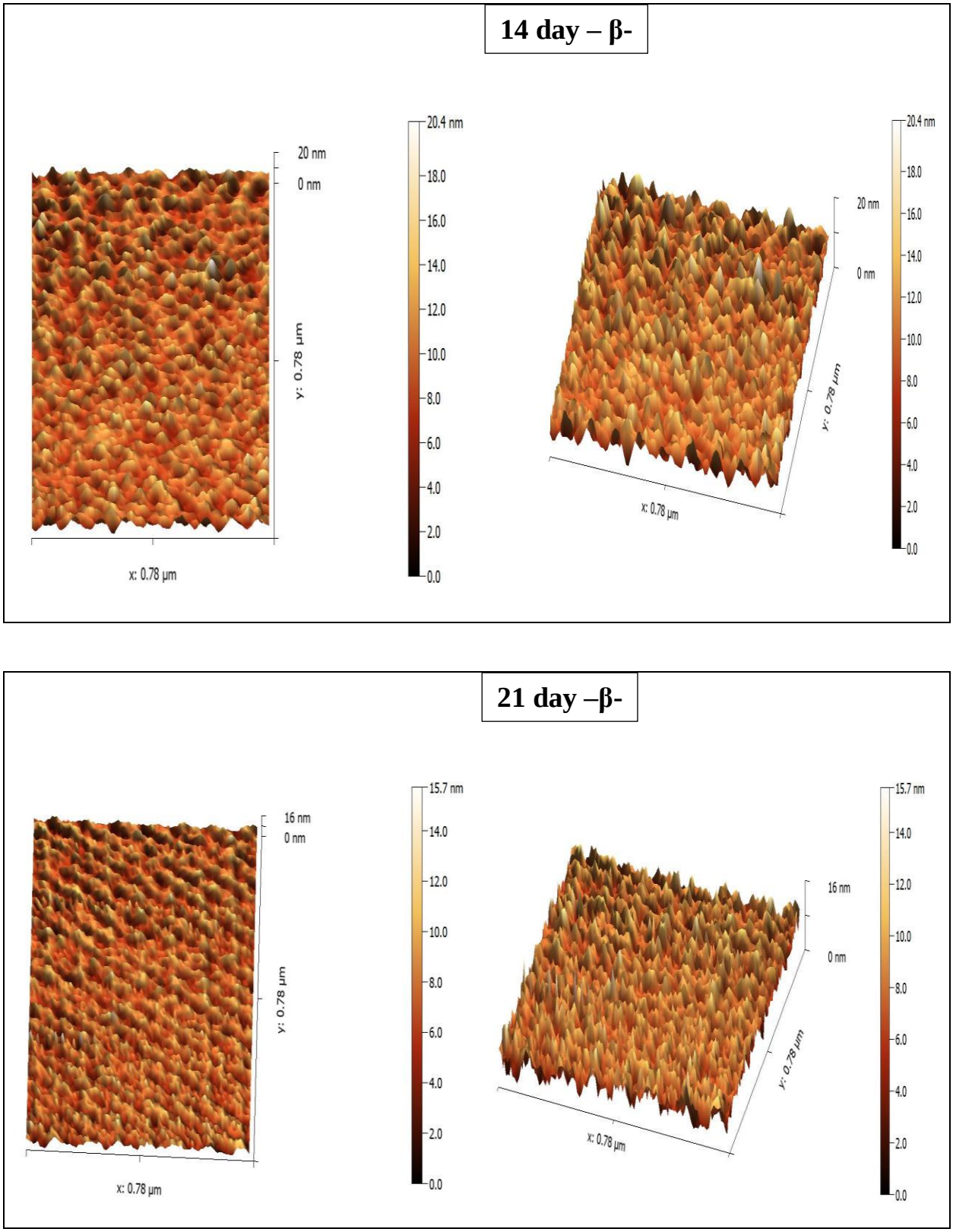

Figure (4.42): 2D and 3D AFM images with different irradiating time for CuPc thin film irradiated Beta ray source (β-)

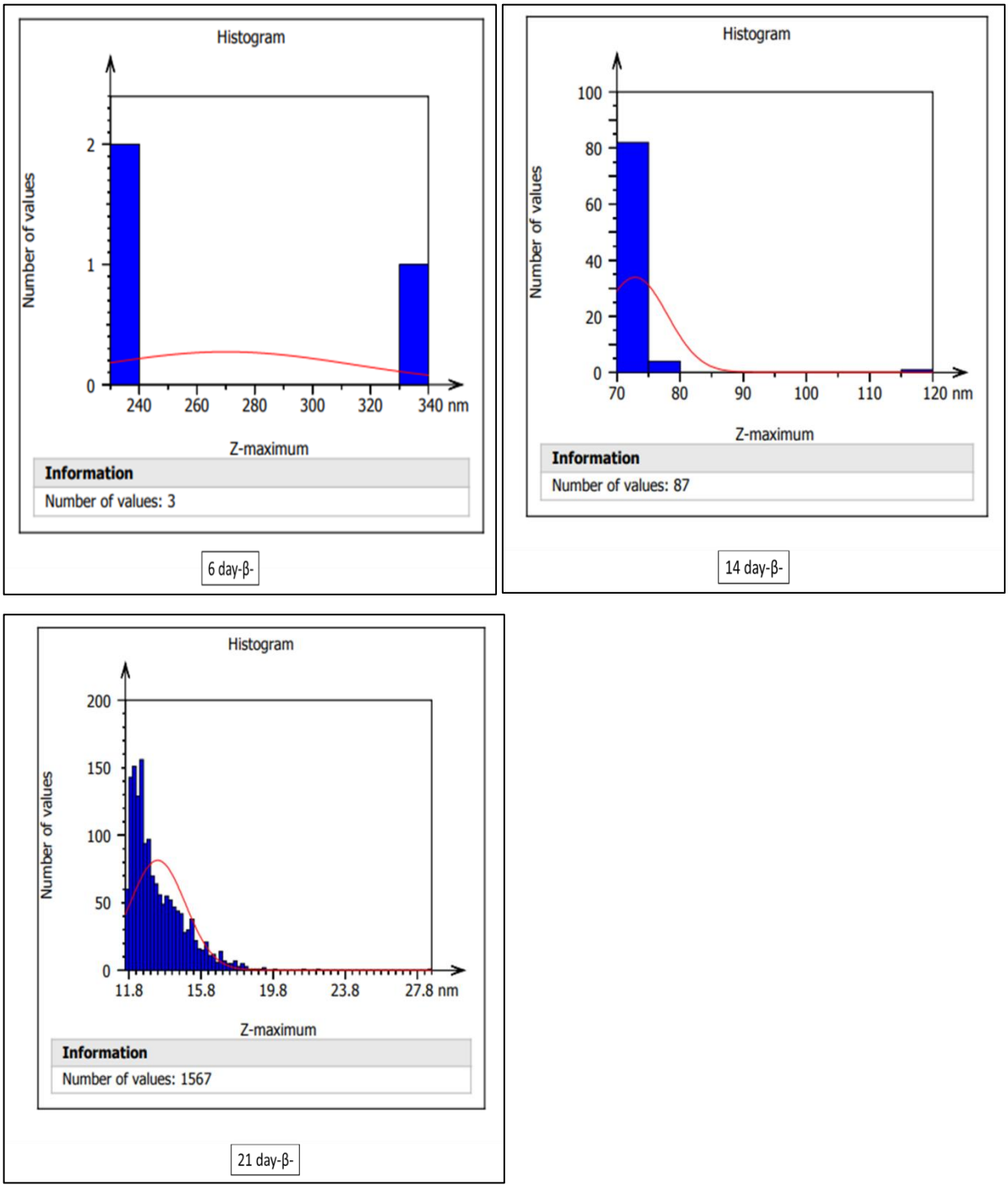

Figure (4.43): granular distribution diagrams of a surface CuPc thin films with a thickness of 214 nm and irradiated with β- at different irradiating times

Table (4.16) :AFM Measurements for CuPc irradiated with Minus Beta ray(β-)

irradiating time (day)	Grain size (nm)	Roughness (nm)	Diameter (nm)	RMS (nm)
0	13.61	11.66	197.7	2.21
6	5.21	9.77	270.0	1.34
14	9.39	3.61	72.87	2.20
21	8.53	1.87	13.40	1.90

Chapter five

Conclusions and Future Works

5.1 Conclusions

In this chapter, we present the most important findings from our research as well as some recommendations for future research. We get to the following conclusion based on the findings of this study:

1. At all periods of plus and minus beta radiation the molecules break down in thin films and solution
2. The negative electron(β-) and the positive positron(β+), and they both act in the same way
3. The energy gap increased and absorbance reduced for solution and thin films for β+β- it is dominant over the optical , electrical and thermal properties
4. The energy gap reduced and increased absorbance all concentrations according for Lambert Law
5. The peaks decrease indicates that the number of crystalline levels with coordinates (hkl) has decreased
6. The roughness and grain size of the surface morphology were reduced at all periods of the radiation

5.2 Suggestions for Future Work

We suggest the following studies as a future work:

1. Study of electrical properties of samples of irradiated solutions and films with positive and negative beta rays
2. Study of the optical, structural, and electrical properties of films and solutions irradiated with radium
3. Study of dispersion coefficients for models of films and solutions with positive and negative beta rays
4. Study of linear and linear optical properties of samples of films and solutions Irradiated positive and negative beta rays.

References

[1] N. J. Bae, Y. J.Lee, H. Kim, T. H.Cho, L. Lee, C. Fleet, A. Hirohata, "Growth and characterization of thin Cuphthalocyanine films on MgO(001) layer for organic light-emitting diodes," *Nanoscale Res. Lett.*, vol. 7, pp. 2–7, 2012, doi: 10.1186/1556-276X-7-650.

[2] M. Della Pirriera, J. Puigdollers, C. Voz, M. Stella, J. Bertomeu, R. Alcubilla, "Optoelectronic properties of CuPc thin films deposited at different substrate temperatures," *J. Phys. D. Appl. Phys.*, vol. 42, no. 14, 2009, doi: 10.1088/0022-3727/42/14/145102.

[3] A. Slodeka, G. Schnurpfeilb, and D. Wöhrle, "Optical limiting of germanium(IV) and tin(IV) phthalocyanines in solution and polymer matrices and comparison to an indium(III) phthalocyanine," *J. Porphyr. Phthalocyanines*, vol. 21, no. 12, pp. 811–823, 2017, doi: 10.1142/S1088424617500833.

[4] K. Sanusi, E. K. Amuhaya, and T. Nyokong, "Enhanced optical limiting behavior of an indium phthalocyanine-single- walled carbon nanotube composite: An investigation of the effects of solvents," *J. Phys. Chem. C*, vol. 118, no. 13, pp. 7057–7069, 2014, doi: 10.1021/jp501469e.

[5] A. Sahki, A. Larbi, and M. C. Boudiaf, "Conductivity modeling of gas sensors based on copper phthalocyanine thin films Modélisation de la conductivité de capteurs de gaz à base de couches minces de phtalocyanine de cuivre," vol. 27, pp. 18–27, 2017.

[6] A. Bengasi, Giuseppe Meunier-Prest, Rita Baba, Kamal Kumar and M. Pellegrino, Anna Lucia Boscher, Nicolas D. Bouvet, "Molecular Engineering of Porphyrin-Tapes/Phthalocyanine Heterojunctions for a Highly Sensitive Ammonia Sensor," *Adv. Electron. Mater.*, vol. 6, no.

12, 2020, doi: 10.1002/aelm.202000812.

[7] M. Isci, Ümit Bouvet, A. Dumoulin, Fabienne Kumar, and M. Isci, Ümit Bouvet, "Tuning of organic heterojunction conductivity by the substituents' electronic effects in phthalocyanines for ambipolar gas sensors," *Sensors Actuators, B Chem.*, vol. 332, no. October 2020, 2021, doi: 10.1016/j.snb.2021.129505.

[8] J. Salvo-Comino, Coral González-Gil, Alfonso Rodriguez-Valentin and M. L. Garcia-Hernandez, Celia Martin-Pedrosa, Fernando Garcia-Cabezon, Cristina Rodriguez-Mendez, "Biosensors platform based on chitosan/AuNPs/phthalocyanine composite films for the electrochemical detection of catechol. the role of the surface structure," *Sensors (Switzerland)*, vol. 20, no. 7, pp. 1–12, 2020, doi: 10.3390/s20072152.

[9] G. Medina-Plaza, Cristina Revilla, E. Muñoz, Raquel Fernández-Escudero, José Antonio Barajas, and M. L. Medrano, Germán De Saja, José Antonio Rodriguez-Mendez, "Electronic tongue formed by sensors and biosensors containing phthalocyanines as electron mediators:," *J. Porphyr. Phthalocyanines*, vol. 18, no. 1–2, pp. 76–86, 2014, doi: 10.1142/S1088424613501137.

[10] M. N. Abbas, M. Ben Saeed, Ayman Ali Ali, and B. Errachid, Abdelhamid Zine, Nadia Baraket, Abdullatif Singh, "Biosensor for the oxidative stress biomarker glutathione based on SAM of cobalt phthalocyanine on a thioctic acid modified gold electrode," *J. Solid State Electrochem.*, vol. 23, no. 4, pp. 1129–1144, 2019, doi: 10.1007/s10008-018-04191-4.

[11] T. Akabane, K. Ohta, T. Takizawa, T. Matsuse, M. Kimura, and S. K. & N. T. Saliha Güngör, Cihat Taşaltın, İlke Gürol, Gülsen Baytemir,

"Copper phthalocyanine-borophene nanocomposite-based non-enzymatic electrochemical urea biosensor," *Appl. Phys. A*, vol. 128, no. 89, pp. 476–492, 2022, doi: 10.1142/S108842461750047X.

[12] N. T. Boileau, O. A. Melville, B. Mirka, R. Cranston, and B. H. Lessard, "P and N type copper phthalocyanines as effective semiconductors in organic thin-film transistor based DNA biosensors at elevated temperatures," *RSC Adv.*, vol. 9, no. 4, pp. 2133–2142, 2019, doi: 10.1039/c8ra08829b.

[13] T. Akabane, K. Ohta, T. Takizawa, T. Matsuse, and M. Kimura, "Discotic liquid crystals of transition metal complexes, 54: Rapid microwave-assisted synthesis and homeotropic alignment of phthalocyanine-based liquid crystals," *J. Porphyr. Phthalocyanines*, vol. 21, no. 7–8, pp. 476–492, 2017, doi: 10.1142/S108842461750047X.

[14] K. Sathiyamoorthy, C. Vijayan, and M. P. Kothiyal, "Low power optical limiting in ClAl-Phthalocyanine due to self defocusing and self phase modulation effects," *Opt. Mater. (Amst).*, vol. 31, no. 1, pp. 79–86, 2008, doi: 10.1016/j.optmat.2008.01.013.

[15] P. P. John Mayall, "PHTHALOCYANINE COMPOUNDS AND THEIR USE IN INK-UET PRINTING," vol. 2, no. 12, 2009.

[16] H. S. S. M.M.El-Nahass, Z.El-Gohary, "Structural and optical studies of thermally evaporated CoPc thin Films," *Opt. Laser Technol.*, vol. 35, no. 7, pp. 523–531, 2003.

[17] K. D. Miller, Janine D. Baron, Elma D. Scull, Heather Hsia, Andrew Berlin, Jeffrey C. McCormick, Thomas Colussi, Valdir Kenney, Malcolm E. Cooper and N. L. Oleinick, "Photodynamic therapy with the phthalocyanine photosensitizer Pc 4: The case experience with

preclinical mechanistic and early clinical-translational studies," *Toxicol. Appl. Pharmacol.*, vol. 224, no. 3, pp. 290–299, 2007, doi: 10.1016/j.taap.2007.01.025.

[18] J. Gui, Li Zhou and S. Zhou, Lin Wei, "A smart copper-phthalocyanine framework nanoparticle for enhancing photodynamic therapy in hypoxic conditions by weakening cells through ATP depletion," *J. Mater. Chem. B*, vol. 6, no. 14, pp. 2078–2088, 2018, doi: 10.1039/c8tb00334c.

[19] B. W. H. Thomas J. Dougherty, Charles J. Gomer and Q. P. Giulio Jori, David Kessel, Mladen Korbelik, Johan Moan, "Photodynamic therapy," *Cancer Manag. Small Anim. Pract.*, vol. 90, no. 12, pp. 163–166, 1998.

[20] K. Sato, Kazuhide Ando, S. Okuyama, Shuhei Moriguchi, M. Ogura, TairoTotoki, Shinichiro Hanaoka, Hirofumi Nagaya, Tadanobu Kokawa, Ryohei Takakura, Hideo Nishimura, and H. Hasegawa, Yoshinori Choyke, Peter L. Ogawa, Mikako Kobayashi, "Photoinduced Ligand Release from a Silicon Phthalocyanine Dye Conjugated with Monoclonal Antibodies: A Mechanism of Cancer Cell Cytotoxicity after Near-Infrared Photoimmunotherapy," *ACS Cent. Sci.*, vol. 4, no. 11, pp. 1559–1569, 2018, doi: 10.1021/acscentsci.8b00565.

[21] N. V. L. and el at T.A.Sergeyeva, "Biosensors and Bioelectronics," vol. 13, no. 3–4, pp. 359–369, 1998.

[22] Alan J. Heeger, "Semiconducting and Metallic Polymers: The Fourth Generation of Polymeric Materials (Nobel Lecture)," *Angew. Chemie Int. Ed.*, vol. 40, no. 14, pp. 2591–261, 2001.

[23] J. Hopkins, K. Fidanovski, A. Lauto, and D. Mawad, "All-Organic Semiconductors for Electrochemical Biosensors : An Overview of

Recent Progress in Material Design," vol. 7, no. September, pp. 1–8, 2019, doi: 10.3389/fbioe.2019.00237.

[24] P. Vilmercati, D. Cvetko, A. Cossaro, and A. Morgante, "Heterostructured organic interfaces probed by resonant photoemission," *Surf. Sci.*, vol. 603, no. 10–12, pp. 1542–1556, 2009, doi: 10.1016/j.susc.2008.11.050.

[25] A. De Oteyza, D. G. El-Sayed, A. Garcia-Lastra, J. M. Goiri, E. Krauss, T. N. Turak, A. Barrena, E. Dosch, H. Zegenhagen, J. Rubio, and J. E. Wakayama, Y. Ortega, "Copper-phthalocyanine based metal-organic interfaces: The effect of fluorination, the substrate, and its symmetry," *J. Chem. Phys.*, vol. 133, no. 21, 2010, doi: 10.1063/1.3509394.

[26] Dimas G de Oteyza, "Fluorinated copper-phthalocyanines in organic thin-films, heterostructures and 2D supramolecular assemblies," University of Madrid, spain, 2006.

[27] M.-W. WitoldWacławek, "The influence of iodine on the electrical properties of lead phthalocyanine," *Thin Solid Films*, vol. 146, no. 1, pp. 1–6, 1987.

[28] D. Wöhrle, G. Schnurpfeil, S. G. Makarov, A. Kazarin, and O. N. Suvorova, "Practical Applications of Phthalocyanines – from Dyes and Pigments to Materials for Optical, Electronic and Photo-electronic Devices," *Macroheterocycles*, vol. 5, no. 3, pp. 191–202, 2012, doi: 10.6060/mhc2012.120990w.

[29] A. Bohrer, Forest I. Sharoni, J. Colesniuc, Corneliu Park, A. C. Schuller, Ivan K. Kummel, and W. C. Trogler, "Gas sensing mechanism in chemiresistive cobalt and metal-free phthalocyanine thin films," *J. Am. Chem. Soc.*, vol. 129, no. 17, pp. 5640–5646, 2007, doi:

10.1021/ja0689379.

[30] Ö. Bekaroğlu, “History, development, and a new concept of phthalocyanines in Turkey,” *Turkish J. Chem.*, vol. 38, no. 6, pp. 903–922, 2014, doi: 10.3906/kim-1404-83.

[31] A. A. Aljuhani, “Covalently Linked Dyads and Triads of Phthalocyanines and Porphyrins,” 2014.

[32] P. Pushpanandan and M. Ravikanth, “Synthesis and Properties of Stable 20π Porphyrinoids,” *Chem. Rec.*, vol. 144, pp. 1–31, 2022, doi: 10.1002/tcr.202200144.

[33] F. W. Marcel Gsänger,David Bialas,Lizhen Huang,Matthias Stolte, “Organic Semiconductors based on Dyes and Color Pigments,” *Adv. Mater.*, vol. 28, no. 19, 2016.

[34] C. C. Leznoff and A. B. P. Lever, *Phthalocyanines: Properties and Applications*, vol. 4. New York: VCH publisher Inc, 1996.

[35] M. D. Platzer, K. M. Sutter, and J. F. S. Jr., “Semiconductors : US Industry, Global Competition, and Federal Policy,” *Congr. Res. Serv.*, 2020.

[36] L. Tsetseris, “Hydrogen- and oxygen-related effects in phthalocyanine crystals: Formation of carrier traps and a change in the magnetic state,” *Phys. Chem. Chem. Phys.*, vol. 16, no. 7, pp. 3317–3322, 2014, doi: 10.1039/c3cp54755h.

[37] N. B. McKeown, “Phthalocyanine-containing polymers,” *J. Mater. Chem.*, vol. 10, no. 9, pp. 1979–1995, 2000, doi: 10.1039/b000793p.

[38] W. Chu, Chih and Y. Shrotriya, Vishal, Li, Gang Yang, “Tuning acceptor energy level for efficient charge collection in copper-phthalocyanine-based organic solar cells,” *Appl. Phys. Lett.*, vol. 88, no. 15, pp. 2012–2015, 2006, doi: 10.1063/1.2194207.

[39] A. A. A. D. M.M. El-Nahass , K.F. Abd-El-Rahman, “Fourier-transform infrared and UV–vis spectroscopes of nickel phthalocyanine thin films,” *Mater. Chem. Phys.*, vol. 92, pp. 185–189, 2005.

[40] N. Papageorgiou, E. Salomon, T. Angot, J. M. Layet, L. Giovanelli, and G. Le Lay, “Physics of ultra-thin phthalocyanine films on semiconductors,” *Prog. Surf. Sci.*, vol. 77, no. 5–8, pp. 139–170, 2004, doi: 10.1016/j.progsurf.2005.01.001.

[41] Keiichi Sakamoto and Eiko Ohno-Okumura, “Syntheses and Functional Properties of Phthalocyanines,” pp. 1127–1179, 2009, doi: 10.3390/ma2031127.

[42] A. Krupski, “Growth morphology of thin films on metallic and oxide surfaces,” *J. Phys. Condens. Matter*, vol. 26, no. 5, 2014, doi: 10.1088/0953-8984/26/5/053001.

[43] M. Stella and J. P. Gonzalez, “Study of Organic Semiconductors for Device Applications,” 2009.

[44] O. Berger, W. Fischer, B. Adolphi, and S. Tierbach, “Studies on phase transformations of Cu-phthalocyanine thin ® lms,” vol. 1, pp. 331–346.

[45] N. D. Ashcroft, N.W. and Mermin, *Solid State Physics*. Philadelphia: Saunders College, 1976.

[46] G. H. Heilmeier and S. E. Harrison, “Implications of the intensity dependence of photoconductivity in metal-free phthalocyanine crystals,” *J. Appl. Phys.*, vol. 34, no. 9, pp. 2732–2735, 1963, doi: 10.1063/1.1729800.

[47] M. Edrissi, B. Nasernejad, and B. Sayedi, “NOVEL METHOD FOR THE PREPARATION OF COPPER PHTHALOCYANIN BLUE NANOPARTICLES IN AN ELECTROCHEMICAL CELL IRRADIATED BY MICROWAVE,” 2007.

[48] B. B. Topuz, G. Gündüz, B. Mavis, and Ü. Çolak, “Synthesis and characterization of copper phthalocyanine and tetracarboxamide copper phthalocyanine deposited mica-titania pigments,” *Dye. Pigment.*, vol. 96, no. 1, pp. 31–37, 2013, doi: 10.1016/j.dyepig.2012.06.010.

[49] M. T. Hussein, “Theoretical IR spectroscopic study of Copper Phthalocyanine (CuPc),” *1 Reg. Conf. Eng. Sci. NUCEJ Spat. ISSUE*, vol. 11, no. 2, pp. 303–306, 2008.

[50] M. Al-amar, “Modifying Copper Phthalocyanine to Improve The Performance of Organic Solar Cells,” 2011.

[51] S. K. Ridhi, R. Saini, G. S.S.Tripathi, “Sensing of volatile organic compounds by copper phthalocyanine thin films,” *Mater. Res. Express*, vol. 4, no. 2, p. aa54d1, 2017, doi: 10.1088/2053-1591/aa54d1.

[52] S. Y. Shoko Kusama, Teruhiko Saito, Hiroshi Hashiba, Akihiro Sakai, “Crystalline Copper(II) Phthalocyanine Catalysts for Electrochemical Reduction of Carbon Dioxide in Aqueous Media,” *Am. Chem. Soc.*, vol. 7, no. 12, 2017.

[53] D. L. Xinran Liu , Fangdi Cong , Mengyao Han , Liwang Zhang , Zhongli Wang , Lu Jiang , Bingqian Liu , Shulin Zhang , Wei Yang , Yongpeng Su , Tao Li , Yingchao Wang, “Copper Phthalocyanine Improving Nonaqueous Catalysis of Pseudomonas cepacia Lipase for Ester Synthesis,” *Appl. Biochem. Biotechnol.*, vol. 1, no. 17, 2022.

[54] J. W. Weigl, J. Mammino, G. L. Whittaker, R. W. Radler, and J. F. Byrne, “Phthalocyanine-Binder Photoreceptors for Xerography,” *Curr. Probl. Electrophotogr.*, pp. 287–300, 2018, doi: 10.1515/9783111507743-034.

[55] R. R. Mohammed and M. T. Hussein, “Linear and Non-Linear Optical Properties for Organic Semiconductor (CuPc) Thin Films,” *Iraqi J.*

Phys., vol. 19, no. 48, pp. 10–20, 2021, doi: 10.30723/ijp.v19i48.639.

[56] E. A. Lukyanets, "Phthalocyanines as Photosensitizers in the Photodynamic Therapy of Cancer," *J. Porphyr. Phthalocyanines*, vol. 3, no. 6–7, pp. 424–432, 1999, doi: 10.1002/(sici)1099-1409(199908/10)3:6/7<424::aid-jpp151>3.0.co;2-k.

[57] P. Singh and N. M. Ravindra, "Optical properties of metal phthalocyanines," *J. Mater. Sci.*, vol. 45, no. 15, pp. 4013–4020, 2010, doi: 10.1007/s10853-010-4476-6.

[58] S. S. Mali, D. S. Dalavi, P. N. Bhosale, C. A. Betty, A. K. Chauhan, and P. S. Patil, "Electro-optical properties of copper phthalocyanines (CuPc) vacuum deposited thin films," *RSC Adv.*, vol. 2, no. 5, pp. 2100–2104, 2012, doi: 10.1039/c2ra00670g.

[59] S. H. Lee, Jaehyun Kim, J. Lee, Woosung Lee, S. Y. An, Byeong Kwan Oh, and J. Kim, Jae Pil Park, "Electrochemical and optical characterization of cobalt, copper and zinc phthalocyanine complexes," *J. Nanosci. Nanotechnol.*, vol. 13, no. 6, pp. 4338–4341, 2013, doi: 10.1166/jnn.2013.7009.

[60] A. H. A. Jalaukhan, "Effect of Substrate Temperature on Optical Properties of Thermally Evaporated CuPc Thin Films. ," *Journal*, vol. 13, no. 2, 2015.

[61] H. Abdulhussien, "Influence of Gamma Ray on the Optical and Structural Properties of Metal Phthalocyanine Thin Films," 2016.

[62] A. Datir, "Synthesis and UV-Visible Characterization Study of Spin Coated Copper Phthalocyanine Films," *Int. Multidiscip.*, vol. IV, no. I, pp. 107–111, 2016.

[63] D. K. Nair and K. S. Kumar, "Development of gamma radiation dosimeter using copper phthalocyanine & zinc phthalocyanine based

OFET," *IEEE Int. Conf. Circuits Syst. ICCS 2017*, vol. 2018-Janua, pp. 427–430, 2018, doi: 10.1109/ICCS1.2017.8326036.

[64] S. Naji and S. Mohammed, "Effect of Beta Ray on the Optical Properties of CuO Thin Films," *Diyala J. Pure Sci.*, vol. 14, no. 4, pp. 40–52, 2018, doi: 10.24237/djps.1404.446b.

[65] M. H. Eisa, "Effects of beta-ray irradiation on optical properties of PbO thin films," *Mater. Sci. Semicond. Process.*, vol. 110, no. January, p. 104966, 2020, doi: 10.1016/j.mssp.2020.104966.

[66] B. K. Alhiti, Laith Sa, Al-rawi, "EFFECT OF ANNEALING TEMPERATURE ON THE OPTICAL PROPERTIES OF COPPER PHTHALOCYANINE (CUPC) THIN FILMS PREPARED BY VACUUM EVAPORATION METHOD," *Physiother. Rehabil.* ·, vol. 32, no. 3, 2021.

[67] A. K. Bhatia, *Interactions of Positrons with Matter and Radiation*. USA, 1928.

[68] K. SIEGBAHN, *Alpha-, Beta- and Gamma-Ray Spectroscopy*, vol. 1. New York: NORTH-HOLLAND COMPANY AMSTERDAM · OXFORD, 1968.

[69] R. Lawson, *An Introduction to Radioactivity*. 1999.

[70] H. Wheat, JM; Currie, GM; Davidson, R; Kiat, "Radionuclide therapy," *Med. Radiat. Sci.*, vol. 58, no. 3, 2011.

[71] C. L. Schott, Robert J. Weaver, R. V. Prelas, Mark A. Oh, Kyuhak Rothen berger, Jason B. Tompson, and D. A. Wisniewski, "Photon intermediate direct energy conversion using a 90Sr beta source," *Nucl. Technol.*, vol. 181, no. 2, pp. 349–353, 2013, doi: 10.13182/NT13-A15789.

[72] and H. S. D. A. Basavaraju, P. Venkataramaiah, K. Cxopala, "Inner

bremsstrahlung accompanying beta decay in Sr90- Y90," *Am. Phys. Soc.*, vol. 28, no. 1, pp. 333–336, 1983.

[73] M. Nazari, "Positron emission tomography," 2010.

[74] j I. Pankove, *Optical Processes in Semiconductors*. New Jersy, 1975.

[75] C. Andres, "Some effects on polymers of low-energy implanted positrons," 2008.

[76] J. I. Pankove, *OpticalProcesses in Semiconductors*. New Jersey: Englewood Cliffs, N.J. : Prentice-Hall, 1971.

[77] B. Streetman, *Solid State Electronic Devices*, 7th ed. Prentice-Hall, Eaglewood Cliffs, 1980.

[78] H. Meier, *Organic semiconductors: Dark- and photoconductivity of organic solids*. Weirnheirn: Verlag Chemie, 1974.

[79] M. Loudon, *Organic Chemistry*, 6th ed. W.H. Freeman, 2015.

[80] R. Grenier, *Semiconductor Device*. McGraw-Hill, Book Co.Inc., 1961.

[81] Donald A. Neamen, *Semiconductor Physics and Semiconductor Devices*, vol. 28, no. 9. 1974.

[82] R. Hoffmann, C. Janiak, and C. Kollmar, "Macromolecules," vol. 24, no. 13, 1991.

[83] J. Millman, *Microelectronics*. Murray – Hill,Book Company Kogakusha, 1969.

[84] R. Elliot and A.I.Gibson, *An Introduction to Solid State Physics and Application*, 1st editio. Macillian Inc, 1974.

[85] Gerald Burn, *Solid State Physics*, 1st Editio. Harcourt Brace Jovanovich, New York: Academic Press, Inc, 1985.

[86] J. Tauc, R. Grigorovici, and A. Vancu, "Optical Properties and Electronic Structure of Amorphous Germanium," *Phys. Status Solidi*, vol. 15, no. 2, pp. 627–637, 1966, doi: 10.1002/pssb.19660150224.

[87] K. K. N. S.M. Sze, *Physics of Semiconductor Devices*. John Wiley & Sons, 2006.

[88] H. Suhail and R. A. Ahmed, "Structural, optical and electrical properties of doped copper ZnS thin films prepared by chemical spray pyrolysis technique," *Pelagia Res. Libr. Adv. Appl. Sci. Res.*, vol. 5, no. 5, pp. 139–147, 2014, [Online]. Available: www.pelagiaresearchlibrary.com.

[89] B. Ray, *II-VI Compounds*, 1st editio. Pergamon Press, 1969.

[90] T. S. Moss, *Optical Properties of Semiconductors*. London: Butterworth's Scientific Publication LTD, 1959.

[91] M. E. Azim-Araghi and A. Krier, "Optical characterization of chloroaluminium phthalocyanine (ClAlPc) thin films," *Pure Appl. Opt. (Print Ed. (United Kingdom)*, vol. 6, no. 4, pp. 443–453, 1997, doi: 10.1088/0963-9659/6/4/007.

[92] Adnan H. Al-Aarajiy, "Preparation and Characterization of NiPc / Si Organic Solar Cell."

[93] R. A. Grenier, *Semiconductor Device*. McGraw-Hill, Book Co. Inc, 1961.

[94] T. .J, *Amorphous and liquid semiconductors*. London and New York: Plenum Press, 1974.

[95] T. S. Moss, *Optical Properties of Semiconductor*. London: Butter Worthes Scientific Publications LTD, 1959.

[96] A. H. C. L.Kazmerski, *Electrical properties of polycrystalline semiconductor thin films*. Academic Press, 1980.

[97] B. Valeur, *Molecular Fluorescence Principles and Applications*, vol. 8. 2001.

[98] W. H. Bragg and W. L. Bragg, "The reflection of X-rays by crystals,"

Proc. R. Soc. London. Ser. A, Contain. Pap. a Math. Phys. Character, vol. 88, no. 605, pp. 428–438, 1913, doi: 10.1098/rspa.1913.0040.

[99] C. Yang *et al.*, "Impact of Stokes Shift on the Performance of Near-Infrared Harvesting Transparent Luminescent Solar Concentrators," *Sci. Rep.*, vol. 8, no. 1, pp. 1–10, 2018, doi: 10.1038/s41598-018-34442-3.

[100] L. Brand and M. L. Johnson, "An Introduction to Fluorescence Spectroscopy," p. 15, 2011, [Online]. Available: http://books.google.com/books?id=GgFXweh0hmQC&pgis=1.

[101] S. K. Shailaja Mahamuni, Deepti Sidhaye, *Foundations of Experimental Physics*. New Delhi: CRC Press, 2021.

[102] S. Ersoy and H. Kantekin, "Synthesis of fluorine-containing phthalocyanines and investigation of the photophysical and photochemical properties of the metal-free and zinc phthalocyanines," vol. 24, no. 5, pp. 259–265, 2018.

[103] C. Diederichs, "The resonance fluorescence of single semiconductor quantum dots for the generation of indistinguishable photons . To cite this version : HAL Id : tel-01416901," 2016.

[104] F. Xiong, Xiaoqing , Song, Y. Wang, Jingyun , Zhang, L. Xue, Yingying , Sun, P. Jiang, Na, Gao, and X. Tian, Lu , Peng, "Thermally Activated Delayed Fluorescence of Fluorescein Derivative for Time-Resolved and Confocal Fluorescence Imaging," *Am. Chem. Soc.*, 2014.

[105] A. Ali, Y. W. Chiang, and R. M. Santos, "X-Ray Diffraction Techniques for Mineral Characterization: A Review for Engineers of the Fundamentals, Applications, and Research Directions," *Minerals*, vol. 12, no. 2, 2022, doi: 10.3390/min12020205.

[106] J. Patterson and B. Bailey, *Solid-state physics: Introduction to the*

theory. 2010.

[107] M. A. Asadabad and M. J. Eskandari, "Electron Diffraction," *Mod. Electron Microsc. Phys. Life Sci. Emiss.*, p. 5, 2016, doi: 10.5772/61781.

[108] A. Monshi, M. R. Foroughi, and M. R. Monshi, "Modified Scherrer Equation to Estimate More Accurately Nano-Crystallite Size Using XRD," vol. 2012, no. 2, pp. 154–160, 2012.

[109] C. B. Wolfschmidt, Holger, M. Gsell, Stefan , Fischer, and U. Schreck, Matthias And Stimming, "STM, SECPM, AFM and Electrochemistry on Single Crystalline Surfaces," no. 111, pp. 4196–4213, 2010, doi: 10.3390/ma3084196.

[110] B. Kyeyune, "Atomic Force Microscopy," 2018.

[111] P. J. Haynes, G. Wells, and J. A. Hartley, "Atomic force microscopy — A tool for structural and translational DNA research," vol. 031504, pp. 1–16, 2021, doi: 10.1063/5.0054294.

[112] P. K. Roy, Shatter Turner, Aubrey Bhattacharya, "Developing a Gaertner Ellipsometer for Thin Film Thickness Measurement," 2022, doi: 10.18260/1-2-620-38784.

[113] P. K. C. Huaiyu Wang, *Characterization of Biomaterials*. United State: Newnes, 2013.

[114] J.Sanderson, "Contrast Enhancement Techniques for Light Microscopy." pp. 15–19, 1998.

[115] D. Titus, E. James Jebaseelan Samuel, and S. M. Roopan, *Nanoparticle characterization techniques*. Elsevier Inc., 2019.

[116] S. R. Falsafi, H. Rostamabadi, and S. M. Jafari, *X-ray diffraction (XRD) of nanoencapsulated food ingredients*. Elsevier Inc., 2020.

[117] B. Szabó, "ATOMIC FORCE MICROSCOPY," *J. Assoc. Pediatr.*

Oncol. Nurses, vol. 3, no. 2, pp. 35–35, 1986, doi: 10.1177/104345428600300214.

[118] S. M. F. Sahar Naji Rashid, "Effect of Beta Ray on the Optical Properties of CuO Thin Films," *Diyala J. Pure Sci.*, vol. 14, no. 4, 2018.

الخلاصـــة

تم تحضير محلول ثالوسيانين النحاس (CuPc) من مسحوق ثالوسيانين النحاس المذاب في الكلوروفورم بتركيز (0.15g/l) وتم تشعيعه بمصدرين مختلفين من الاشعة بيتا النووية الموجبة(Na-22) بمصدر طاقة (0.544Mev) والسالبة (Sr-90) بمصدر طاقة(0.546 Mev) تم قياس الخواص البصرية قبل وبعد التشعيع وتبين أن الامتصاصية والانعكاسية يتناقصان مع زيادة زمن التشعيع وتزداد النفاذية وفجوة الطاقة البصرية ذو الانتقال غير مباشر كما تم حساب الثوابت البصرية مثل معامل الامتصاص ، معامل الانكسار ، معامل الخمود وثابت العزل الكهربائي الحقيقي والخيالي والتوصيلية البصرية قبل وبعد التشعيع .

كما حضرت محاليل (CuPc) بتراكيز g/l (0.2,0.1،0.15) وتم شعيعها بالأشعة بيتا النووية الموجبة (Na-22) ومصادر بيتا السالبة (Sr-90). تم قياس الخواص البصرية قبل وبعد التشعيع وتبين أن الامتصاص والانعكاس يتزايدان مع زيادة زمن التشعيع وتقل النفاذية وفجوة الطاقة البصرية ذو الانتقال غير مباشر كما تم حساب الثوابت البصرية مثل معامل الامتصاص ، معامل الانكسار ، معامل الخمود وثابت العزل الكهربائي الحقيقي والخيالي والتوصيلية البصرية قبل وبعد التشعيع .

كذلك حضرت أغشية رقيقة (CuPc) بقيم سمك ثابته وبدرجات حرارية ثابته بتقنية الترسيب على ركائز زجاجية بسمك (197nm, 214) بعد ذلك تم تشعيعها بأشعة بيتا باستخدام مصدرين مختلفين من الأشعة (Na-22) ذو معدل طاقة (0.544Mev)و مصدر (Sr-90) ذو طاقه (0.546Mev).

فحوص الخواص البصرية تضمنت فحوص طيف الاشعة فوق البنفسجية والمرئية ‘UV- Visible) وكذلك طيف الفلوره (PL). تم تشخيص المادة و تحديد الاواصر الكيميائية لمسحوق ثالوسيانين النحاس CuPc بواسطة جهاز تحويل فورير للأشعة تحت الحمراء (FTIR).

اظهرت فحوص UV- Vis ان اغشية CuPc تمتلك نقصان في الامتصاصية و الانعكاسية وزيادة في النفاذية وفجوه طاقه بصرية ذات الانتقال المباشر .كذلك تم حساب الثوابت البصرية مثل معامل الامتصاص ومعامل الانعكاس ومعامل التهيج وطيف الفلوره لوحظ زيادة قيمة فجوة الطاقة البصرية

فحصت الخواص التركيبية لمسحوق CuPc وللأغشية المحضرة على ركائز زجاجية بواسطة حيود الأشعة السينية (X-ray) , أظهرت نتائج حيود الأشعة السينية أن المسحوق متعدد التبلور,نظام ثلاثي الميل وان معدل الحجم البلوري يزداد بزيادة مدة التشعيع.

تم فحص مورفولجية السطح لأغشية (CuPc) قبل وبعد التشعيع ولفترات زمنية مختلفة ومن ثم تحديد الحجم الحبيبي والخشونة بواسطة مايكروسكوب القوه الذرية (AFM) لنوعين من مصادر الطاقة لأشعة بيتا وكانت قيمتها تقل بزيادة زمن التشعيع لكل المصدرين اشعة بيتا الموجبة والسالبة

وزارة التعليم العالي والبحث العلمي

جامعة بابل

كلية العلوم / قسم الفيزياء

تأثير التشعيع بجسيمات بيتا على الخواص التركيبية و البصرية للأغشية الرقيقة لـ ثالوسيانين – معدن

رسالة مقدمة إلى

مجلس قسم الفيزياء – كلية العلوم – جامعة بابل

وهي جزء من متطلبات نيل درجة الماجستير في العلوم/ الفيزياء

من قبل

رهام خالد كريم كاظم

بكالوريوس علوم الفيزياء / ٢٠١٦

بإشراف

م. د. عدنان حمود محمد عبد الحسين الاعرجي

١٤٤٤هـ ٢٠٢٢م